PREPARATION OF FERRIC AND MANGANESE COATED ON MODIFIED WATER TREATMENT SLUDGE AS CATALYST IN OZONATION FOR PHENOL REMOVAL FROM AQUEOUS SOLUTION

APIRADEE SUKMILIN

A THESIS SUBMITTED IN FULFILLMENT OF THE REQUIREMENT FOR THE
DEGREE OF DOCTOR OF PHILOSOPHY IN APPLIED CHEMISTRY
DEPARTMENT OF CHEMISTRY FACULTY OF SCIENCE
KING MONGKUT'S INSTITUTE OF TECHNOLOGY LADKRABANG
2019
KMITL-2019-SC-D-010-021

PREPARATION OF FERRIC AND MANGANESE COATED ON MODIFIED WATER TREATMENT SLUDGE AS CATALYST IN OZONATION FOR PHENOL REMOVAL FROM AQUEOUS SOLUTION

APIRADEE SUKMILIN

A THESIS SUBMITTED IN FULFILLMENT OF THE REQUIREMENT FOR THE
DEGREE OF DOCTOR OF PHILOSOPHY IN APPLIED CHEMISTRY
DEPARTMENT OF CHEMISTRY FACULTY OF SCIENCE
KING MONGKUT'S INSTITUTE OF TECHNOLOGY LADKRABANG
2019
KMITL-2019-SC-D-010-021

Thesis Title	Preparation of ferric and manganese coated on modified water treatment sludge as catalysts in ozonation for phenol removal from aqueous solution
Student Name	Ms. Apiradee Sukmilin
Student ID	55650351
Degree	Doctor of Philosophy
Department	Chemistry
Year	2018
Thesis Advisor	Assoc. Prof. Dr. Banjong Boonchom
Thesis Co-advisor	Asst. Prof. Dr. Chalor Jarusutthirak

Abstract

In this study, iron and manganese coated on water treatment sludge (WTS), designated as Fe/WTS and Mn/WTS, respectively, were prepared by hydrothermal method using phosphoric acid and then impregnation with ferric nitrate and manganese sulfate. Physicochemical properties of WTS, acid modified WTS, Fe/WTS, and Mn/WTS were investigated by XRF, XRD, FTIR, BET, SEM, and SEM-EDX techniques. The results of XRD and FTIR for WTS and acid modified WTS revealed that removal of octahedral aluminum cations (Al^{3+}) along with other impurities occurred under acid treatment with hydrothermal conditions. Progressively increasing removal of Al^{3+} ions was caused by phosphoric acid strength of activation. The formation of high crystallinity and increased surface area were occurred from acid treatment. BET results indicated an increment of specific surface area of the WTS from 37.37 m^2/g to 150.07 m^2/g when treated with 5M phosphoric acid. However, there was slightly decrease in surface area when acid strength increased to 10 and 15 M. Acid modified WTS was used as supports for ferric and manganese catalysts. The results from XRF and EDX confirmed the abundance of Fe and Mn on the modified WTS. The Fe/WTS and Mn/WTS were successfully used as catalysts in catalytic ozonation for removal of phenol from aqueous solution. The results indicated that the Fe/WTS and Mn/WTS catalysts significantly improved the removal efficiencies of phenol. Factors affecting phenol removal efficiency including Fe and Mn content, catalyst dosage, pH, and reaction times, were investigated and optimum conditions for catalytic ozonation in phenol degradation were obtained. At the optimum conditions when Fe/WTS catalyst was used, i.e. Fe content in Fe/WTS of 2%, catalyst dosage of 1 g/L, pH of 11, and reaction time of 120 min, phenol removal efficiency was up to 99.16%. The optimum conditions for Mn/WTS catalyst were indicated as follows: Mn content in Mn/WTS of 2%, catalyst dosage of 3 g/L, pH of 11, and reaction time of 120 min. At this condition, phenol removal efficiency of 89.98% was achieved, which was higher than that of ozonation with WTS catalyst (59.35%) and sole ozonation (44.61%). Hydroxyl radicals ($OH^\bullet$) generated from ozone decomposition on the surface of the catalyst surface were responsible for phenol removal. The results of kinetic analyses indicated that the reactions of catalytic ozonation in the presence of Fe/WTS and Mn/WTS catalysts followed pseudo-first order kinetic model with observed rate constants (k_{obs}) of 0.0362 and 0.0190 min^{-1}, respectively, while those of ozonation with WTS and ozonation alone were 0.0063 min^{-1} and 0.0046 min^{-1}, respectively. This finding presented the potential use of novel catalysts prepared from ferric and manganese coated on modified water treatment sludge in catalytic ozonation for phenol removal from aqueous solution.

Keywords: acid activation, catalytic ozonation, ferric, manganese, water treatment sludge

ACKNOWLEDGEMENTS

I would like to start this dissertation with profound gratitude and indebtedness to my advisors, Assoc. Prof. Dr. Banjong Boonchom and Asst. Prof. Dr. Chalor Jarusutthirak, for their stimulating ideas, numerous constructive suggestions, guidance, and encouragement throughout this study.

I am greatly indebted to my chairman, Asst. Prof. Dr. Suchat Leungprasert for his valuable advice, guidance, and comments that helped in sharping the research.

Words to thanks must also be conveyed to the members of my supervision committee, Assoc. Prof. Dr. Usarat Thawornchaisit, Asst. Prof. Dr. Suwannee Junyapoon, and Dr. Chawan Sriwong for all their valuable comments and critical idea through which the scope of the work could be enhanced.

I gratefully acknowledged the Office of the Higher Education Commission (OHEC) and Phranakhon Rajabhat University (PNRU) for generously providing the scholarship and financial support for this research.

I wished to present deepest sincere thanks to all staffs in the Department of Chemistry at KMITL, Chemistry Program of PNRU, and Environmental Engineering Program at AIT for friendship, help, and moral support, which contributed in various ways to the completion of this dissertation.

Finally, I would like to express my deepest gratitude and dedicate this research work to my family and special friends who always assisted and supported me through difficult times and contributed to the success of this study.

Ms. Apiradee Sukmilin

Table of Contents

Table of Contents (con't)

Table of Contents (con't)

List of Tables

List of Figures

List of Figures (con't)

List of Figures (con't)

Abbreviations/Symbols

BET	Brunauer-Emmett-Teller
Fe	Iron, Ferric
Fe/WTS	Ferric coated on acid modified water treatment sludge
hr	Hour
ICP-OES	Inductively couple plasma optical emission spectrometer
L.O.I	Loss of Ignition
Mn	Manganese
Mn/WTS	Manganese coated on acid modified water treatment sludge
Min	Minute
MWA	Metropolitan Waterworks Authority
$OH^{\bullet}$	Hydroxyl radicals
SEM	Scanning electron microscope
SEM-EDX	Scanning electron microscopy with energy dispersive X-ray spectroscopy
WTS	Water treatment sludge
XRD	X-ray diffractometer
XRF	X-ray fluorescence spectrometry

CHAPTER 1

Introduction

1.1 Research motivation

Water treatment sludge (WTS) is a by-product from water treatment process. Its generation increased rapidly due to rapid growth of population leading to high domestic and industrial water consumption as well as the trend of urbanization and industrialization (Ahmad et al., 2016; Seiple et al., 2017). It was reported that the amount of WTS from Metropolitan Waterworks Authority (MWA) has been increasing from 61,320 tonnes/year in 2009 (Wetchasat et al., 2010) to 100,000-120,000 tonnes/year in 2017 (Nimwinya et al., 2016; Pumkumarn, 2017). Large amount of sludge from water treatment process led to high cost of disposal. Typically, WTS is classified as a waste material, nevertheless, it contains a lot of useful chemical compositions, such as iron, silicon, and alumina (Kizinievic et al., 2013). Many researchers tried to recycle WTS by various applications such as plantation, ceramic production (Kizinievic et al., 2013), and geo-polymer because its properties are similar to clay (Vinitnantharat et al., 2010). However, the recycle of the water treatment sludge for more valuable application is still challenging. Suasamserm (2002) investigated the properties of WTS and found that the properties of water treatment sludge were equivalent to those of kaolin. Kaolinite is the major mineral component of kaolin, which may contain quartz, mica, and feldspar (Panda et al., 2010). Kaolin employs a very fine particle size with chemical structure of 1:1 layer sheet structured hydrated aluminum silicate with one silicon oxygen (SiO_4) tetrahedral layer and one alumina octahedral layer with pseudo-hexagonal symmetry, bonded together through sharing of apical oxygens (Panda et al., 2010). This kaolin-like compound is one of the mineral clay widely used for a large number of applications, such as in ceramics, paper coating, filling paper, paint extender, rubber filler, plastic filler, cements, or catalysts (Benlalla et al., 2015; Ling et al., 2017; Ling et al., 2018; and Wolff et al., 2015). However, WTS was usually used in fields without pretreatment, which is difficult to meet required specification. So it is very necessary to modify the WTS by assistant materials before using it in several applications.

Acid activation has been widely studied as a chemical assistant method for improvement of clay or sludge properties, for example, surface area, particle size, morphology, crystallinity, amorphous, and catalytic activity. Chemical assistant compounds such as hydrochloric (HCl), sulfuric (H_2SO_4), nitric (HNO_3), and phosphoric (H_3PO_4) acids have been widely used in acid activation (Ayodele et al., 2012; Panda et al., 2010; Wisniowsk and Włodarczyk-Makuła, 2018). These acids play significant roles in leaching the clays or sludge, leading to disaggregation of clay particles, elimination of mineral impurities, and dissolution of the external layers, thus altering the chemical composition and the structure of the clays or sludge (Kooli et al, 2015; Kormadel, 2016; Gao et al, 2016). The acid treatment is beneficial in terms of modified properties with respect to the parent clays and specific applications (Parsons and Daniels, 1999; Gao et al, 2016). From previous study, modified clay or sludge using acid activation employed increasing pore volume and BET surface area which was suitable for use as a catalyst support (Panda et al., 2010). In this study, the WTS was interesting to be modified its properties for use as catalyst support. However, information regarding to phosphoric acid activation on water treatment sludge is insufficient and still challenging. Therefore, phosphoric acid activation on WTS was investigated to modify physicochemical properties prior to utilize it in specific application.

Transition metals, such as Fe, Mn, Cu, and Ni, have been used as catalysts (Wang et al., 2011). Fe-and Mn-based catalysts have been widely used in ozonation for wastewater treatment because of high efficiencies in mineralization of organic pollutants (Li et al., 2018; Ghuge and Saroha, 2018). Comparing with other metals, Fe and Mn enhanced high efficiencies to degrade micropollutants (Guo et al., 2018). Fe-doped MCM 41 acted as a catalyst in catalytic ozonation process to degrade diclofenac with a percent removal of 70%, while Mn-doped SBA could mineralize norfloxacin to 54% (Chen et al., 2017). Fe and Mn as catalysts performed good catalytic activity with ozonation (Li et al., 2018; Ghuge and Saroha, 2018), so both Fe and Mn were interesting to be used as catalysts especially in catalytic ozonation process.

Catalytic ozonation is one type of advanced oxidation processes using catalyst in ozonation to promote decomposition of ozone on its surface to produce hydroxyl radicals. The catalytic ozonation also facilitates the adsorption and reaction of organic compounds with ozone on the surface of the catalyst, thereby, increasing the degradation of organic compounds (Chen et al., 2017; Ghuge and Saroha, 2018). Catalytic ozonation can be divided into two types including homogeneous catalytic ozonation and heterogeneous catalytic ozonation, based on the type of catalysts used in the process. In homogeneous catalytic ozonation, transition metal ions such as Mn^{2+}, Fe^{3+}, Fe^{2+}, and Co^{2+}, are used to decompose ozone and generate $OH^{\bullet}$ (Li et al., 2018). However, using metal ions has several disadvantages such as insufficient active sites and limited specific surface area, high consumption of the catalysts, and complexity of these technologies (Farzadkia et al., 2014). Moreover, this technology is to introduce ions into an aqueous phase and results in secondary pollution, which leads to the increase cost of water treatment (Li et al., 2018). In heterogeneous catalytic ozonation, solid catalyst, such as metal, metal oxide, and metal on support, accelerates the decomposition of ozone into $OH^{\bullet}$. The solid catalyst in ozonation also enhances degradation of organic pollutants by adsorbing them on its surface in order to accelerate subsequent reaction between pollutant and ozone (Shahamat et al., 2014; Ghuge and Saroha, 2018).

Phenol is known as a hazardous pollutant found in aqueous effluents from various industries such as petrochemical plant, petroleum refinery and plastics industry. It is considered as a refractory organic compound by the US EPA with high toxicity and carcinogenic properties (He et al., 2008). Conventional biological processes represent an environmentally friendly way of treatment with reasonable costs, however, they are not adequate to treat such a toxic and refractory compound, otherwise, a long residence time for microorganisms is required. Thus, there is a need to use effective strategies of treatment to achieve high quality of effluent prior to discharge to natural receiving water (Farzadkia et al., 2014; Wang et al., 2016). Among the advanced oxidation processes (AOPs), ozone-based processes appear as promising technologies for the removal of refractory compounds [14]. With high oxidation potential, ozone (O_3) can react directly with various organic compounds and/or indirectly when ozone is decomposed into hydroxyl radicals ($OH^•$), which have higher oxidizing rate than ozone itself. However, direct ozonation has a few disadvantages due to relatively low solubility and instability in water, which is limited to a certain extend of mineralization. To overcome these limitations, catalytic ozonation is able to increase the reaction rate compared with ozonation alone.

In this research, phenol was used as a model pollutant in aqueous solution to be degraded by catalytic ozonation in the presence of the Fe/WTS and Mn/WTS catalysts. The WTS was modified with phosphoric acid at different acid strengths during hydrothermal process. Modified WTS was impregnated with ferric nitrate and manganese sulfate to load ferric and manganese catalysts into the acid modified WTS support. Physicochemical properties of WTS, acid modified WTS, Fe/WTS, and Mn/WTS were investigated by XRF, XRD, FTIR, BET, SEM, and SEM-EDX techniques. The FE/WTS and Mn/WTS were used as catalysts in catalytic ozonation for degradation of phenol in aqueous solution. The objectives of this study are to prepare novel catalysts from acid modified WTS coated with ferric and manganese and to study feasibility of Fe/WTS and Mn/WTS as catalysts in catalytic ozonation for degradation of phenol. Factors affecting phenol removal efficiencies, including Fe and Mn content, catalyst dosage, pH, reaction time, were investigated. Reaction kinetics of catalytic ozonation catalyzed by Fe/WTS and Mn/WTS catalysts were analyzed and compared to that of sole ozonation. The results from this research exhibit achievements of the utilization of Fe/WTS and Mn/WTS catalysts in catalytic ozonation which can be applied to degrade other phenolic compounds containing in aqueous solution.

1.2 Objectives of the study

1.2.1 To prepare Fe and Mn coated on acid modified water treatment sludge for use as catalysts in catalytic ozonation.

1.2.2 To investigate removal efficiency and optimum conditions of as-prepared catalysts in catalytic ozonation for removal of phenol from aqueous solution.

1.2.3 To study the reaction kinetics of catalytic ozonation using Fe/WTS and Mn/WTS catalysts in degradation of phenol.

1.3 Hypotheses

Ferric and manganese coated on acid modified water treatment sludge can be prepared and used in catalytic ozonation process to enhance the performance in degradation of phenol. Hydroxyl radicals ($OH^{\bullet}$) generated from ozone decomposition enhanced by Fe/WTS and Mn/WTS catalysts play important role in degradation of phenol.

1.4 Scopes of the Study

1.4.1 Water treatment sludge (WTS) was collected from filter press of a water treatment plant. The WTS was dried naturally for 7 days.

1.4.2 WTS was modified by phosphoric acid at varying concentrations via hydrothermal method. Acid modified WTS was used as a support for Fe and Mn.

1.4.3 Ferric and manganese were coated on modified WTS by wet impregnation method with varying metal contents of 1, 2, and 3%.

1.4.4 As-prepared catalysts were characterized by XRD, BET, XRF, SEM, SEM-EDX and pH_{pzc}.

1.4.5 Phenol was used as a model pollutant in aqueous solution. Catalytic ozonation for phenol removal was studied by batch experiment. Factors affecting phenol removal efficiency were investigated as follows:

- catalyst type: Fe/WTS, Mn/WTS, and WTS
- % metal doped: 1%, 2%, 3% (wt /wt)
- catalyst dosage: 1, 2, 3 g/L.
- pH: 3, 7, 11
- reaction time: 0-120 min.

1.4.6 Role of $OH^{\bullet}$ in catalytic ozonation was investigated by using *tert*-butanol (TBA) as a radical scavenger.

1.4.7 Reaction kinetic was studied according to experimental data. Rate constants were obtained.

1.5 Benefits of the study

1.5.1 Novel catalysts prepared from acid modified water treatment sludge for the use in catalytic ozonation were obtained.

1.5.2 Removal efficiencies for degradation of phenol by catalytic ozonation using Fe/Mn doped on WTS as catalysts and optimum conditions were explored.

1.5.3 Rate constant of catalytic ozonation using Fe/WTS and Mn/WTS as catalysts in degradation of phenol were accomplished.

1.5.4 Catalytic ozonation using Fe/WTS and Mn/WTS can be applied for treatment of other recalcitrant compounds in wastewater.

CHAPTER 2

Theory and Literature Reviews

2.1 Water treatment sludge

Water treatment sludge (WTS) is by product generated from water treatment process. As shown in Figure 2.1, conventional water treatment process involved coagulation and flocculation, clarification, rapid filtration, and disinfection. The function of coagulant is to purify water by neutralizing the electrical double layer of fine colloids so as to allow agglomeration (Benlalla et al., 2015). Types of coagulants mostly used were aluminum salts (e.g. $Al_2(SO_4)_3.18H_2O$) or iron salts (e.g. $FeCl_3.6H_2O$, $FeCl_2$, $FeSO_4.7H_2O$) (Ahmad et al., 2016). These salts get hydrolyzed in water to form their respective hydroxide precipitates. Colloidal and suspended impurities such as sand, silt, clay, humic particles present in the raw water are removed by charge neutralization, sweep floc mechanism, and adsorption onto hydroxide precipitates (Trinh and Kang, 2011). The hydroxide precipitate along with sand, silt, clay and humic particles removed from the raw water mainly constitute the solids present in the sludge. Moisture content of the wet sludge is generally above 80 wt % (Tantawy et al., 2015). Large amount of sludge or residues are generated during the processing of raw water to clarified water for drinking purpose. The daily inevitable type of waste at water treatment facilities requires proper handling and disposal. In Bangkok, Thailand, it was reported that the amount of water treatment sludge from Metropolitan Waterworks Authority (MWA) has been increasing from 61,320 tonnes/year in 2009 (Wetchasat et al., 2010) to 100,000-120,000 tonnes/year in 2017 (Pumkumarn, 2017). The amount of WTS seems to be increasing year by year because of rapid growth of population leading to high domestic and industrial water consumption as well as the trend of urbanization (Ahmad et al., 2016).

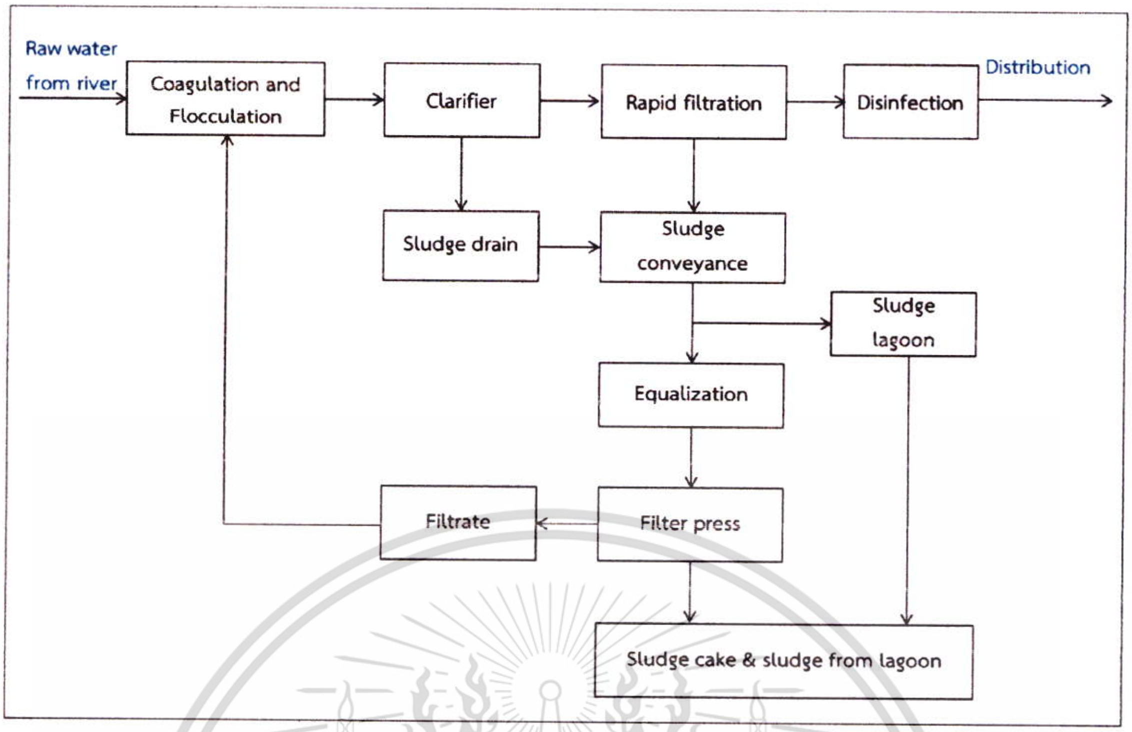

Figure 2.1 Water treatment process and source of water treatment sludge
Source: Adapted from Pumkumarn (2017)

Although WTS was classified as a waste material, this waste included a lot of useful chemical compositions, such as iron, silicon and alumina as listed in Table 2.1 (Kizinievic et al., 2013). Three main components containing in WTS were SiO_2, Al_2O_3 and Fe_2O_3, approximately 70% in total. SiO_2 and Al_2O_3 were parent clay of kaolin clay. The WTS presented a large particle size range (1 to 600 μm), whose median size was about 5 μm. High percentage of fine particles of the WTS was essentially related to the presence of kaolinite (Rodrigues and Holanda, 2015). For this reason, WTS was likely suitable to develop as a catalyst support.

Table 2.1 Composition of water treatment sludge

Component	Percent weight (% wt)			
	Junbuala et al. (2018)	Ahmad et al. (2016)	Abo-El-Enein et al. (2017)	Rodrigues and Holanda (2015)
SiO_2	46.59	52.78	36.51	29.59
Al_2O_3	21.93	14.38	22.21	31.18
Fe_2O_3	8.36	5.20	5.65	10.21
K_2O	2.35	3.62	0.49	1.27
MgO	1.27	3.08	1.34	n/a
TiO_2	0.89	0.61	n/a	1.04
CaO	1.31	4.39	2.66	0.34
Na_2O	0.35	0.97	1.35	n/a
MnO_2	0.33	0.08	n/a	0.14
P_2O_5	0.85	0.17	n/a	n/a
ZnO	n/a	0.01	n/a	0.02
Loss of Ignition (L.O.I)	15.77	n/a	28.10	24.50

2.2 Kaolin

Kaolin, or China clay, is nearly white in color. It is distinguished from other industrial clays based on its fine particle size and pure coloring. Its ability to disperse in water make it an ideal pigment. Kaolin is derived from the mineral kaolinite which comes from the Earth's crust. It is an aluminum silicate represented as Al_2O_3-$2SiO_2$-$2H_2O$, as shown in Figure 2.2. The primary constituent in kaolin is the mineral kaolinite, a hydrous aluminum silicate formed by the decomposition of minerals such as feldspar.

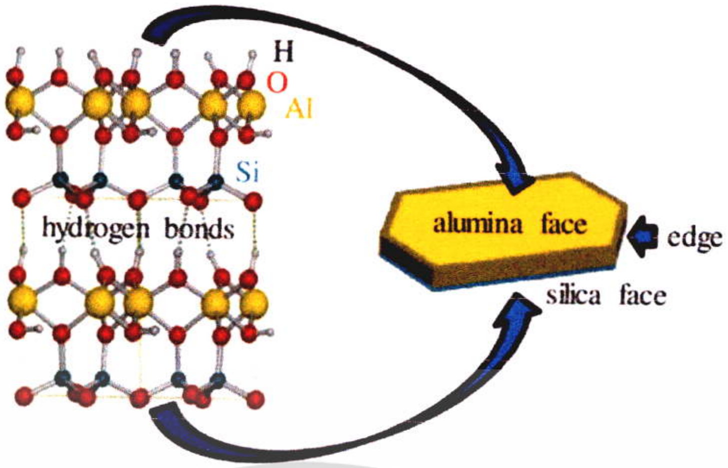

Figure 2.2 Molecular structure of kaolin

Source : Penkavova et al. (2017)

Kaolin employs a very fine particle size with chemical structure of 1:1 layer sheet structured hydrated aluminum silicate with one silicon oxygen (SiO_4) tetrahedral layer and one alumina octahedral layer with pseudo-hexagonal symmetry, bonded together through sharing of apical oxygens (Panda et al., 2010). This kaolin-like compound is one of the mineral clay widely used for a large number of applications, such as in ceramics, paper coating, filling paper, paint extender, rubber filler, plastic filler, cements, or catalysts (Benlalla et al., 2015; Ling et al., 2017; Ling et al., 2018; and Wolff et al., 2015).

Kaolinite displays low reactivity, low adsorption capacity, or small surface area. Several modification processes have been proposed to enhance their adsorption capacities for the removal of contaminants and catalyst support, as well as enlarge their surface area. The two most common methods for modification of clay minerals are thermal treatment and acid activation. These two methods have proven successful for kaolin treatment by causing structural and textural changes in clay minerals that enhance the products' adsorption capacity. Moreover, acid modified clay and thermal treatment have a benefit including easy modification, less chemical usage, and low cost. For this reason, acid modified kaolin was interesting to modify WTS as catalyst support.

2.3 Modification of Clay

Acid activation is a chemical treatment method to improve the surface and catalyst properties. The method involves leaching of the clays with inorganic acid such as hydrochloric, sulfuric, nitric and organic acid such as acetic, citric, oxalic and lactic causing disaggregation of clay particles, elimination of mineral impurities, and dissolution of the external layers to alter the chemical composition and the structure of the clays (Kumar et al., 2013)

The acid treatment is beneficial in terms of increased surface area, porosity, and number of acid center with respect to the parent clay. This high surface area of clays is competitive in different industrial uses and very promising as sorbents or as catalyst supports (Panda et al., 2010). The data in Table 2.2 show the process to produce the acid activated clay via reflux method to avoid evaporation during the experiments (Motlagh et al., 2011). The period of activation was 2-4 h at temperatures of 60-110-° C. Surface area and pore volume of acid activated clay are higher than parent clay because the presence of Al-O-Si bonds at the octahedral layer was attached during acid modification. Moreover, the XRF characterization showed that the proportional of parent clay were changed to increase Si/Al ratio due to the dealumination of acid activated clay can be ascribed to the leaching of the Al^{3+} ions from the octahedral layer because of hydrolysis under acidic condition. (Panda et al., 2010), as shown in Figure 2.3 (Komadel, 2016).

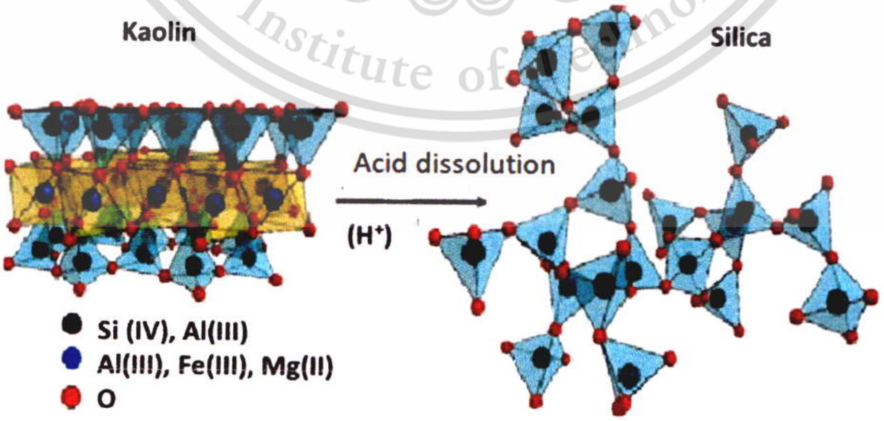

Figure 2.3 Molecular structure of acid modified kaolin

Source: Adapted from Komadel (2016)

The changes in textural and physicochemical properties of acid activated clay are dependent on temperature, time, concentration of acid, and solid to liquid ratio. Table 2.2 summarized the parameters for acid activation by reflux method of different types of clay. The reflux method has been used to synthesize various nanostructured materials such as nanoparticles, nanowires, nanorods, nanostructures. In this method the energy necessary for the reaction is supplied by heating the reaction solution over long periods of time (Figure 2.4 a). Through this method one can control the size, morphology, and crystallinity of the materials by varying parameters such as the reaction time, concentration of precursors and the type of solvent employed (Aditha et al., 2016). Additionally, hydrothermal method can be defined as a method of synthesis of single crystals which depends on the solubility of clay in hot water under high pressure (Figure 2.4 b). The crystal growth is performed in an apparatus consisting of a steel pressure vessel called an autoclave, in which a nutrient is supplied along with water. A temperature gradient is maintained between the opposite ends of the growth chamber. At the hotter end the nutrient solute dissolves, while at the cooler end it is deposited on a seed crystal, growing the desired crystal. Advantages of the hydrothermal method over other types of crystal growth include the ability to create crystalline phases which are not stable at the melting point. Also, materials which have a high vapor pressure near their melting points can be grown by the hydrothermal method. The method is also particularly suitable for the growth of large good-quality crystals while maintaining control over their composition. Disadvantages of the method include the need of expensive autoclaves, and the impossibility of observing the crystal as it grows. For this reason, hydrothermal method was an interesting technique to synthesis acid modified clay. This might growth the crystalline structure of acid clay, leaching aluminum from clay structure to enhance the structure of modified clay for catalyst support.

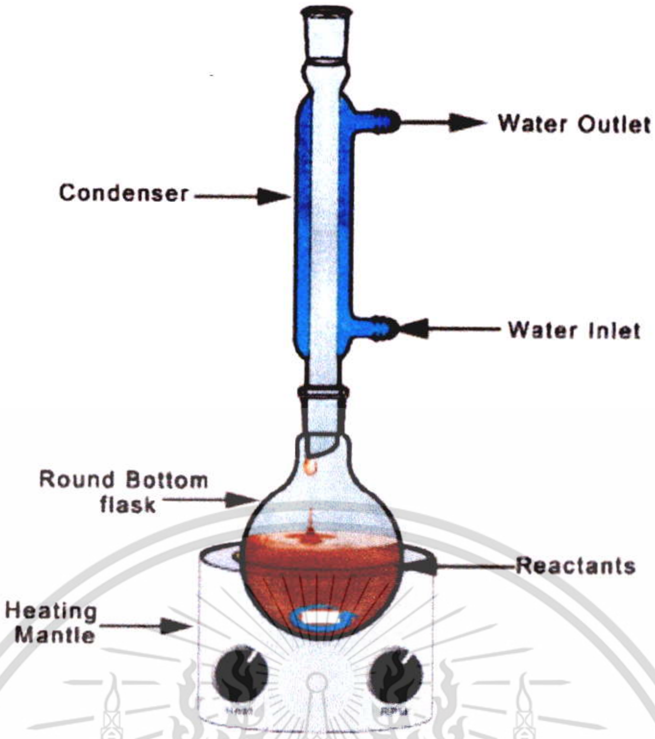

(a) Reflux method

(b) Hydrothermal method

Figure 2.4 Methods for acid activation of clay (a) Reflux method and (b) Hydrothermal method

Source: Aditha et al. (2016) ; Cheng et al. (2016)

Table 2.2 Parameters for acid activation of different types of clay

Type of clay	Type of acid	Process	Conc. (M)	Time (h)	Temp.(°C)	Solid: liquid ratio	References
Kaolin	sulfuric	reflux	1,3,5,10	4	110	1:100	Panda et al (2010)
Kaolin	phosphoric	reflux	5	2	110	1:4	Ayodele et al. (2012)
Kaolin	nitric, hydrochloric, phosphoric, acetic, sodium hydroxide	reflux	3	4		1:100	Kumar et al. (2013)
Smectite	hydrochloric	reflux	2,4.5,7	0.33,2, 3.66	62.85, 79.85, 96.85	1:2.3,1:4, 1:7.3	Rozic et al. (2008)
Kaolin	phosphoric	reflux	5,10	2	110	1:4	Ayodele (2013)
Meta-kaolin	sulfuric	n/a	1	4	90	N/A	Lenarda et al. (2007)
Bentonite	hydrochloric	reflux	2-7	0.34-3.66	63-67	1:2.3-1:7	RoZic et al. (2010)
Water treatment sludge	acetic	heat + stir	0.01-2	4	60	1:10	Vinitnantharat et al. (2010)
Montmorillonite	sulfuric	reflux	1-10	2	80-85	1:20	Angaji et al. (2013)
Bentonite	sulfuric	reflux	2-7	2	80	1:20	Motlagh et al. (2011)

2.4 Metal coated on catalyst support

Metal coated on catalyst support is one type of heterogeneous catalyst. This process aims to push metal to adsorb onto catalyst support surface. The concept of this method is to increase surface area versus weight of metal. This method achieves high surface area per unit volume on the surface of the support. There are several processes to prepare metal coated on catalyst support, some are mentioned herewith in this research.

1) Precipitation

Precipitation method has been widely used for preparation of solid catalyst. Precipitate are generated by adding precipitating agent to a solution of iron salt, and then the precipitate is washed, dried, and calcined under different conditions. Similarly, co-precipitation method uses more kinds of cations, such as Si, Co, Mn, Cu, Ni, and Al, to prepare composite materials. In precipitation method, the types of precipitating agent and their concentrations, precipitation temperature, precipitation pH, stirring speed, and feeding order, have impacts on the properties of the precipitation products. Therefore, the operational conditions are very important and must be optimized.

2) Wet impregnation

Wet impregnation method is one of the most commonly used methods for preparing supported catalysts. The host oxide was immersed into a solution, which contains the required some precursor. After that, the mixture is dried and heated. Size, pore structure, and surface area of products are basically determined by the support. In this method, the active ingredient content of the catalyst is generally low, so the dosage of catalyst is high. This method is usually used for the synthesis of supported Fe-based catalyst, such as Fe_2O_3/Al_2O_3, Pd/FeOOH. X-ray characterization (XRD) is usually used to confirm the composition. The amounts of iron loading depend on impregnation time. This method is easy to operate, but the iron leaching can decrease the catalytic activity.

3) Sol-gel method

In sol-gel method, high chemical active ingredient compounds are used as precursors. Metal salts are mixed in the liquid phase, and the sol system is formed by hydrolysis and condensation reaction. Sol is slowly polymerized among these aging colloidal particles, the three-dimensional network structural gel is formed and finally prepared by drying and sintering. The catalyst prepared by this method is more uniform, but the organic matters used should be removed clearly in case of secondary pollutant entering into water.

4) Thermal decomposition

In thermal decomposition method, the required metal salts are mixed with a suitable organic fuel. Then, the mixture is heated to fire, after the self-sustaining combustion, the products are obtained. The reaction occurs under a high-boiling point container. This method is complex, but the product is well-dispersed and uniform. It can overcome the agglomeration at high temperature. The products have the characteristics of high purity, good dispersion, uniform, no agglomeration, good crystal shape and environmental purification. The process and optimum conditions to prepare catalyst on the support such as activated carbon, acid clay, and metal oxide, are summarized in the Table 2.3.

In this research, in preparation of catalysts on WTS supported, wet impregnation method was proposed. The period of impregnation was in the range from 10 min to 6 h. The temperature of impregnation was 25 to 60 °C. After that calcination process was required to change metal ion to metal oxide which was increase its stable. The period of calcination was 1 to 4 h and the temperature of calcinations was 300 to 700 °C. From the literature review, it is interesting to coat Fe and Mn on the acid modified WTS support by using wet impregnation method and calcination was 550 °C for 2 h.

Table 2.3 Parameters for wet impregnation and calcination in preparation of catalysts on supporting material

Supporting Material	**Process**	**Type of metal**	**Amount of support (g)**	**Metal amount (g)**	**Impregnation**		**Calcination**		**References**
					Temp (°C)	**Time (h)**	**Temp (°C)**	**Time (h)**	
Activated carbon	impregnation	$Mn(NO_3)_2$	n/a	n/a	25	2	n/a	n/a	Wou et al. (2010)
Modified activated carbon	Impregnation by sonicate bath	$Fe(NO_3)_3$	25	100	n/a	n/a	700	1	Farzadkia et al. (2014)
Activated carbon	impregnation	$Cu(NO_3)_3$	10	13.6	55-60	10 min	300	4	Yi-fei et al. (2010)
Modified kaolin	impregnation	$Fe_2C_6O_{12}$	n/a	2	50	6	450	4	Ayodele et al. (2012)
Modified activated carbon	impregnation by sonicate bath	$Fe(NO_3)_3$	25	100	n/a	n/a	700	1	Shahamat et al. (2014)
Modified bauxite	impregnation	$Fe(NO_3)_3$, $Mn(CH_3COO)_2$	0.2 mol/l: 100 ml	n/a	n/a	16	600	4	Qi et al. (2012)
y-Al_2O_3	impregnation	$Mn(CH_3COO)_2$	n/a	10% w of MnO_2	n/a	n/a	500	3	Rosl et al. (2010)

2.5 Ozonation

Ozone is an effective oxidant with a redox potential of 2.07 volts. It can selectively oxidize unsaturated double bonds and aromatic structures (Maddila et al., 2013). Ozonation is very attractive effluent treatment technique as it has the potential to degrade toxic organic compounds, thereby, increasing the biodegradability of the effluent (Jagadevan et al. 2016). Figure 2.6 illustrated the mechanism of ozone reaction. Ozone attacks organic compounds via two mechanisms: (1) direct ozonation by ozone molecules and (2) indirect free radical (or radical type) mechanism involving highly oxidative hydroxyl radical ($OH^{\bullet}$). Ozone molecules can easily degrade aromatic organic pollutants by destructing aromatic ring to form intermediates like small chain carboxylic acids, aldehydes and ketones (Ikhlaq et al., 2014).

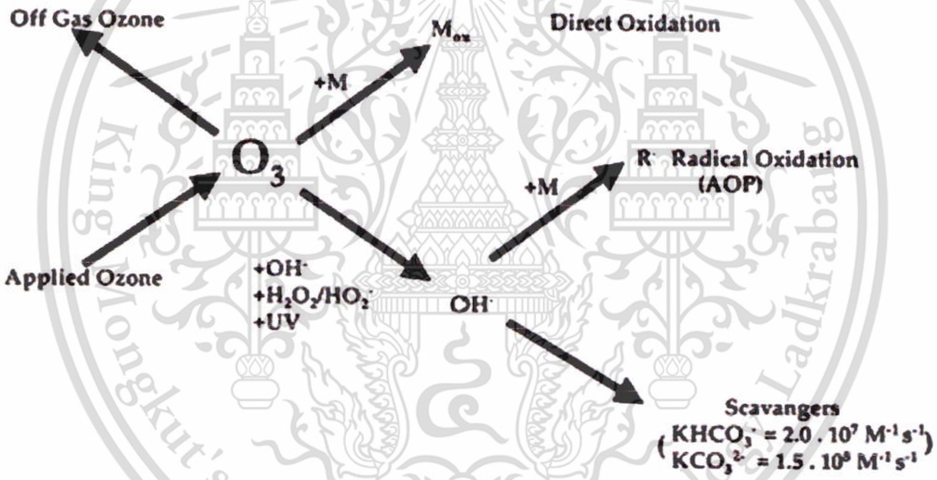

Figure 2.5 Ozone reaction mechanisms in aqueous solution

Source: Adapted from Forero et al. (2001)

Chemical properties of ozone depend on molecular structure of ozone. Two extreme forms of resonance structures of ozone molecule can be expressed as shown in Figure 2.6. Ozone can react as a dipole, an electrophilic or nucleophilic agent. One arm of ozone is plenty of electrons. So, this could act as strong lewis base. As a result of its high reactivity, ozone is very unstable in water. The half-life time of molecular ozone varies from a few seconds up to few minutes and depends on pH, water temperature and concentration of organic and inorganic compounds in water.

However, these intermediates are resistant to ozone attack, thereby, accumulate in the solution. Therefore, direct ozonation mechanism involving the reaction of ozone molecules with the organic pollutant is not sufficient to achieve high degradation efficiency. On the other hand, indirect free radical mechanism achieves high degradation efficiency as in this mechanism; ozone gets transformed into hydroxyl radicals ($OH^{\bullet}$) employing a redox potential of 2.86 volts which is higher oxidation capacity than ozone molecules. The hydroxyl radicals are non-selective in nature and can mineralize all types of organic and inorganic compounds (von Gunten, 2003)

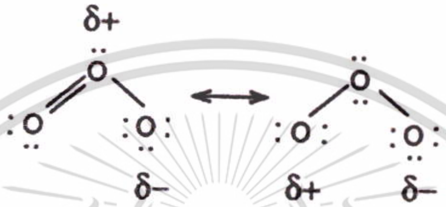

Figure 2.6 Ozone structure

Source: Kasprzyk-Hordern et al. (2003)

However, ozonation also has a limitation of short half-life of ozone which requires continuous generation of ozone, thus, increasing energy consumption and operating cost of the process (Tang et al., 2016). Therefore, it is needed to optimize generation of ozone and its utilization in order to make the effluent treatment process cost attractive. Ozonation in combination with hydrogen peroxide, UV light, or catalyst is used to facilitate generation of hydroxyl radicals which enhances the degradation efficiency and reduces operational time and cost. Recently, ozonation in presence of catalyst, called catalytic ozonation, has emerged as an efficient treatment method for the complete removal of all types of organic matter from the effluent (Wang et al., 2016).

2.6 Catalytic ozonation

Catalytic ozonation has received increasing attention due to its higher effectiveness in the degradation of organic pollutants. Catalytic ozonation is beneficial in enhancing the degradation of refractory organic pollutants present in the effluent. The catalyst in ozonation promotes decomposition of ozone on its surface to produce hydroxyl radicals (Nawrocki and Kasprzyk-Hordern, 2010; Jeirani and Soltan, 2016). Catalytic ozonation is classified into homogeneous and heterogeneous types based on the type of catalysts used in the process. In homogeneous catalytic ozonation, transition metal ions are used to decompose ozone whereas in heterogeneous catalytic ozonation, solid catalysts are employed for ozone decomposition (Ghuge and Saroha, 2018).

2.6.1 Homogeneous catalytic ozonation

In homogeneous catalytic procedure, transition metal ions (Fe^{2+}, Mn^{2+}, Ni^{2+}, Co^{2+}, Cd^{2+}, Cu^{2+}, Ag^{+}, Cr^{2+}, Zn^{2+}) are usually used as the catalysts, to degrade the organic pollutants in water. The Mn^{2+} and Co^{2+} ions had a relatively high catalytic activity but their toxicity limited the application of those ions. On the other hand, ferrous ion is nontoxic and helpful in coagulation stage, so this ion is widely used as catalyst in homogeneous catalytic ozonation (Zeng et al., 2012) Mechanisms of homogeneous catalytic ozonation is based on an ozone decomposition reaction followed by the generation of hydroxyl radicals. The metal ions accelerate the decomposition of ozone to produce the $\bullet O_2$, and then electron of $\bullet O_2^-$ transfer to O_3 to gain $\bullet O_3$, OH• is accepted successfully (Ghuge and Saroha, 2018). Although, homogeneous catalytic ozonation can effectively improve the removal efficiency of organic pollutants in water. Nevertheless, the disadvantage of this technology is to introduce ions and result in the secondary pollutants into effluent leading to not only lead to increase the cost of water treatment, but also high consumption of catalyst (Guo et al., 2012),

2.6.2 Heterogeneous catalytic ozonation

The main catalysts types for the process of heterogeneous catalytic ozonation were metal oxides such as MnO_2, TiO_2, Al_2O_3 and, metals or metal oxides on metal oxide supports such as Cu-Al_2O_3, Cu-TiO_2, Ru-CeO_2, V-O/TiO_2, V-O/silica gel and TiO_2/Al_2O_3, Fe_2O_3/Al_2O_3. The catalytic activity of the catalysts mentioned is mainly based on the catalytic decomposition of ozone and the enhanced generation of hydroxyl radicals. The efficiency of the catalytic ozonation process depends to a great extent on the catalyst and its surface properties as well as the pH of the solution that influences the properties of the surface-active sites and ozone decomposition reactions in aqueous solutions. Kaolin is also used as a catalyst for ozonation in removal of methylene blue. Comparing with ozonation alone, the removal rate is increased from 16.0 to 98.9% and COD reduction increased from 33.3 to 88.36 percent in 10 minutes. (Gau et al., 2009). Water treatment sludge could perform as a catalyst for ozonation. It increased ozone decomposition up to 78.7 percent in 10 minutes. This result is very interesting to investigate the efficiency of water treatment sludge to remove other organic pollutants such as phenol or productive product care (Muruganandham et al.,2007)

Two representative mechanisms of heterogeneous catalytic ozonation are proposed as follows:

(1) Interfacial reaction mechanism. In this mechanism, the main function of catalysts is to act as adsorptive material. First, using its large surface to adsorb and then remove the organic pollutants. Second, provide active adsorptive site and combine with aim molecules to form active complexes with lower activation energy, all of these make the pollutants could be oxidized simply by gaseous ozone and ozone or $OH^•$ in solution. And then, the intermediates can be further oxidized in the surface of catalysts, or desorbed to the aqueous solution to be oxidized by ozone or $OH^•$.

(2) $OH^•$ mechanism. This mechanism proposes that the metal oxide catalysts can increase the solubility of ozone and initiates the ozone decomposition. This mechanism speculates that surface hydroxyl groups of metal oxides play a vital role in the formation of $OH^•$, as shown in Figure 2.7. Soluble ozone in aqueous solution is adsorbed to the surface of the catalyst, a series of radical chain transfer are occurred to generate much $OH^•$, which hold a high oxidation potential and can oxide the organic pollutants in wastewater. The catalytic ozonation system with poor adsorptive ability can be explained by this mechanism, the procedure is shown in Figure 2.8.

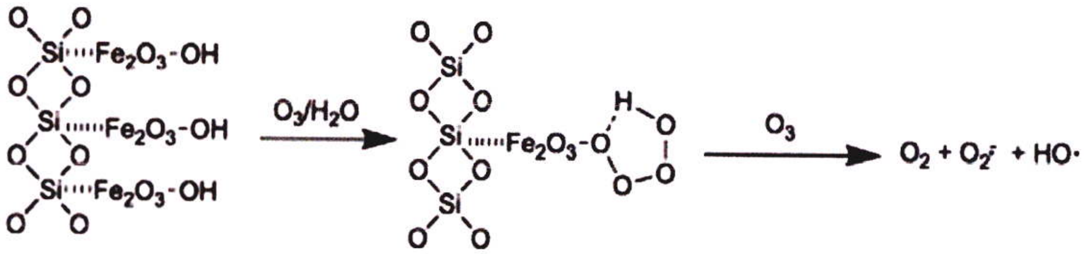

Figure 2.7 Possible mechanisms for the formation of hydroxyl radical

Source: Wang and Bai (2011)

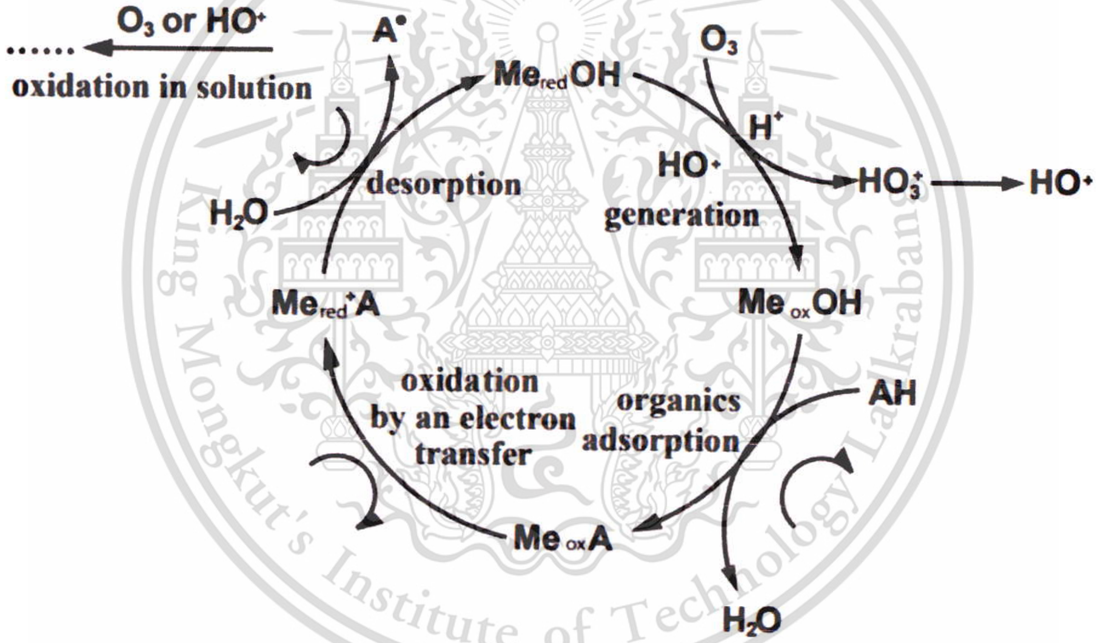

Figure 2.8 Possible mechanisms for $OH^\bullet$ or other radical species generation by reaction of ozone during heterogeneous catalytic ozonation

Source: Gao et al. (2012)

2.7 Phenol

Phenol is colorless or white crystal, with sickly sweet smell and a sharp burning taste. Phenol occurs naturally as coal tar and is formed during decomposition of organic materials (Limsuwan, 2008). Phenol is also used in the production of drugs, weed killers, and synthetic resins. Phenol and its derivatives are present in the wastewaters such as coking, pulp mills, paint and dyes, wine distilleries, oil and gasoline, synthetic rubber, textiles, pharmaceuticals, solvent, manufacture of pesticides, paper and wood (Mungmart et al., 2011). Occupational exposure to phenol has been reported during its production and use of phenolic resins in the wood product industry. Toxic organic contaminants such as heterocyclic and phenolic compounds, presenting environmental risks should be eliminated before discharge into natural water bodies. Concentrations of phenol and its products in municipal wastewater vary from trace quantities up to 1000 µg/l. There have been reports of toxic organic compounds remaining in trace quantities (µg/l) in treated effluent of many wastewater treatment plants. It is noted that the phenolic compounds contamination in drinking water at a concentration of 1 µg/l cause significant taste and odor problems making it unfit for use (Turhan and Uzman., 2008). The acceptable phenolic compound concentration must be controlled at the industrial effluent standard (1 mg/L). Physical and chemical properties of phenol are shown in Table 2.4.

Treatment of aqueous effluents polluted with phenol and phenolic species is attended due to toxicity and low biodegradability of these organic compounds. In chemical industries, phenolic compounds are very difficult to be treated by conventional treatment methods, such as activated sludge digestion, solvent extraction, chemical treatment, adsorption (Mohammadi et al., 2014). The possible processes for phenol removal according to its initial concentration are listed in Table 2.5.

Table 2.4 Physical and chemical properties of phenol

Properties	Value/Characteristic
1. Chemical name	Phenol
2. Synonym	Benzenol, Phenyl hydrate, Phenel alcohol, monophenol, Phenelic acid
3. Chemical formula	C_6H_6O
4. Chemical structure	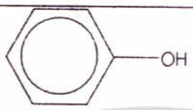
5. Molecular weight	94.11
6. Appearance	Colorless to light pink
8. Boiling point	181.87 °C
9. Melting point	40.89 °C
10. Vapor pressure	0.35 mmHg at 35 °C
11. Odor	Distinct aromatic, somewhat sickening, sweet and acrid odor
12. Vapor density	3.24 (Air = 1)
14. Log K_{ow}	1.46
15. Log K_{oc}	1.21-1.96
16. Solubility in water 20^0C	8.28 g/100 mL
17. Henry's law constant	3.0×10^{-7} atm.m^3/mol

Source: Adapted from Turhan and Uzman (2008)

Table 2.5 Categorization of phenol removal methods based on initial concentration

Concentration range	Concentration (mg/L)	Technique
High Concentration	As high as 15,000	Thermal decomposition
	Up to 10,000	Membrane pervaporation
	Over 3,000-6,000	Liquid liquid extraction
	Over 5,000	Membrane based solvent extraction
	Up to 4,000	Adsorption
Medium Concentration	300 - 3,000	Adsorption/ Wet air oxidation/ Catalytic wet air oxidation/ Emulsion liquid membrane/ Distillation
	0.5 - 750	Reverse Osmosis/Nano Filtration
	20 - 500	Liquid-liquid extraction
Low Concentration	10 - 90	Solid Phase Extraction
	50	Chemical oxidation/ Photocatalytic oxidation/ Ozonation
	Less than 50	Biodegradation

Source: Adapted from Mohammadi et al. (2013)

2.8 Literature reviews

Li et al. (2018) synthesized Fe-MCM-48 catalyst via hydrothermal method, and the mineralization efficiency of diclofenac (DCF) by Fe-MCM-48/O_3. Characterizations of catalyst revealed that Fe existed in the framework of MCM-48. Regarding to mineralization efficiency, the addition of Fe-MCM-48 significantly increased total organic carbon (TOC) removal, up to 49.9%. TOC were removed through the Fe-MCM-48/O_3 process at 60 min, which was 2.0 times higher than that in sole ozonation. DCF removal in the Fe-MCM-48/O_3 process was primarily based on ozone direct oxidation. The improvement of mineralization efficiency was attributed to the function of generated hydroxyl radicals ($OH^{\bullet}$), which indicated that the presence of Fe-MCM-48 accelerated ozone decomposition. Moreover, the negatively charged surface of Fe-MCM-48 and the proper pH value of the DCF solution played an essential role in hydroxyl radical generation.

Chen et al. (2017) studied the degradation of norfloxacin by MnOx/SBA-15/O3 process. The prepared catalyst possessed a large surface area ranging from 405 to 671 m^2 g^{-1}. The loaded MnOx on SBA-15 successfully increased its adsorption ability and catalytic activity, and its surface property played an important role in catalytic process. Both O_3 and MnOx/SBA-15/O_3 systems were effective for norfloxacin removal. A high mineralization efficiency (54%) was achieved by MnOx/SBA-15/O_3 process at 60 min, 1.36 times higher than that of single ozonation process. The protonated surface hydroxyl groups were the main reaction sites. Oxalic acid, formic acid, acetic acid were detected, and the concentration of oxalic acid in MnOx/SBA-15/O_3 process was lower than that in sole ozonation process because more hydroxyl radical was generated in catalytic ozonation.

Chen et al. (2016) studied degradation of diclofenac (DCF) in Fe-MCM-41/O_3 process. High mineralization efficiency (76.3%) was achieved in Fe-MCM-41/O_3 process, which was 2.8 times higher than sole ozonation. Hydroxyl radicals were found to be the main active species. Formic acid, acetic acid, oxalic acid were also detected and their accumulation in catalytic ozonation process was less than that in ozonation as a result of more generation of hydroxyl radical. Small molecular carboxylic acids accounted for 70% of the remaining TOC in catalytic ozonation process, only 32.5% in sole ozonation process. The intermediates accumulated in the first 15 min were more toxic than its initial status. It had a high level of detoxification after 30 min treatment.

Sun et al. (2015) investigated the catalytic ability of MnOx/SBA-15 for the ozonation of clofibric acid (CA) and its reaction mechanism. Compared with ozonation alone, the degradation of CA was barely enhanced, while the removal of TOC was significantly improved by catalytic ozonation (O_3/MnOx/SBA-15). The more remarkably inhibition effect of sodium bisulfite ($NaHSO_3$) on the removal of TOC in catalytic ozonation than in ozonation alone elucidated that MnOx/SBA-15 facilitated the generation of hydroxyl radicals ($OH^{\bullet}$), which was further verified by electron spin-resonance spectroscopy (ESR). Highly dispersed MnOx on SBA-15 were believed to be the main active component in MnOx/SBA-15. Some intermediates were identified and different degradation routes of CA were proposed in both ozonation alone and catalytic ozonation. The amounts of small molecular carboxylic acids (i.e., formic acid (FA), acetic acid (AA) and oxalic acid (OA) generated in catalytic ozonation were lower than in ozonation alone, resulting from the generation of more $OH^{\bullet}$.

Qi et al. (2012) studied the efficiency and mechanism of catalytic ozonation of 2,4,6-trichloroanisole (TCA) by metal oxide modified bauxite. TCA was effectively degraded by catalytic ozonation in the presence of iron- or manganese-modified bauxite (IMB or MMB). The effect of water pH on catalytic ozonation indicated that surface property was the key factor that influenced the activity of catalyst. Results of both catalytic ozone decomposition and radical scavengers experiments indicated that catalytic ozonation by IMB or MMB followed a hydroxyl radical reaction pathway. The main reaction pathway was proposed that adsorption of both ozone and TCA in the micropores and subsequent interaction (direct and indirect oxidation) between them that was confirmed by the analysis of the surface pore volume and surface hydroxyl groups, being followed by the diffusion of ozone and TCA on the mesoporous surface, in which surface hydroxyl groups covering mesoporous surface-initiated ozone decomposition to generate $OH^{\bullet}$, resulted in TCA degradation.

CHAPTER 3

Research Methodology

3.1 Chemical and Instruments

3.1.1 Apparatus and Instruments

1) pH meter (Lab 850, Schott, Singapore)

2) Hot air oven (Din 40050, Memmert, Germany)

3) Furnace (Type 48000, Thermolyne, Germany)

4) Ozone generator

5) Air compressor (model BM-25, Automatic max, China)

6) X-ray diffractometer (XRD a Philips X-Pert-MPD X-ray diffractometer with Cu Kα radiation, UK)

7) X-ray fluorescence (XRF: Horiba XGT-2000W, Germany)

8) Scanning electron microscope (SEM: JSM-6355 FE, JEOL Japan)

9) Scanning electron microscopy with energy dispersive X-ray spectroscopy (SEM-EDX : SEM-EDS: Philips XL 30 series USA)

10) Brunauer - Emmett-Teller (BET) (Autosorb-1 Chrantachrome, BEL model)

11) Scanning Electron Microscope (SEM-EDS XL 30 series, Philips, USA.)

12) Inductively Couple Plasma Optical Emission Spectrometer (ICP-OES (PerkinElmer: Avio 200)

3.1.2 Chemicals

1) 4-Amino antipyrine (AR grade, Fluka)

2) Ferrous cyanide (AR grade, Ajax)

3) Ferrous nitrate (AR grade, Ajax)

4) Manganese nitrate (AR grade, Panrac)

5) Phenol (AR grade, Panrac)

6) Phosphoric acid (AR grade, Ajax)

7) Potassium Iodide (AR grade, Ajax)

8) Sodium hydroxide (AR grade, Merck)

9) Sodium thiosulfate (AR grade, Ajax)

10) Sulfuric acid (AR grade, Scharlau)

3.2 Experimental Setup

The overall scope of the experiments is shown in Figure 3.1. The experiments were divided into 3 phases including 1) preparation of Fe and Mn catalysts coated on modified water treatment sludge 2) investigating the efficiency of catalytic ozonation on removal of phenol by batch operation and 3) study of reaction kinetics on degradation of phenol by catalytic ozonation.

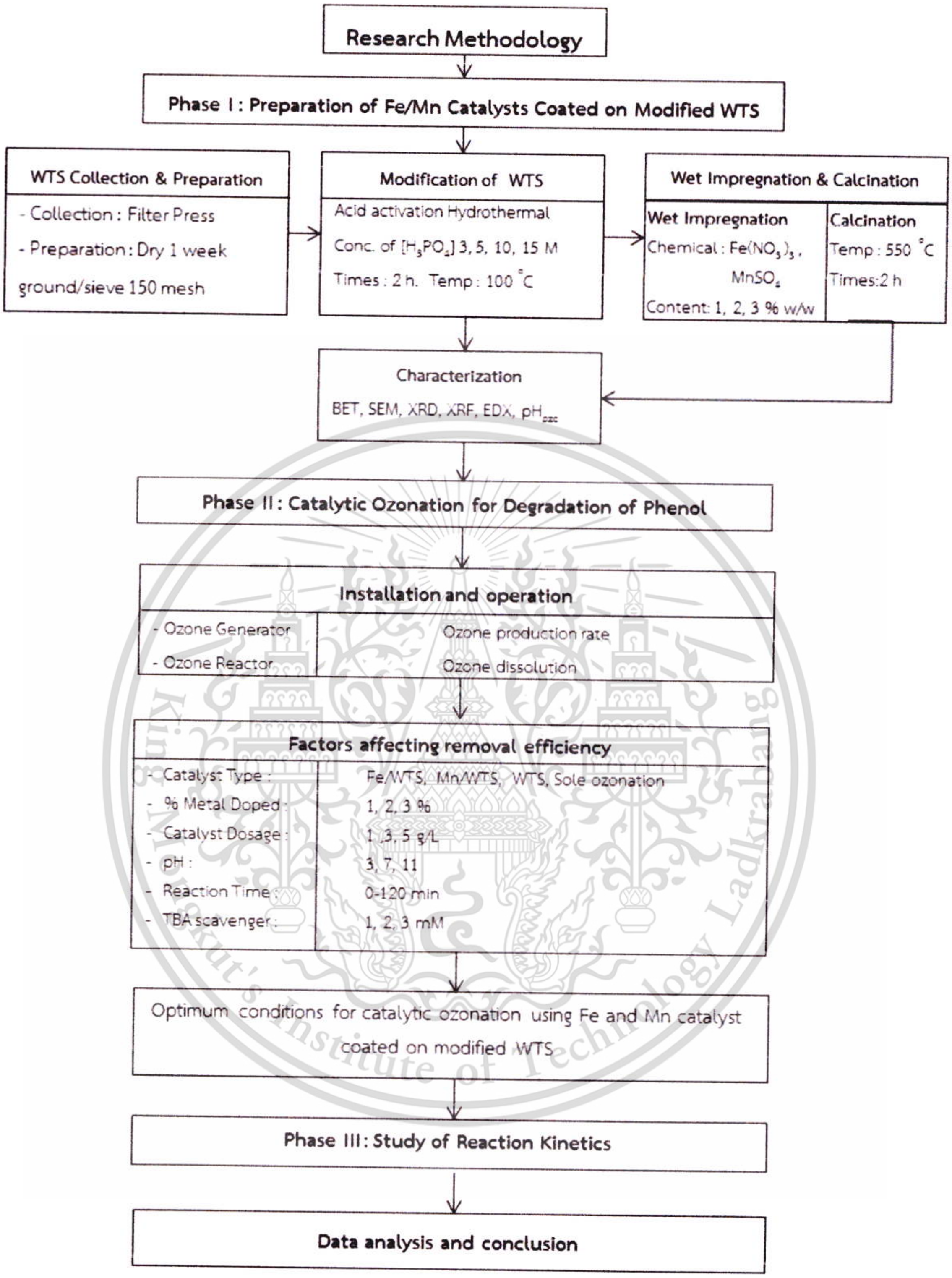

Figure 3.1 Flow diagram of the study

3.2.1 Preparation of Fe and Mn catalyst supported on modified water treatment sludge

1) Source of water treatment sludge

Water treatment sludge used in the experiment was collected from filter press of a water treatment plant in Bangkok. Sludge cake from the filter press was designed as WTS sample. The sample was dried naturally for 7 days, then grounded and sieved with 150-mesh screen. The sieved sample was kept in desiccator before use. The samples were characterized by XRD, XRF, BET, SEM, ICP and pH_{pzc}.

2) Acid activation

Acid activation was carried out by adding 10 g of WTS sample to phosphoric acid solution at the different concentrations. The slurry was equipped by hydrothermal method at temperature of 100 °C for 2h. The reaction was immediately quenched by adding iced water followed by centrifugation and repeated washing with RO water to remove any unspent acid for several times. The resulting clay was dried in an oven at 60 °C for 16 h., then grinded with a mortar to be powder. The acid modified water treatment sludge was characterized by XRD, XRF, BET, SEM, SEM-EDX, and pH_{pzc}.

3) Fe/Mn catalyst coated on modified WTS

Fe/Mn catalysts coated on modified WTS were prepared by wet impregnation method. The concentration of Fe and Mn on acid activated clay was varied with % metal content on catalysts at 1, 2, 3 % (w/w) using ferric nitrate and manganese sulfate, respectively. Solid samples were dried at 60 °C for 16 h. before calcination. The samples were calcined at 550 °C for 2 h. The catalysts were characterized by XRD, BET, XRF, SEM-EDX, and pH_{zpc}. The catalyst powder was cooled at room temperature and kept in desciccator prior to used.

3.2.2 Characterization of as-prepared catalysts

1) X-ray diffraction

X-ray diffraction (XRD) analysis was employed in order to identify the phases present in the catalysts and to determine their crystallinity. The XRD patterns were recorded on a Bruker D_8 advance diffractometer using nickel-filtered Cu Kα (0.15418 nm) radiation with 40 mA and 40 kV. The data were collected over 2θ range of 20 –

80° with a 0.02° step size and using a counting time of 1s per point. The signal intensity versus refraction angle was recorded.

2) Brunauer-Emmett-Teller (BET)

BET surface areas were obtained by N_2 adsorption on a Micromeritics Gemini 2360 instrument. Prior to analysis, the sample of about 0.100 g was degassed to remove moisture and contaminants under nitrogen gas flow at 150°C for 3 h. Then, surface area was analyzed with surface analyzer while nitrogen gas flowed constantly through the sample at -196 ˚C

3) X-ray fluorescence spectrometer (XRF)

The elemental analyses of metal components including Si, Al, Fe, and Mn in catalysts were determined by the X-ray fluorescence spectroscopy technique, by means of an energy-dispersive XRF spectrometer equipped with the liquid nitrogen-cooled Si (Li) detector. The AXIL software package was used for spectral deconvolution and for the calculation of the components.

4) Scanning electron microscopy with energy dispersive X-ray spectroscopy (SEM-EDX)

The EDX technique detects X-rays emitted from the sample during bombardment by an electron beam to characterize the elemental composition of the analyzed volume. Features or phases as small as 1 µm or less can be analyzed. When the sample was bombarded by the SEM's electron beam, electrons were ejected from the atoms comprising the sample's surface. The resulting electron vacancies were filled by electrons from a higher state, and an X-ray was emitted to balance the energy difference between the two electrons' states. The X-ray energy was characteristic of the element from which it was emitted.

5) pH_{pzc}

To measure pH_{pzc}, standard test for pH of soil (ASTM D4972) was conducted. Sample of 1 g/L was added to 0.005 M $CaCl_2$. The pH was adjusted to 5, 6, 7, 8, 9 (± 0.1 pH units) with 0.1 M HNO_3 and/or 0.1 M NaOH as needed in each sample. Then the samples were shaken for 24 h in a revolving shaker to reach equilibrium. After this time each resulting pH was measured and the initial pH (pH_o) vs. the difference between the initial and final pH values (pH) was plotted (Yang et al., 2004).

6) Metal content in catalyst support

Solid sample of 0.1 g was digested by 20 mL of 1% nitric acid at 200°C for 2.5 h. Then, solution was filtrated and analyzed by ICP-MS. Percent abundance of metals on acid modified WTS was determined on the basis of mass balance.

7) Leaching test

To determine the possibility of Fe and Mn leaching out from the modified WTS, leaching extraction test was conducted according to the EPA standard method for soil extraction (EPA Method 3050B) (EPA, 1996). Solid sample of 10 g with RO water of 100 mL was shaken for 24h. Then, 1 mL of solution was digested by added 20 mL of 1% nitric acid at 200°C for 2.5h. Then, solution was filtrated and analyzed by ICP-MS.

3.2.3 Installation and Operation

1) Ozone generator

Ozonation generator consisted of 10 corona discharges using to generate ozone in the experiment. This method has been widely used as it produced a high ozone concentration for the applied electrical energy.

2) Ozone reactor

Ozone reactor was designed as an ideal fluidized bed reactor integrated with ideal plug flow. The reactor made of acrylic employed diameter of 10 cm with 60 cm height. The total volume of reactor was 2.7 L. The schematic of catalytic reactor is shown in Figure 3.2.

3) System installation and operation

Ozonation system was operated in an ambient temperature. Ozone was produced by ozone generator supplied with dry air generated by air compressor. Dry compressed air at a flow rate of 5 L/min was used to provide oxygen gas as a raw material for ozone production. In the experiment of phenol degradation by sole ozonation, the reactor was filled with 2.7 liter phenol solution at initial concentration of 50 mg/L. Ozone gas was fed into the reactor through gas diffusers.. In catalytic ozonation processes, as-prepared catalyst, i.e. FE/WTS, Mn/WTS, or WTS, was filled in the reactor. The catalyst was mixed simultaneously using ozone bubbles. Unreacted ozone was trapped by 2% potassium iodide (KI) solution containing in two gas absorption bottles in series, as shown in Figure 3.3.

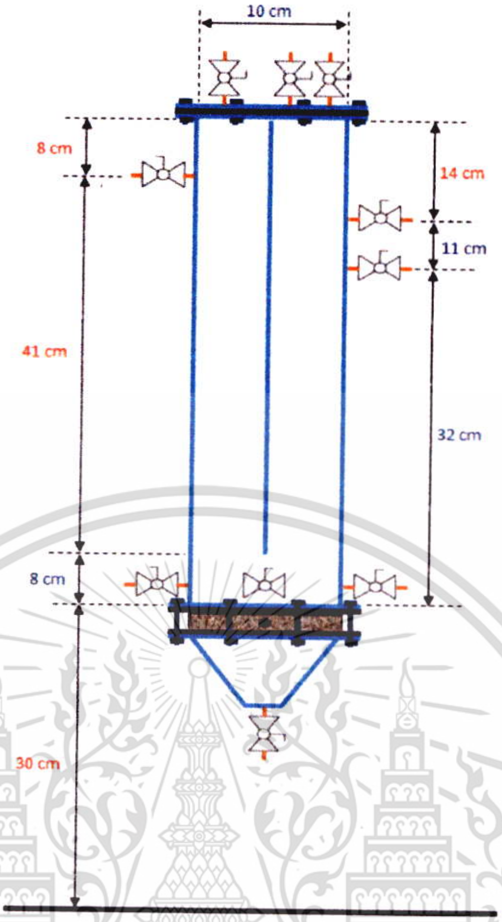

Figure 3.2 Schematic diagram of ozone reactor

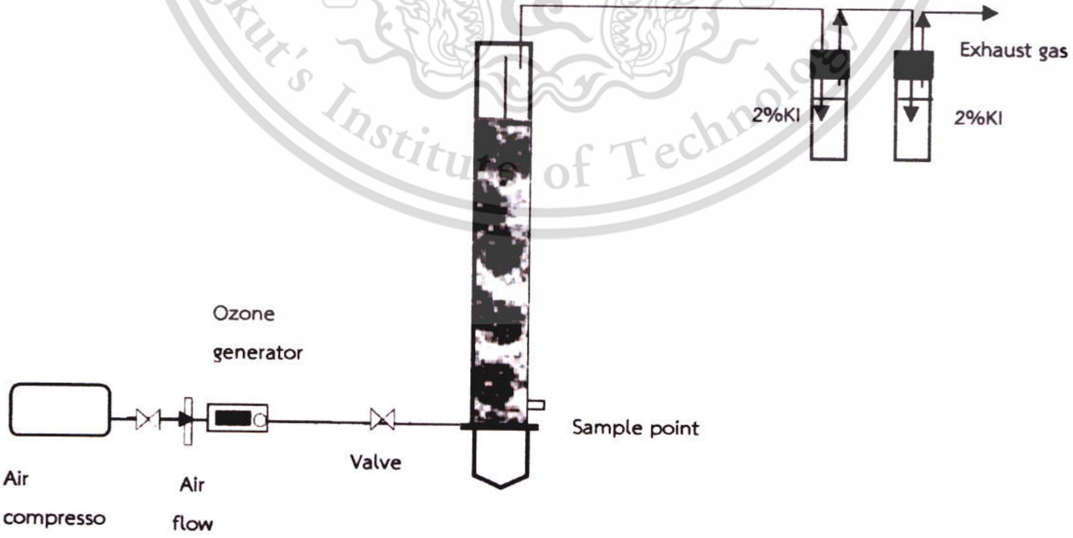

Figure 3.3 Schematic diagram of catalytic ozonation system

4) Measurement of ozone production rate

Ozone concentration in the gas phase was determined by iodometric method By using 2% potassium iodide (APHA, 1998). Ozone produced was transferred to react with KI directly. The iodide liberated was then treated with 0.2 M sodium thiosulfate redundant solution. The stoichiometric of the chemical reaction between ozone and potassium iodide is shown by Eq.3.1.

The reaction of ozone and potassium iodide

$$O_3 + 2I^- + H_2O \rightarrow I_2 + O_2 + 2OH^- \qquad (3.1)$$

The released iodine is titrated with sodium thiosulfate as shown in Eq. 3.2.

$$I_2 + 2S_2O_3^{2-} \rightarrow 2I^- + S_4O_6^{2-} \qquad (3.2)$$

3.2.4 Study of catalytic ozonation for degradation of phenol

1) Source of wastewater

Synthetic wastewater was used as source of wastewater in this study. It was prepared from phenol with an initial concentration of 50 mg/L. Phenol was analyzed by colorimetric by using 4-amino antipyrine in formation of phenol complex, then determined by UV-Vis spectrophotometer at a wavelength of 510 nm (Li et al., 2018).

2) Effect of pH

Catalytic ozonation was performed in the reactor at ambient temperature (26-27 °C). Ozone was produced by ozone generator supplied with dry air by an air compressor at a flow rate of 5 L/min. Phenol solution at initial concentration of 50 mg/L was filled in the reactor. To study the effect of pH, the pH of solution was varied at 3, 7, and 11. As-prepared catalyst, i.e. Fe/WTS, Mn/WTS, or WTS was filled in the reactor. The following parameters were kept controlled, i.e. catalyst dosage of 1 g/L, metal content of 1% (w/w). Aliquoted samples of 20 mL were taken from the reactor at certain time interval up to 120 minutes. For phenol analysis, each sample was spiked with 0.025M sodium thiosulfate ($Na_2S_2O_3$) to quench any residual ozone and stop the reaction between ozone and phenol. The experiments were performed in triplicates. Data presenting in figures and tables were average values calculated from three initial values.

Control experiments were conducted simultaneously with catalytic ozonation experiments at the same conditions. One was sole ozonation of which catalyst was excluded from the protocol. Another control experiment was conducted by adding each type of catalyst into the reactor and then feeding compressed air instead of ozone gas.

3) Effect of catalyst dosage

The catalysts including Fe/WTS, Mn/WTS, and WTS, were investigated. Catalyst dosage was varied at 1, 3, and 5 g/L during catalytic ozonation experiments. The following parameters were controlled, i.e. phenol concentration of 50 mg/L, solution pH of 11, and metal content of 1% (w/w). The experiments were conducted at the same protocol as mentioned earlier.

4) Effect of metal content

The effect of metal content in each type of catalyst including Fe/WTS and Mn/WTS was investigated. Metal content was varied at 1, 2 and 3 % (w/w). The following parameters were controlled, i.e. phenol concentration of 50 mg/L, solution pH of 11, catalyst dosages at optimum values obtained from previous study. The experiments were conducted at the same protocol as mentioned earlier.

5) Effect of *tert*-butanol

Effect of tert-butanol (TBA) as a radical scavenger was investigated. The optimum conditions from previous studies were used in this study. *Tert*-butanol (TBA) was used as a radical scavenger at varied concentrations of 1, 2 and 3 mM. The following parameters were controlled, i.e. phenol concentration of 50 mg/L, solution pH of 11, metal content of 1%, and catalyst dosages at optimum values obtained from previous study. The experiments were conducted at the same protocol as mentioned earlier.

3.2.5 Determination of apparent kinetics

The reaction between ozone and phenol can be described by direct or indirect reaction, i.e. through the reaction with O_3 or $OH^{\bullet}$. Degradation of phenol can be described by the following reactions (Eqs. 3.3-3.4):

$$[O_3] + [\text{Phenol}] \longrightarrow k_{O3}\,P \qquad (3.3)$$

$$[OH^{\bullet}] + [\text{Phenol}] \longrightarrow k_{OH\bullet}\,P \qquad (3.4)$$

The degradation rate of phenol in both ozonation and catalytic ozonation by Fe/WTS can be expressed in Eq. 3.5.

$$-\frac{d[phenol]}{dt} = k_{o_3}[O_3][phenol] + k_{OH\bullet}[\mathrm{OH}\bullet][phenol] \quad (3.5)$$

where k_{o3} and $k_{OH\bullet}$ are constants for ozone and $OH^\bullet$ reacting with phenol, respectively. Eq 3.5 can be transformed to Eq. 3.6.

$$-\frac{d[phenol]}{dt} = (k_{o_3}[O_3] + k_{\cdot OH}[\cdot OH])[phenol] \quad (3.6)$$

By defining, Eq 4.16 can be transformed to Eqs. 3.7 and 3.8.

$$k_{obs} = k_{o_3}[O_3] + k_{\cdot OH}[\cdot OH] \quad (3.7)$$

$$-\frac{d[phenol]}{dt} = k_{obs}[phenol] \quad (3.8)$$

To determine apparent kinetics (k_{obs}) of catalytic ozonation reaction using different catalysts, i.e. including Fe/WTS, Mn/WTS, and WTS, in removal of phenol, the above-mentioned approaches were conducted. The optimum conditions obtained from batch study were used. The samples were collected at 0, 5, 10, 15, 30, 60, 90, and 120 minutes for determination of phenol concentration. Plots of Ln $[C]/[C_0]$ versus reaction time of the sole ozonation and catalytic ozonation by Fe/WTS, Mn/WTS and WTS. A good linear fit was observed for pseudo first order for each catalyst. Apparent kinetics (k_{obs}) were obtained by determination of slope.

3.2.6 Statistical analysis

The experiments were performed in triplicates. Data presenting in figures and tables were average values calculated from three initial values. The difference among group means of experimental data sets were analyzed by analysis of variance (ANOVA) test. That performed by p-value with 95% confidence level.

CHAPTER 4

Results and Discussion

4.1 Characterization of WTS and modified WTS

WTS and modified WTS were characterized by XRD, XRF, SEM, and BET.

4.1.1 XRD analysis

The types of phases that occurred in the water treatment sludge materials due to acid treatment were studied using X-ray diffraction technique. Figure 4.1 shows the XRD profiles of untreated and acid treated water treatment sludge powders. All patterns of water treatment sludge powders show well defined reflections at the 2 theta degree values of 21° and 27° (corresponding to the reflection form [0 0 1] (Panda et al., 2010) which are typical characteristic peaks of kaolinite ($Al_2Si_2O_5$) and quartz (SiO_2), respectively (Ling et al., 2018 : Panda et al.,2010). Again, the peaks corresponding to the 2theta degree values at 34-36, 38-42, 49-51, 61-63, 69-71^{O} are characteristics for kaolinite, hematite (Fe_2O_3), kaolinite, kaolinite, and quartz, respectively (Ling et al., 2017). Upon acid treatment the peak intensity of the water treatment sludge was found to increase progressively. This is due to the structural order of phases (kaolinite and quartz) that occurred owing to the acid treatment, which affects the crystallinity of the sludge. Since activation is quite severe in this acidic strength, the layered structure of the water treatment sludge integrates to give a crystal phase.

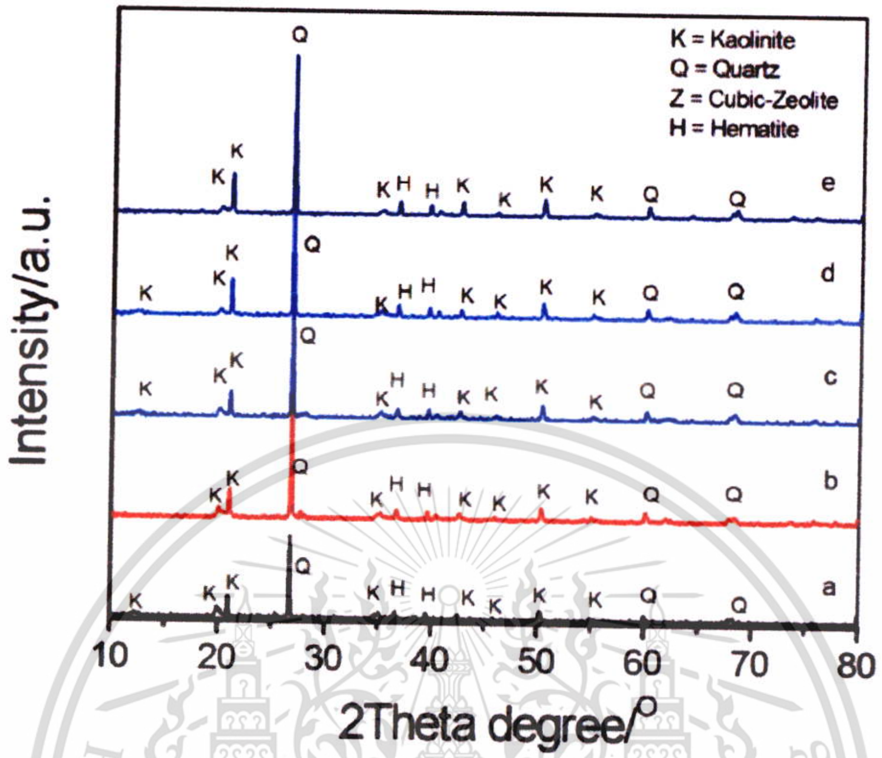

Figure 4.1. XRD patterns of WTS and acid modified WTS. (a) WTS, (b) 3M-acid modified WTS, (c) 5M-acid modified WTS, (d) 10M-acid modified WTS, and (e) 15M-acid modified WTS

4.1.2 XRF and BET analysis

XRF analysis was carried out to determine chemical compositions of WTS and acid modified WTS. While BET analysis provided specific surface area of the tested materials. Table 4.1 exhibited the results from XRF and BET analyses of WTS and WTS activated with different concentration of phosphate acid. The table shows that silica was major constituents in all tasted materials. WTS contained high fraction of Al as aluminum sulfate was used during coagulation and flocculation processes of water treatment. Iron of 10.4% found in WTS possibly due to the iron from the earth.

Table 4.1 XRF and BET analyses of WTS and acid modified WTS

Material	Component content (%)								BET surface area (m^2/g)
	SiO_2	Al_2O_3	Fe_2O_3	K_2O	CaO	MgO	TiO_2	P_2O_5	
WTS	49.90	24.40	10.40	3.17	2.02	1.52	1.50	0.55	37.37
3M H_3PO_4 modified WTS	62.3	21.8	4.62	3.32	0.21	1.08	1.60	1.76	114.42
5M H_3PO_4 modified WTS	65.0	17.3	2.97	3.59	0.17	0.98	1.83	0.95	150.07
10M H_3PO_4 modified WTS	67.3	13.6	3.01	3.69	0.15	0.84	1.57	4.25	147.63
15M H_3PO_4 modified WTS	69.6	11.5	3.27	2.76	0.16	0.68	1.54	5.63	131.01

Acid activation using H_3PO_4, considerable changes in the composition of modified WTS were observed. As the strength of the acid increased, Al, Fe, Mg, and Ca fraction in the acid modified WTS. The XRF results clearly showed that acid activation caused leaching these metals out of WTS structure. The parent water treatment sludge contains silica and alumina which are in major quantities where as other oxides of iron, potassium, calcium, magnesium and titanium and phosphorus are present in trace amounts (Ling et al., 2018: Ling et al., 2017). After phosphoric acid activation, considerable changes in the composition of water treatment sludge were observed. As the strength of the acid increases the Al_2O_3, Fe_2O_3, MgO, and CaO contents in the acid treated material decrease while the SiO_2 and P_2O_5 contents increase. The TiO_2 and K_2O contents were slightly change. The Al_2O_3 and MgO contents in the acid treated material decrease progressively with increasing acid strength but Fe_2O_3 content decrease with the acid treated sludge between 3-5 M and increase when 10-15 M. Simultaneously, the CaO content in the acid treated sludge decreased slightly with increasing acid strength of 3-15 M, which indicated that acid strength did not affect this metal. The fraction of SiO_2 was found to increase from 49.90% to 71.00% while Al_2O_3 fraction clearly decreased from 24.40% to 17.30%, which indicated that acid treatment increased the Si/Al ratio from 2.04 to 4.10. The XRF results clearly indicate that phosphoric acid strength have affected on leaching metal of water treatment sludge, which may be useful to specific applications.

BET surface area of WTS was 37.37 m^2/g. When increased acid strength from 3 M to 5 M, BET surface area of modified WTS increased while added phosphoric acid to 10M and 15 M, BET surface area was decreased, which is summarized in Table 4.1. Upon 3 M phosphoric acid treatment, the new surface area of the original material is three times and the highest surface area is four times when acid strength is 5 M phosphoric acid. However, there are slightly decreased surface areas when increased acid strength to 10 and 15 M phosphoric acid. These phenomena might be the parent water treatment sludge was destroyed porosity by high acid strength, which may be corresponded to higher crystallinity that revealed by XRD results.

4.1.3 SEM analysis

Scanning electron micrographs illustrated the morphological treatment of the WTS and acid modified WTS, as presented in Figure 4.2 (a-e). The SEM micrograph of WTS and acid modified WTS revealed the presence of large particles that appeared to have been formed by several flaky particles stacked together to form of agglomerates. The SEM image of 3, 5, 10, and 15 M phosphoric acid treated show different particle morphology. The micrographs of 3 and 5 M acid phosphoric treated indicate the disaggregation and decreasing in size of sludge structure on acid treatment. At 10 and 15 M of phosphoric acid treatment show well-bonded aggregates rather than detached particles. Regarding to characterization of acid modified WTS, it was found that 5 M phosphoric acid treated WTS had the highest BET surface area which was suitable for further study as catalyst support. For this reason, modified WTS with 5M H_3PO_4 was chosen to use as catalyst support in further study.

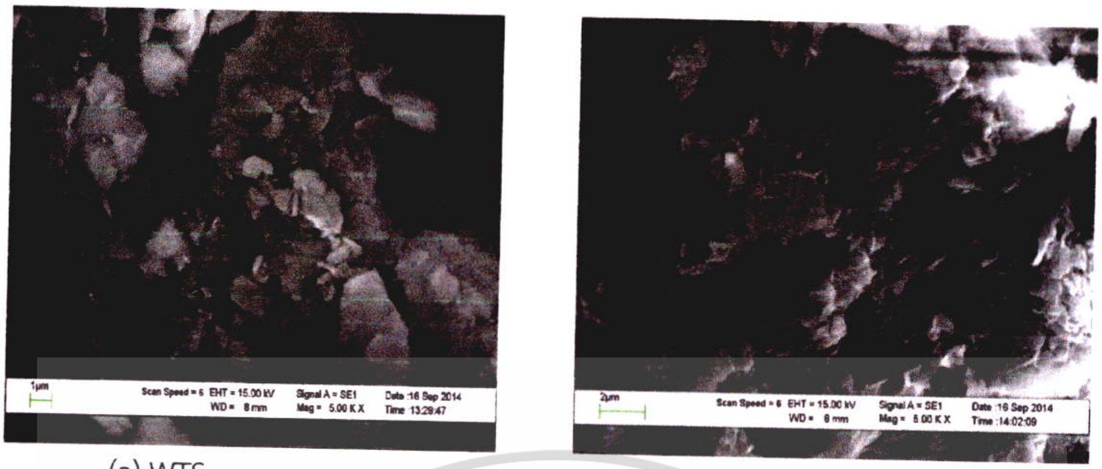

(a) WTS

(b) 3M H_3PO_4 modified WTS

(c) 5 M H_3PO_4 modified WTS

(d) 10M H_3PO_4 modified WTS

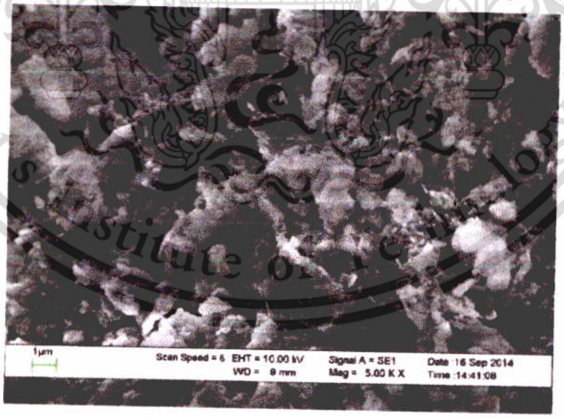

(e) 15M H_3PO_4 modified WTS

Figure 4.2 SEM morphology: (a) WTS, (b) 3M H_3PO_4 modified WTS, (c) 5M H_3PO_4 modified WTS, (d) 10M H_3PO_4 modified WTS and (e) 15M H_3PO_4 modified WTS

4.1.4 FTIR analysis

FTIR spectra of water treatment sludge and acid activated water treatment sludge powders are shown in Figure 4.3. The absorption board bands in the range of 3500-3700 cm^{-1} were assigned to the O-H stretching modes from silanol group of silica and inner hydroxyl group of kaolinite (Panda et al., 2010). The O-H stretching and H-O-H bending observed in all spectra at centered at 3440 cm^{-1} and 1630 cm^{-1} were assigned to the water-absorbing surface. The strong peak at 1042 cm^{-1} observed in all spectra was assigned to Si-O bond stretching. Meanwhile, another sharp peak at 930 cm^{-1} was assigned to the Al-OH bending vibration of kaolinite sheet, which was observed the low intensity when the acid treatment was increase in the acid strength. The characteristic peaks of quartz vibration observed at 795 and 693 cm^{-1} are appointed Si-O inner surface and inner layer. The absorption peaks at below 536 cm^{-1}were referred to Metal-O stretching (O-Fe, Si-O, O-Al) and Si-O-Si, Si-O-Fe bending (Ayodele et al., 2013).

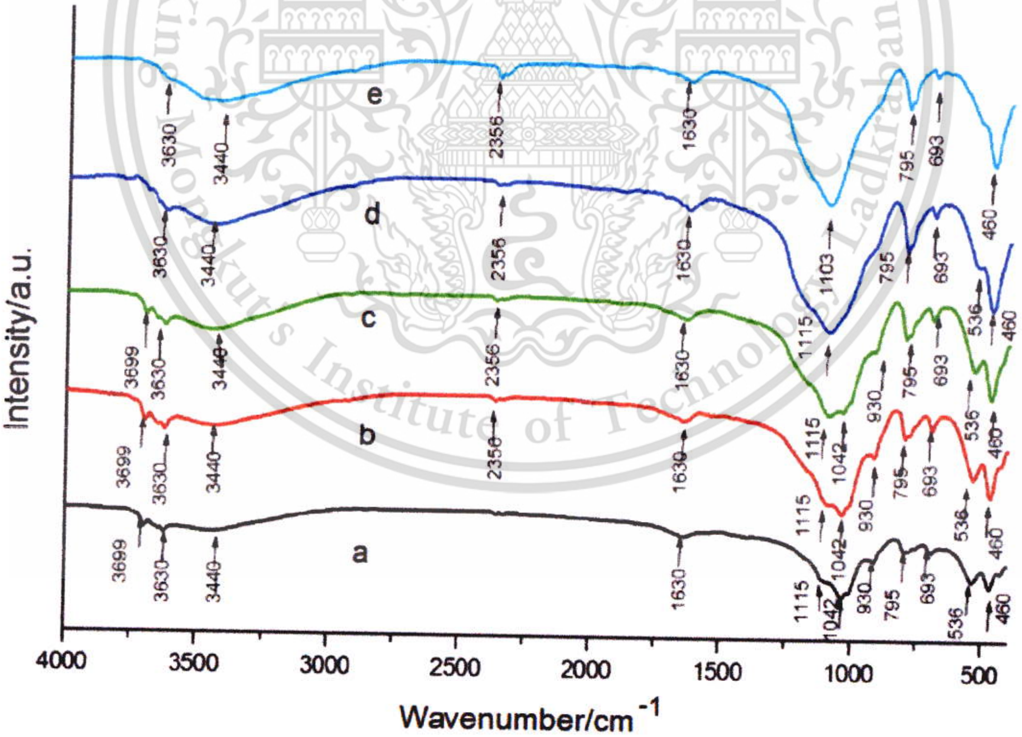

Figure 4.3 FTIR spectra of WTS and acid modified WTS (a) WTS, (b) 3M H$_3$PO$_4$ modified WTS, (c) 5M H$_3$PO$_4$ modified WTS, (d) 10M H$_3$PO$_4$ modified WTS and (e) 15M H$_3$PO$_4$ modified WTS

4.1.5 Molar ratio analysis of WTS and acid modified WTS

Molar ratio of SiO_2: kaolinite was calculated based on chemical structure of kaolin, i.e. $Al_2O_3.2SiO_2.2H_2O$ and XRF results from Table 4.1. When WTS was modified by increasing acid concentration, it was found that kaolinite ($Al_2O_3.2SiO_2.2H_2O$) phase decreased, and SiO_2 phase increased. These phenomena corresponded to XRD analysis, representing that Q position (quartz) of XRD increased intensity (Figure 4.1). Increase in acid strength led to increase in disintegration of clay sheets. However, higher concentration led to agglomeration of the kaolin particles (Yahaya et al., 2017). Silicon and aluminum are the two major elements identified by XRF analysis. For 5M H_3PO_4 modified WTS, which BET surface area was 150 m^2/g, it was found that molar ratio of SiO_2: kaolinite was 2.5:1. It was also found that BET surface area decreased when the molar ratio of SiO_2: kaolinite was either lower or higher than 2.5:1. It can be explained that mole fraction of SiO_2 affected the crystallization of modified WTS. In case the molar ratio of SiO_2: kaolinite was lower than 2.5, increase of acid strength from 3M to 5M facilitated dealumination and elimination of impurities in the WTS structure, leading to the increase of surface area of modified WTS. However, when molar ratio of SiO_2: kaolinite increased more than 2.5:1, high strength of acid increased the crystalline and caused agglomeration of SiO_2, causing the reduction of surface area. The Al-O-Si bond in acid modified WTS was broken during acid leaching, leaving Si-O tetrahedron in favor of silica (Luo et al., 2017).

Table 4.2 Molar ratio of SiO_2: kaolinite WTS and acid modified WTS

Material	Weight % *		Mass composition (mole)				Molar ratio
	SiO_2	Al_2O_3	SiO_2	Al_2O_3	Residual SiO_2	$Al_2O_3.2SiO_2.2H_2O$	SiO_2 : Kaolinite
WTS	49.9	24.4	0.832	0.239	0.353	0.478	0.737
3M H_3PO_4 modified WTS	62.3	21.8	1.038	0.214	0.611	0.427	1.428
5M H_3PO_4 modified WTS	71.0	17.3	1.183	0.170	0.844	0.339	2.487
10M H_3PO_4 modified WTS	67.3	13.6	1.122	0.133	0.855	0.266	3.204
15M H_3PO_4 modified WTS	69.6	11.5	1.160	0.113	0.934	0.225	4.142

Note: * Results from XRF analysis

4.2 Characterization of Fe/WTS and Mn/WTS catalysts

Ferric and manganese catalysts coated on acid modified WTS support were characterized by XRD, XRF, BET, SEM and SEM-EDX.

4.2.1 XRD analysis

XRD patterns determined the crystal phase of Fe/WTS and Mn/WTS which was shown in Figure 4.3. It was found that there was no difference among XRD patterns of Fe/WTS, Mn/WTS, and acid modified WTS because iron content and manganese content was low (2%). This result was similarly to Wang et al. (2016) that studied Mn doping on Al_2O_3. It was found that no difference in XRD diffraction peak of manganese oxide due to low content of Mn. However, the XRD pattern of 4% was observed. The intensity was notable decreased compared with acid modified WTS. This indicated that the addition of Fe and Mn led to decrease in crystallinity of modified WTS because. most of Fe_2O_3 and MnO_2 attached the acid modified WTS surface and changed its structure.

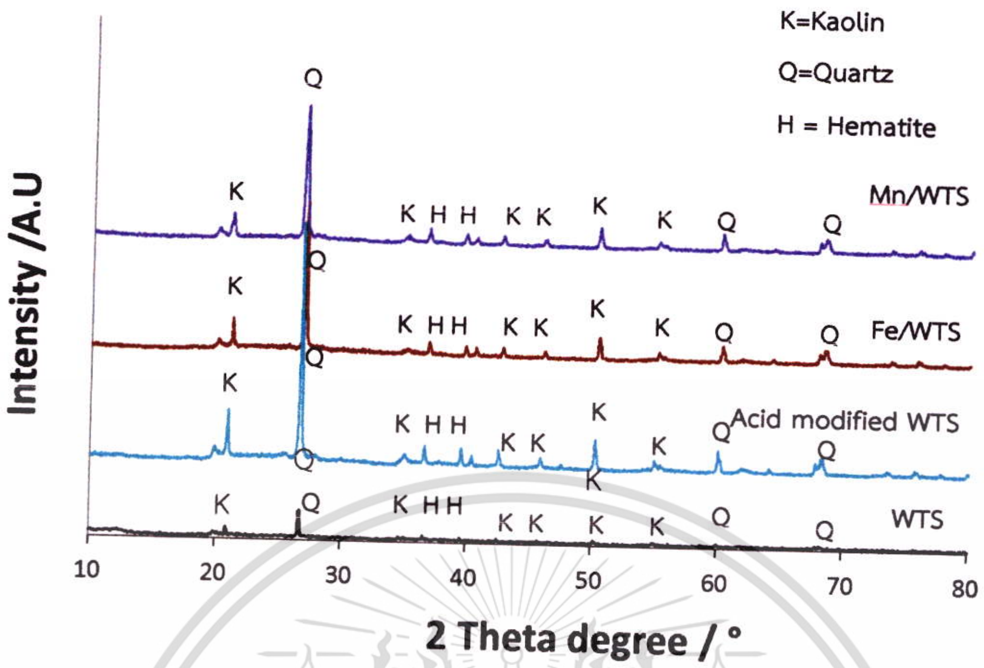

Figure 4.4 XRD patterns of Fe/WTS and Mn/WTS compared with WTS and acid modified WTS.

4.2.2 XRF and BET analysis

The results of XRF analysis are shown in Table 4.3, Fe content increased from 2.97 to 4.02% when adding higher amount of Fe into modified WTS. At the same time, Al fraction was found to decrease. BET results indicated that BET surface area of Fe/WTS and Mn/WTS decreased when increased % of Fe and Mn. The enlargements of pore size and pore volume are attributed to the replacement of Fe and Mn in the structure of acid modified WTS. However, at 3% Fe and Mn, BET surface area sharply decreased possibly due to metal agglomeration on the surface. For this reason, 2% Fe/WTS and 2% Mn/WTS catalysts were used in further study.

Table 4.3 XRF and BET analysis of acid modified/WTS, Fe/WTS and Mn/WTS

Material	Component content (%)									BET surface area (m^2/g)
	SiO_2	Al_2O_3	Fe_2O_3	K_2O	CaO	MgO	TiO_2	P_2O_5	MnO	
Modified WTS	71.0	17.3	2.97	3.59	0.16	0.97	1.83	0.94	n/a	150.07
1% Fe/WTS	72.3	19.8	3.21	3.32	0.21	0.88	1.60	1.26	n/a	118.51
2% Fe/WTS	71.0	17.3	3.97	3.59	0.16	0.97	1.83	1.04	n/a	109.84
3% Fe/WTS	69.3	13.6	4.02	3.69	0.15	0.83	1.57	1.25	n/a	28.78
1% Mn/WTS	71.3	18.8	3.15	3.25	0.28	0.86	1.59	1.27	n/a	142.52
2% Mn/WTS	69.8	16.8	3.11	3.57	0.16	0.97	1.83	1.87	n/a	116.86
3% Mn/WTS	67.6	11.5	3.07	3.76	0.15	0.68	1.54	1.63	n/a	54.46

4.2.3 SEM analysis

Scanning electron micrographs of Fe/WTS and Mn/WTS samples were presented in Figure 4.5 (a-c) and Figure 4.6 (a-c), respectively. The SEM micrographs of Fe/WTS and Mn/WTS indicated the disaggregation and the decrease in size of acid modified structure.

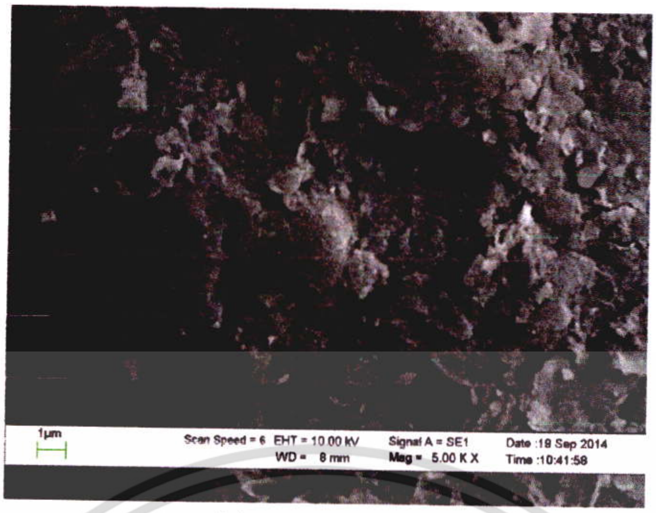

(a) 1% Fe/WTS

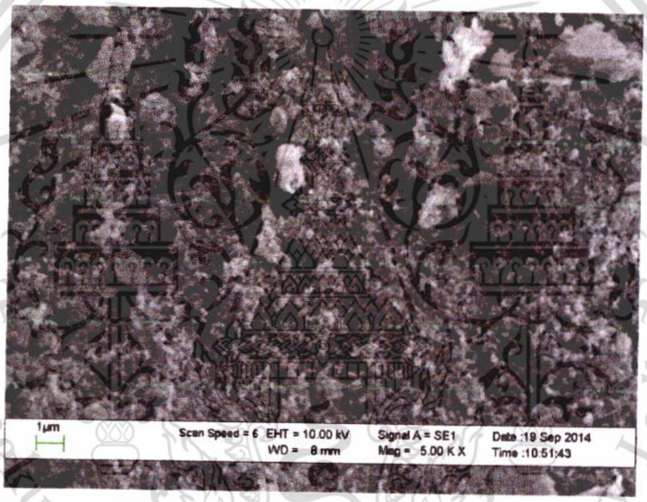

(b) 2% Fe/WTS

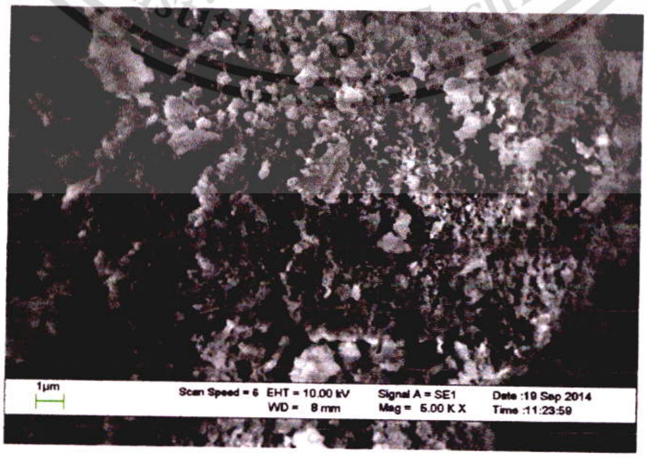

(c) 3% Fe/WTS

Figure 4.5 SEM analysis of Fe/WTS: (a) 1% Fe/WTS, (b) 2% Fe, and (c) 3% Fe/WTS

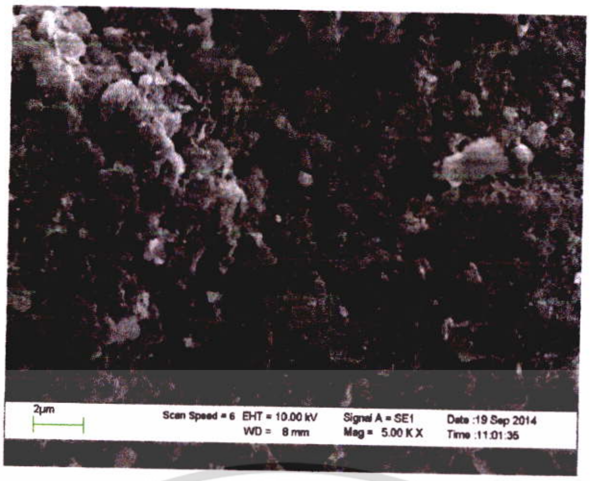

(a) 1% Mn/WTS

(b) 2% Mn/WTS

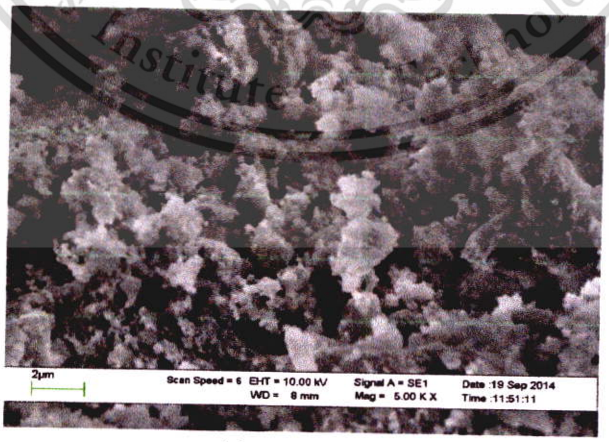

(c) 3% Mn/WTS

Figure 4.6 SEM analysis of Mn/WTS: (a) 1% Mn/WTS, (b) 2%Mn/WTS, and (c) 3%Mn/WTS

4.2.4 SEM-EDX analysis

SEM-EDX was used to determine the presence of chemical elements to estimate their relative abundance. EDX also helped to measure multi-layer coating thickness of metallic coatings and analysis of various alloys. Figure 4.7 illustrates the results of EDX analysis of Fe/WTS and Mn/WTS compared with WTS and acid modified WTS. EDX results confirmed that Fe and Mn penetrated in the structure acid WTS.

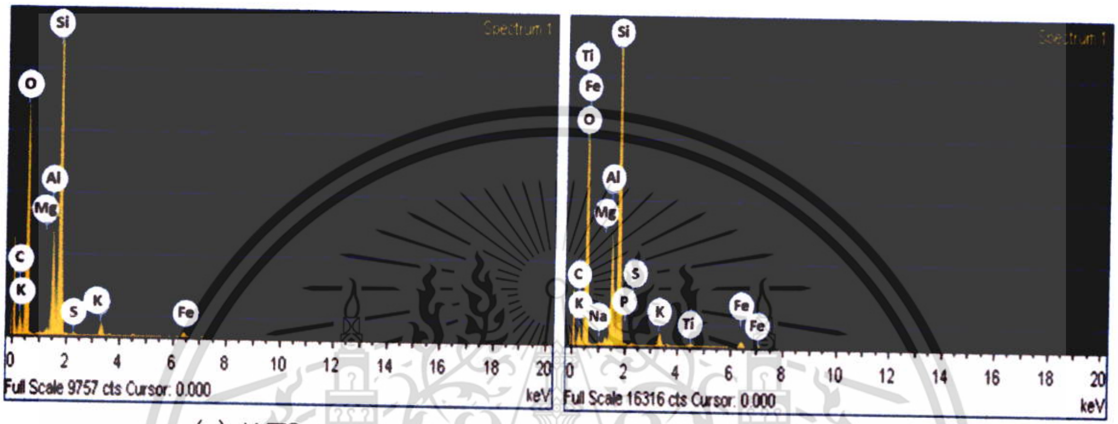

(a) WTS (b) acid modified WTS

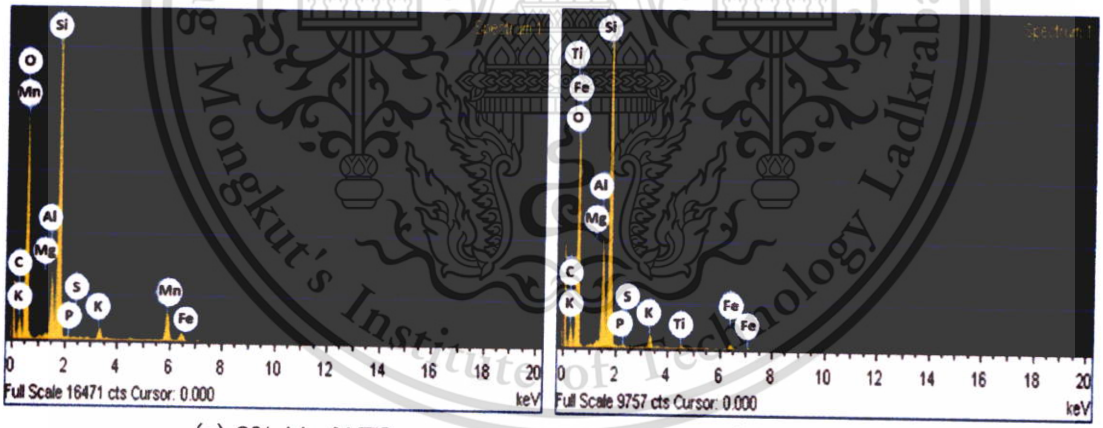

(c) 2% Mn/WTS (d) 2% Fe/WTS

Figure 4.7 SEM-EDX analysis of catalysts: (a) WTS, (b) acid modified WTS, (c) 2% Mn/WTS, and (d) 2% Fe/WTS

Regarding to Figure 4.7, it indicated that Si was found to be major element. Fe, Mn and other metals were found in WTS structure. In Figure 4.7 (b), some elements decreased because of acid activation. This phenomena could confirm the results from BET and SEM morphology in Table 4.1 and Figure 4.2, respectively. In Figure 4.7 (c) and

(d) , it was found that the peaks of Fe and Mn increased, when Fe and Mn were added into structure of acid modified WTS. These findings were equivalent to the results from XRF, except Mn which was missing in the XRF results. This result confirmed the abundance of Fe and Mn coated into the surface of acid modified WTS.

4.2.5 Mass balance analysis

To confirm the abundance of metals in the structure of acid modified WTS, the catalysts were digested by HNO_3 then analyzed for Fe and Mn by ICP-MS. The results were shown in Table 4.4. It was found that Fe and Mn were found originally in WTS. When WTS was treated by acid, it was confirmed that acid leached some minerals from WTS structure, so Fe and Mn contents in acid modified WTS was found to decrease compared to its parent materials. When Fe and Mn of 2% (w/w) were impregnated into acid modified WTS, Fe and Mn were contained into the structure of modified WTS at the weight percent of 1.49% and 1.56%, respectively.

Table 4.4 Abundance of Fe and Mn in modified WTS support.

Sample	Element	Weight percent (%wt)
WTS	Fe	5.038
	Mn	0.246
modified WTS	Fe	1.532
	Mn	0.006
Fe/WTS	Fe	3.028
Mn/WTS	Mn	1.564

To determine the possibility of Fe and Mn leaching out from the modified WTS, leaching extraction test was conducted according to the EPA standard method for soil extraction (EPA Method 3050B) (EPA, 1996). Fe/WTS and Mn/WTS of 10g was placed in 100 mL of water and then shaken for 24h. After that, Fe and Mn in supernatant were determined by ICP-MS. The results are shown in Table 4.5.

Table 4.5 Fe and Mn leaching test

Sample	Element	Weight percent (%wt)
Fe/WTS	Fe	0.5750
Mn/WTS	Mn	0.5746

It was found that Fe of 0.575% and Mn of 0.575% were leached from Fe/WTS and Mn/WTS catalysts. Leached Fe/Mn possibly dispersed on the surface of acid modified WTS and readily leached out. This result indicated that the abundance of Fe and Mn into the pore of acid modified WTS and showed the stability of as-prepared catalysts.

4.2.6 Molar ratio analysis of Fe/WTS and Mn/WTS

Mole ratio analysis of Fe/WTS and Mn/WTS was calculated according to chemical structure of kaolin, i.e. $Al_2O_3.2SiO_2.2H_2O$. The result was shown in Table 4.6. It was found that molar ratio of SiO_2 : kaolinite was 2.5:1 for 5M acid modified WTS. When 2% of Fe and Mn were added into 5M acid modified WTS, the ratio of SiO_2: kaolinite of 2% Fe and Mn were equivalent to that of acid modified WTS. It indicated that 2% of Fe and Mn doped penetrated well into the acid modified WTS. Addition of Fe and Mn decreased the surface area of acid modified WTS because surface area of acid modified WTS employed negative charge which attracted cation (Jozefaciuk, 2002) When the content of Fe and Mn increased over the ratio SiO_2: kaolinite of 2.5:1, the content of Fe and Mn affected the SiO_2 : kaolinite crystalline. The surface area sharply decreased because both Fe and Mn dispersed on the surface of acid modified WTS and possibly caused metal agglomeration. This phenomenon corresponded to the results from XRD and SEM morphology as mentioned earlier.

Table 4.6 Molar ratio of SiO_2: kaolinite Fe/WTS and Mn/WTS

Material	Weight % *		Mass composition (mole)				Ratio
	SiO_2	Al_2O_3	SiO_2	Al_2O_3	Residual SiO_2	$Al_2O_3.2SiO_2.2H_2O$	SiO_2 : Kaolinite
Modified WTS	71.0	17.3	1.183	0.170	0.844	0.339	2.487
1% Fe/WTS	72.3	19.8	1.205	0.194	0.817	0.388	2.102
2% Fe/WTS	71.0	17.3	1.183	0.170	0.844	0.339	2.487
3% Fe/WTS	69.3	13.6	1.155	0.133	0.888	0.266	3.329
1% Mn/WTS	71.3	18.8	1.188	0.184	0.820	0.368	2.222
2% Mn/WTS	69.8	16.8	1.163	0.165	0.834	0.329	2.530
3% Mn/WTS	67.6	11.5	1.127	0.113	0.901	0.225	3.994

Note: * Results from XRF analysis

4.2.7 pH_{pzc} analysis

Point of zero charge (pzc) is the pH at which the surface of material is globally neutral. The pH_{pzc} of prepared materials were measured and presented in Table 4.7. The significance of pH_{pzc} was that a given catalyst surface had positive charge at solution pH less than the pH_{pzc} and could absorb anions. On the other hand, catalyst surface had negative charge at solution pH greater than the pH_{pzc} and possibly adsorbed cations. The results showed that pH_{pzc} of acid modified WTS was lower than WTS because some H^+ attached to the surface of WTS. While, the pH_{pzc} of Fe/WTS and Mn/WTS decreased because Fe and Mn coated on the structure of acid modified WTS (Ayodele et al., 2012).

Table 4.7 pH_{pzc} of catalyst

Samples	**pH_{pzc}**
WTS	6.17
Acid modified WTS	4.42
Fe/WTS	5.73
Mn/WTS	5.68

4.3 Ozone production rate

In this study, ozone was generated by corona discharge method. The production rate of ozone generator was determined. Ozone was applied directly to 2% potassium iodide (KI) solution. Iodide ion was oxidized to iodine by ozone and the liberated iodine was titrated with sodium thiosulfate to a starch endpoint (APHA, 1998). The graph of ozone generated versus time is plotted in Figure 4.8. The slope of linear curve indicated the ozone production rate which was 0.57 mg/min.

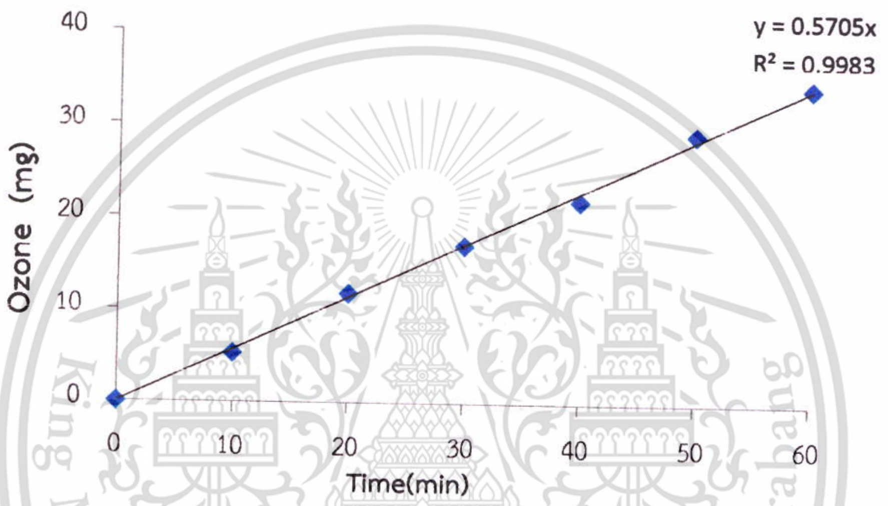

Figure 4.8 Ozone production rate

4.4 Catalytic ozonation

4.4.1 Effect of catalyst type

To determine the efficiency on phenol degradation of each catalyst. Catalyst ozonation experiment were controlled at pH of 11 by using different types of catalysts. It was noted that control experiment were conducted by sole ozonation without any catalysts as well as using catalysts without ozone applied. The catalysts including Fe/WTS, Mn/WTS, and WTS were applied at a dosage of 1g/L. The result was shown in Figure 4.9, while the detail of experimental data was shown in Table A1-A3 of Appendix A.

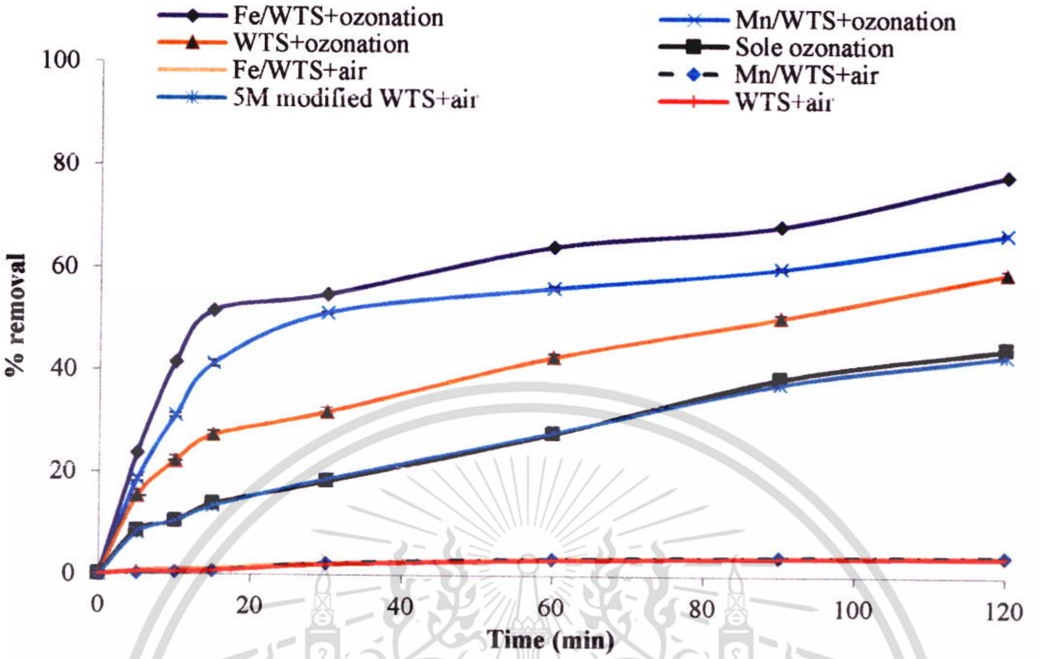

Figure 4.9 Catalytic activities of Fe/WTS and Mn/WTS
(Experimental conditions: O_3 generation 0.57 mg/min, [phenol] 50 mg/L,
Fe/WTS, Mn/WTS and WTS = 1g/L, Fe and Mn content = 1%, solution pH = 11)

Regarding to Figure 4.9, it was found that at 60 min and pH of 11, the use of Fe/WTS Mn/WTS and WTS as catalysts in catalytic ozonation achieved 64.30%, 56.2% and 42.77%, respectively. Compared with ozonation alone the percent removal of phenol was only 27.78% which was not different when acid modified WTS and calcinated modified WTS were added. The adsorption showed minor effect only 3.33% of phenol removal at 60 min. According to ANOVA test, it was found that the results of Fe/WTS and Mn/WTS with ozonation were significantly different from their control experiments including Fe/WTS (or Mn/WTS) with air and sole ozonation at 95% confidence level. Detailed information was shown in Table A33-A35 in Appendix A. The presence of Fe in Fe/WTS catalyst and Mn in Mn/WTS during catalytic ozonation facilitated ozone decomposition to enhance degradation of phenol. The results were corresponding to those of several researchers (Li et al., 2009; Chen et al., 2016; Peng et al., 2018). It can be explained that in the presence of Fe/WTS as a catalyst, Fe facilitated decomposition of ozone and generation of hydroxyl radical $OH^{\bullet}$, according to Eq 4.1-4.3. Hydroxyl radicals ($OH^{\bullet}$) played a key role in the degradation of phenol (Chen et al., 2016; Wang and Bai, 2017). While, Mn/WTS as catalyst can be explained in Eqs.4.4-4.6 (Fei et al., 2018).The pH_{pzc} of Fe/WTS and Mn/WTS were 5.73 and 5.68, respectively. As a result, the Fe/WTS and Mn/WTS catalyst was successfully used to degrade phenol compared with using WTS catalyst and sole ozonation.

$$\equiv FeOH \longrightarrow \equiv FeO^{-} + O_3 \longleftrightarrow \equiv FeO(O_3)^{-} \tag{4.1}$$

$$\equiv FeO(O_3)^{-} \longleftrightarrow \equiv FeO^{\bullet} + {}^{\bullet}HO_3/\ {}^{\bullet}O^{-}_3 \tag{4.2}$$

$$\equiv FeO^{\bullet} + H_2O \longleftrightarrow \equiv FeOH + OH^{\bullet} \tag{4.3}$$

$$\equiv MnOH \longrightarrow \equiv MnO^{-} + O_3 \longleftrightarrow \equiv MnO(O_3)^{-} \tag{4.4}$$

$$\equiv MnO(O_3)^{-} \longleftrightarrow \equiv MnO^{\bullet} + {}^{\bullet}HO_3/\ {}^{\bullet}O^{-}_3 \tag{4.5}$$

$$\equiv MnO^{\bullet} + H_2O \longleftrightarrow \equiv MnOH + OH^{\bullet} \tag{4.6}$$

When reaction time increased from 60 to 120 min, percent removal of phenol by Fe/WTS slightly increased from 64.33 to 78.39 %, while that by Mn/WTS slightly increased from 56.20 to 67.03 %. For this reason, ozonation time of 60 min was selected and used in further study.

4.2.2 Effect of initial pH

The solution pH is an important factor affecting ozone decomposition because hydroxide ion (OH^{-}) was found to be an initiator of the chain reaction in ozone decomposition process (Qi et al., 2012). The effect of solution pH on the degradation of phenol by catalytic ozonation using 1 % Fe/WTS catalyst and 1% Mn/WTS at a dosage of 1 g/L were investigated. The results are shown in Figure 4.10, while the experimental data are shown in Table A1-A4 in Appendix A.

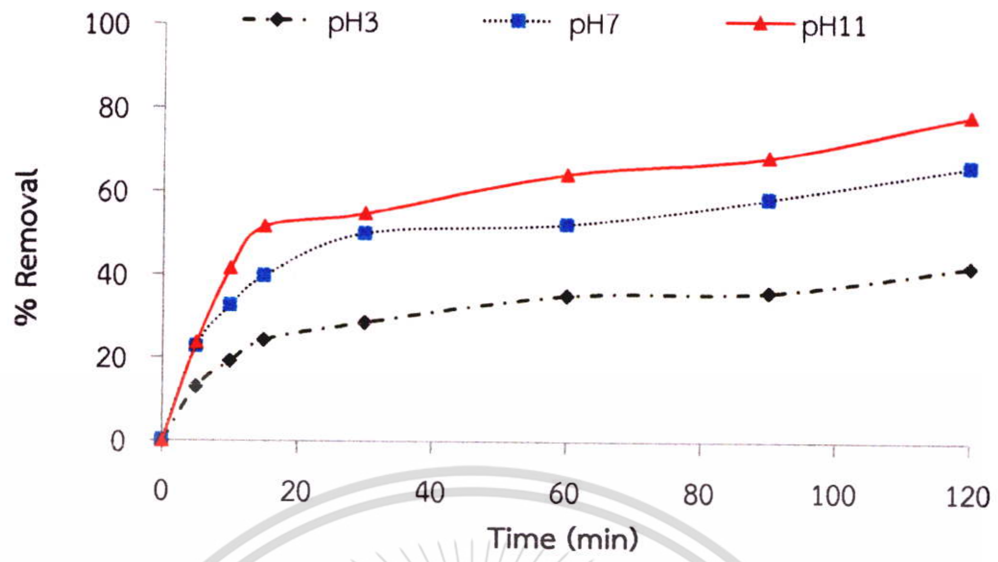

(a) Fe/WTS

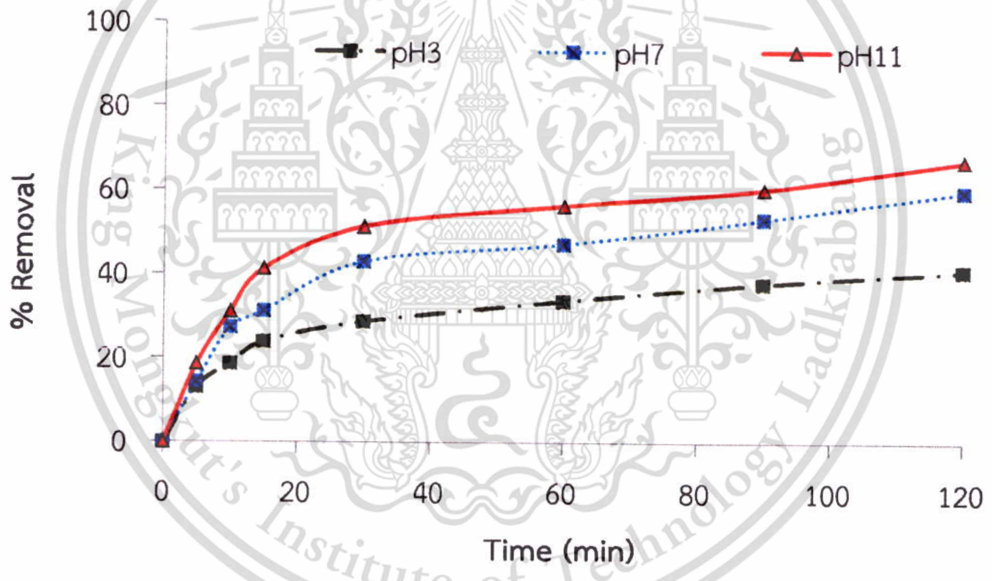

(b) Mn/WTS

Figure 4.10 Effect of solution pH on catalytic activities of Fe/WTS and Mn/WTS (Experimental conditions: O_3 generation = 0.57 mg/min, [phenol] = 50 mg/L, Fe/WTS and Mn/WTS= 1g/L, Fe and Mn content = 1%)

As shown in Figures 4.9 (a) and (b), where the solution pH increased, the degradation of phenol became increased. At 120 min and pH of 3, 7, and 11, removal efficiencies of phenol by using Fe/WTS as a catalyst in ozonation were 41.98, 65.77, and 78.29 %, respectively. The removal of phenol when using Mn/WTS catalyst were

40.90, 59.69, and 67.03% at pH 3, 7, and 11, respectively. It can be explained that increasing pH promoted ozone decomposition and formation of hydroxyl radical ($OH^\bullet$) which was very powerful radical and reacted with phenol and its by products in non-selective mode (Li et al., 2009). Comparing with the control experiments using WTS as catalyst and ozonation alone, as shown in Figure 4.10, it was found that at 60 min and pH of 11, the use of Fe/WTS and Mn/WTS as a catalyst in catalytic ozonation to degrade phenol achieved 64.30% and 60.22%, while the percent removal of phenol by using ozonation alone and WTS-catalytic ozonation were 24.67 and 43.09 %, respectively. It can be explained that as the pH_{pzc} of Fe/WTS and Mn/WTS were 5.73 and 5.78, respectively. Therefore, their surface hydroxyl groups appeared in deprotonated form when pH was higher than 5.73 and 5.78. According to previous study, a negatively charged surface had a strong reactivity to ozone and hydroxyl radicals ($OH^\bullet$) were generated from the reaction of deprotonated surface hydroxyl groups ($\equiv FeO^-$) and O_3 through Eqs. 4.1-4.3 (Chen et al., 2016).

Regarding to Chen et al. 2017, when pH of solution was higher than pH_{zpc} the surface of catalyst changed into $Mn\text{-}O^-$ while, pH solution was lower than pHzpc, most of the surfaec hydroxyl group protonated ($Mn\text{-}OH_2^+$). So, ozone molecule attracted with this surface throught electrostatic forces or/and hydrogen bonding which was described in Eqs. 4.7 and 4.8 (Chen et al., 2017). For this reason, Fe/WTS and Mn/WTS can generate hydroxyl radical both acid and base solution. While sole ozone can generate hydroxyl radical only in base solution.

$$Mn\text{-}OH_2^+ + O_3 \longrightarrow Mn\text{-}OH^{+\cdot} + HO_3\cdot \qquad (4.7)$$

$$Mn\text{-}OH^{+\cdot} + H_2O \longrightarrow Mn\text{-}OH^+_2 + HO\cdot \qquad (4.8)$$

However, when pH solution decreased, the leaching of metal possibly led to the decrease of degradation efficiency. So, at pH solution of 11, the percent removal of phenol was higher than pH of 3 and 7 because of ozone decomposition by hydroxide ion and by metal in catalyst.

4.4.3 Effect of catalyst dosage

The effect of catalyst dosage in catalytic ozonation for phenol degradation was studied by adding 1% Fe/WTS and 1% Mn/WTS at various dosages. The results are shown in Figure 4.11. The experimental data was shown in Table A6-A8 in Appendix A.

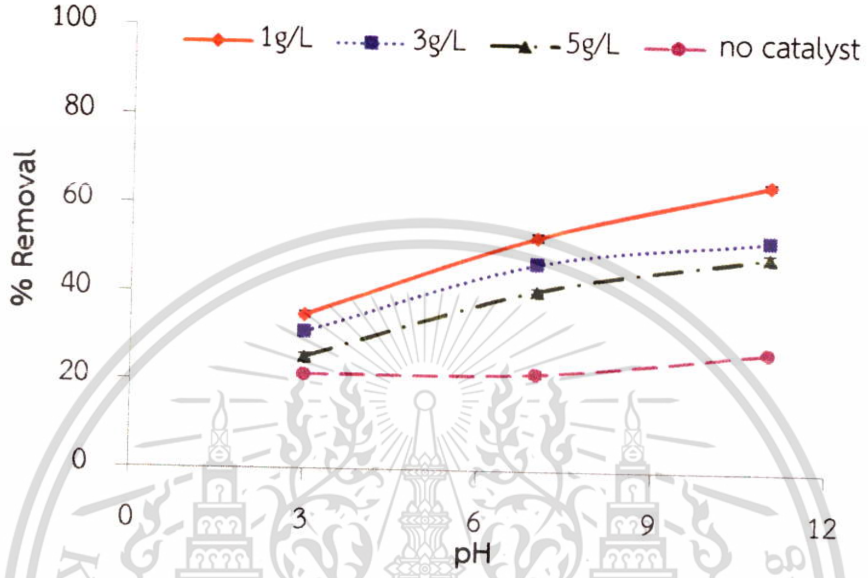

(a) Fe/WTS

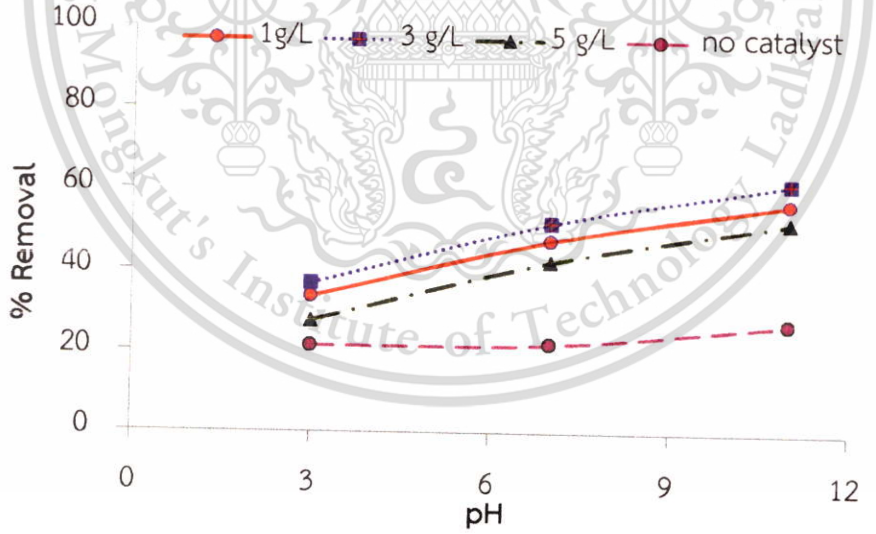

(b) Mn/WTS

Figure 4.11 Effect of catalyst dosage on the catalytic activities of catalyst (Experimental conditions: O_3 generation = 0.57 mg/min, [phenol] = 50 mg/L, time = 60 min, Fe and Mn content = 1%)

Figure 4.11 (a) exhibited that as the Fe/WTS dosages increased, the performance of catalytic ozonation in phenol degradation reduced. At the Fe/WTS dosages of 1, 3, and 5 g/L removal efficiencies for phenol degradation were 64.65, 53.12, and 49.23%, respectively. According to Figure 4.11 (b), when Mn/WTS dosage increased, the % removal of phenol increased from 56.86 to 61.91 at 1 to 3 g/L, respectively. However, at 5g/L, the percent removal of phenol was decreased to 52.38% while that of sole ozonation was 26.27% at 60 min. As mentioned earlier, in the presence of Fe/WTS and Mn/WTS as catalyst, hydroxyl radicals played a key role in the degradation of phenol. More catalyst dosage provided more active sites for the catalytic reaction, leading to more formation of $OH^{\bullet}$. Many literatures reported that the surface hydroxyl groups of the metal oxides were the active sites of catalytic ozonation (Qi et al., 2009; Peng et al., 2018). Higher dosage of catalyst provided more surface hydroxyl groups for catalytic ozonation, leading to high performance on phenol degradation (Li et al., 2018) However, excess $OH^{\bullet}$ generated by high catalyst dosage led to self-quenching, as expressed in the Eq 4.9 and 4.10 (Peng et al., 2018).

$$OH^{\bullet}+OH^{\bullet} \longleftrightarrow H_2O_2 \tag{4.9}$$

$$OH^{\bullet}+HO_2 \longleftrightarrow H_2O+O_2 \tag{4.10}$$

As the $OH^{\bullet}$ was quenched, the performance of catalytic ozonation on phenol degradation was limited. Thus, 1 g/L of Fe/WTS catalyst and 3 g/L of Mn/WTS catalyst were selected for further study.

4.4.4 Effect of metal content in catalyst

The study of Fe and Mn doped in WTS was shown in Figure 4.12 (a) and (b) and The experimental data was shown in Table A9-A10 of Appendix A. The removal efficiencies by Fe/WTS catalyst with Fe content of 1, 2, and 3% were 64.65, 81.85, and 55.5%, respectively. While, the removal of phenol by Mn/WTS with Mn content of 1, 2, and 3% were 61.91, 76.36, and 50.31%, respectively.

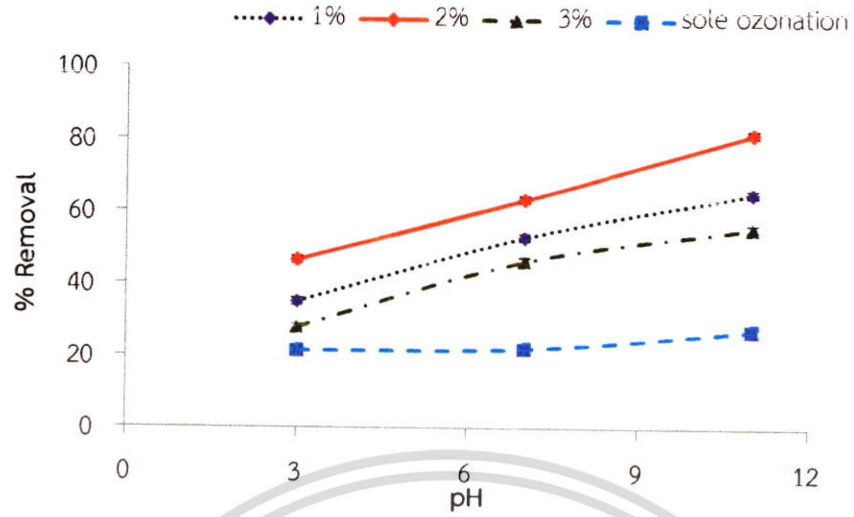

(a) Fe/WTS

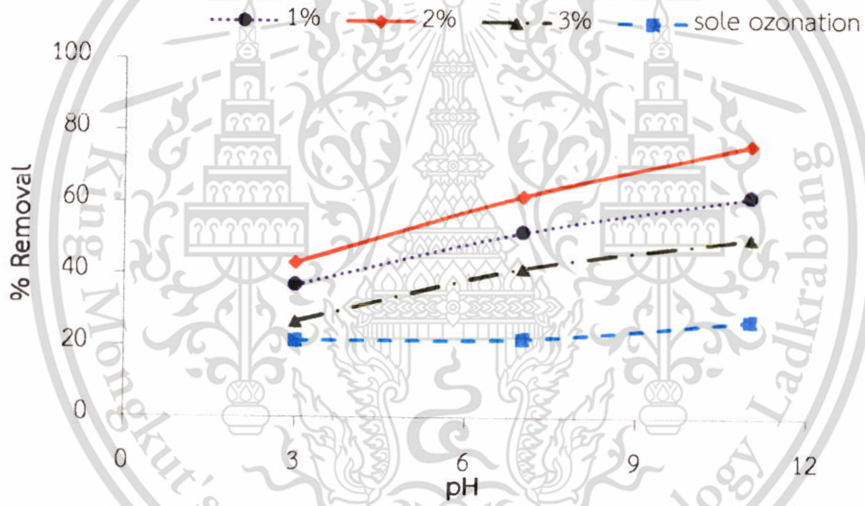

(b) Mn/WTS

Figure 4.12 Effect of % Fe doped on the catalytic activities of Fe/WTS catalyst (Experimental conditions: O_3 generation = 0.57 mg/min, [phenol] = 50 mg/L, time = 60 min, Fe/WTS dosage = 1 g/L and Mn/WTS dosage = 3 g/L)

It was found that increasing iron and manganese content in Fe/WTS and Mn/WTS from 1% to 2% caused the removal efficiency increased, but at 3% Fe doped, the efficiency decreased. High content of Fe and Mn in WTS facilitated excess $OH^{\bullet}$ generation, possibly leading to self-quenching and the decreasing performance of catalytic ozonation on phenol degradation which was shown in Eq (4.12)-(4.15)

$$OH^{\bullet} + OH^{\bullet} \longleftrightarrow H_2O_2 \quad (4.11)$$

$$OH^{\bullet} + HO_2^{-} \longleftrightarrow H_2O+O_2 \quad (4.12)$$

$$OH^{\bullet} + HO_3^{\bullet} \longleftrightarrow H_2O_2+O_2 \quad (4.13)$$

$$H_2O_2 + O_3 \longleftrightarrow H_2O+O_2 \quad (4.14)$$

4.4.5 Effect of radical scavengers

In general, the key active species in catalytic ozonation were $OH^{\bullet}$ generated during ozone decomposition. In this study, *tert*-butanol (TBA) were used as a radical scavenger at varied concentrations of 1-3 mM to prove the formation of $OH^{\bullet}$ from ozone decomposition and its performance on phenol degradation during catalytic ozonation process (Li et al., 2018). Figure 4.13 (a) and (b) show the results of the effect of radical scavenger (detailed experimental data were shown in Table A11-A13 in Appendix A).

When the concentration of TBA increased, the percent phenol removal simultaneously decreased. The presence of *tert*-butanol obviously inhibited the degradation rate of phenol in catalytic ozonation with WTS. The result was corresponding to several researchers (Zhang et al., 2018; Lan et al., 2013).

Figure 4.14 illustrates a comparison of %removal by sole ozonation at pH 3,7 and 11. It was observed that when TBA was added into sole ozonation, the removal of phenol by ozonation slightly decreased because TBA inhibited the performance of $OH^{\bullet}$. However, TBA did not affect the performance of sole ozonation at pH of 3 in removal of phenol because, in acidic condition, the degradation of phenol by sole ozonation mainly occurred via direct reaction by ozone molecule itself. Therefore, it can be clarified that Fe/WTS and Mn/WTS catalysts accelerated ozone decomposition to generate hydroxyl radical. Some hydroxyl radicals further degraded by products such as carboxylic acid (Li et al., 2018). This finding confirmed that hydroxyl radicals played an important role in the catalytic ozonation.

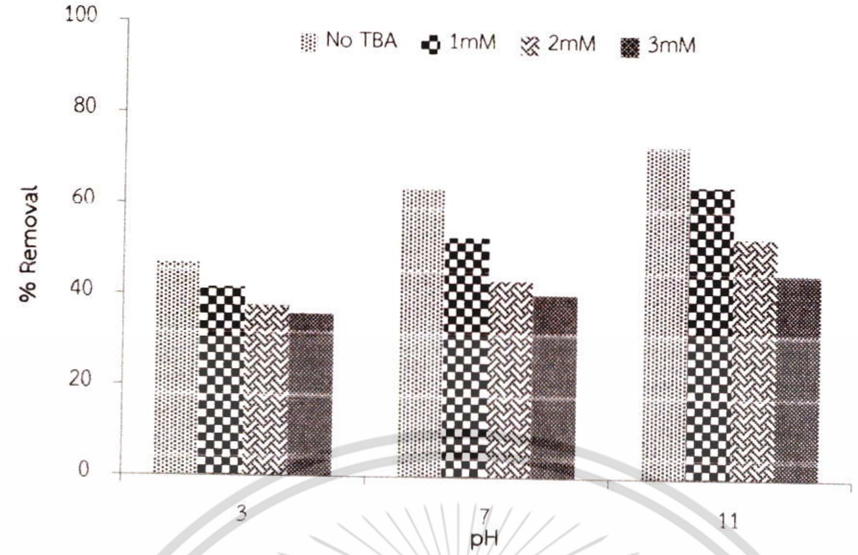

(a) Fe/WTS

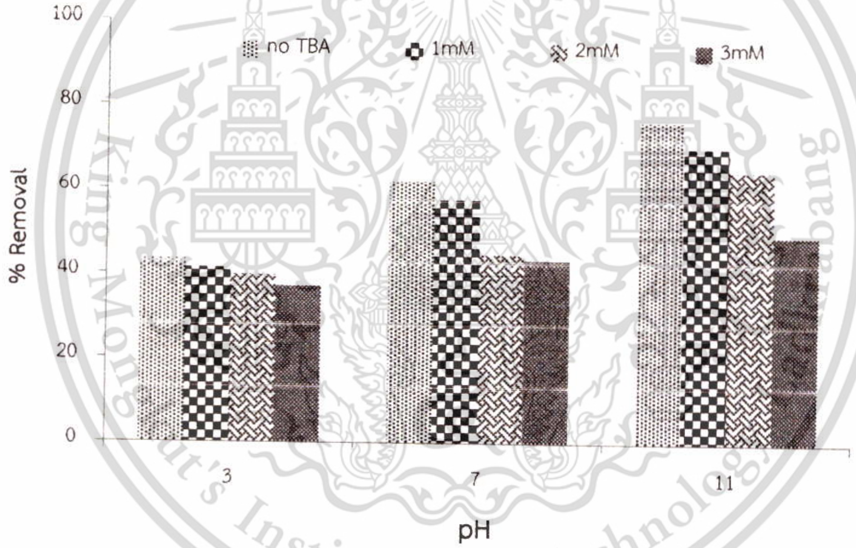

(b) Mn/WTS

Figure 4.13 Effect of TBA on the catalytic activities

(Experimental conditions: O_3 generation = 0.57 mg/min, [phenol] = 50 mg/L, Time= 60 min, Fe/WTS dosage = 1g/L, Mn/WTS dosage = 3 g/L)

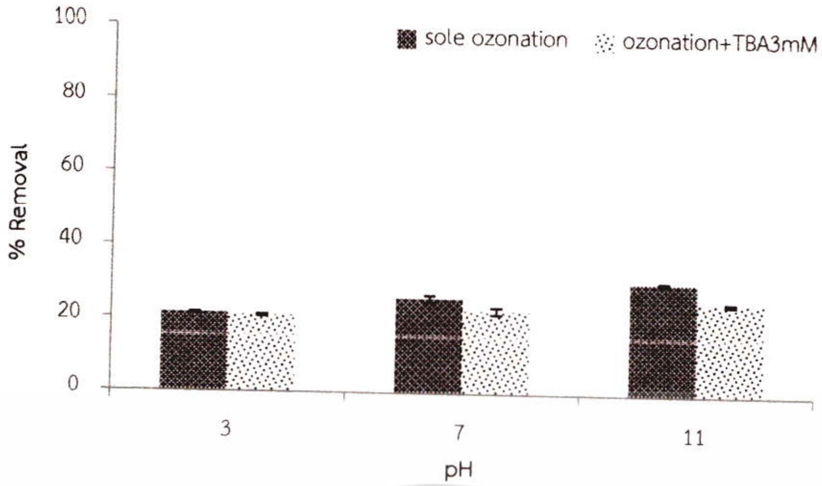

Figure 4.14 Effect of TBA on Ozonation (Experimental conditions: O_3 generation = 0.57 mg/min, [phenol] = 50 mg/L, Time 60 min, [TBA]=3mM)

4.4.6 Reaction kinetics of catalytic ozonation

To achieve high performance of catalytic ozonation using Fe/WTS and Mn/WTS as catalysts, the optimum conditions were identified, i.e. Fe content in Fe/WTS of 2%, catalyst dosage of 1 g/L, pH of 11, and reaction time of 120 min. while Mn content in Mn/WTS of 2%, catalyst dosage of 3 g/L, pH of 11, and reaction time of 120 min. The result was shown in Fig 4.15 and the corresponding experimental data were shown in Table A14-A17 in Appendix A. According to Figure 4.15, it shows that the removal efficiencies of phenol at 120 min were 99.16 % and 89.96 % for Fe/WTS and Mn/WTS, respectively which were higher than that of sole ozonation (44.61%). This optimum condition was used in further study of reaction kinetic.

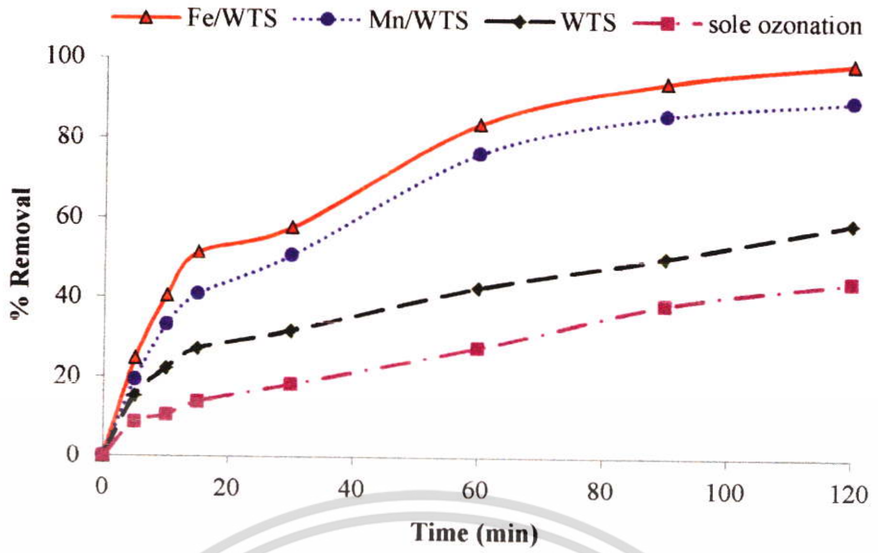

Figure 4.15 Removal efficiency for phenol by catalytic ozonation using different catalysts at optimum conditions (Experimental conditions: O_3 generation =0.57 mg/min, [phenol] = 50 mg/L, pH = 11, Fe/WTS dosage =1g/L, Fe doped = 2%, Mn/WTS dosage = 3 g/L, Mn doped = 2%)

The reaction kinetics of catalytic ozonation using Fe/WTS and Mn/WTS as a catalyst were analyzed. Plots of $\ln([C]/[C]_0)$ versus reaction time of the sole ozonation and catalytic ozonation by Fe/WTS, Mn/WTS, and WTS, are shown in Figure 4.16. A good linear fit was observed for each of ozonation reaction and apparent rate constants (k_{obs}) was determined from slope of the linear curve. According to kinetic analysis, it was found that the experimental data fit well with the pseudo-first order kinetic model with an apparent rate constant (k_{obs}) of 0.0362 min^{-1} for Fe/WTS, 0.019 min^{-1} for Mn/WTS, and 0.0063 min^{-1} for WTS, while sole ozonation exhibited k_{obs} of 0.0046 min^{-1}. The results indicated possibility of Fe/WTS and Mn/WTS as catalysts in catalytic ozonation for phenol removal. The results were corresponding to that investigated by Qi et al. (2012).

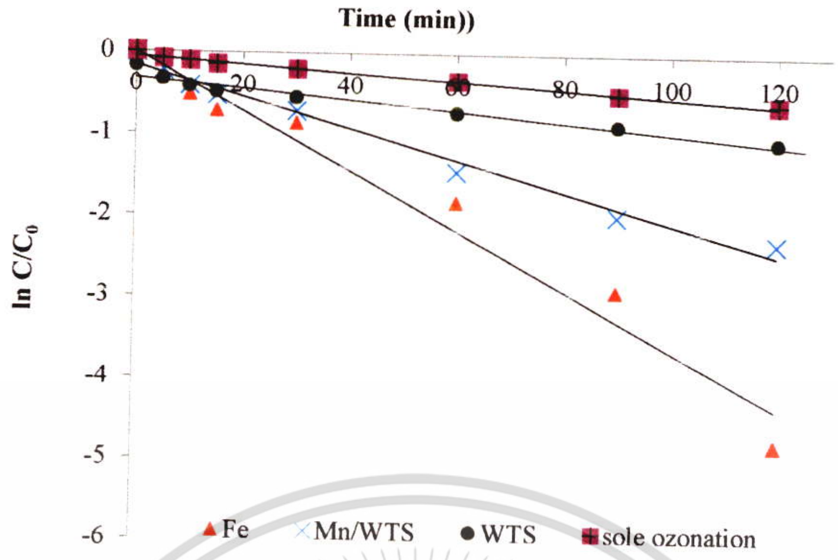

Figure 4.16 Degradation kinetics for phenol by catalytic ozonation (Experimental conditions were: phenol 50 mg/l, $[O_3]$=0.57 mg/min, Fe/WTS=1g/L, Fe doped 2%, Mn/WTS 3 g/L , Mn doped 2%, pH 11)

According to the results, Fe/WTS provided better performance in acceleration of ozone decomposition than Mn/WTS. It can be explained that when acid was used to treat WTS, the surface area of WTS increased (Komadel., 2016). Fe and Mn added into the modified structure of WTS attached the structure by covalent bonds. The surface of metal oxides in aqueous solution was easy to be hydroxylated by dissociative chemisorption of water molecules and acted as Lewis acid and Lewis base (Wang and Bai., 2017), as shown in Figure 4.17. After that, ozone molecule interacted with surface-OH_2^+ through electrostatic forces and/or hydrogen bonding (Chen et al., 2017). As ozone structure employed density of electron in its structure, so ozone acted as strong lewis base. While Fe and Mn were electrophilic, they acted as strong lewis acid. However, electronegativity (EN) of Fe is 1.8 which is more than Mn (1.5). For this reason, Fe was stronger lewis acid than Mn, that favored attraction ozone compared with Mn. Therefore, Fe catalyst decomposed ozone and generated hydroxyl radical more rapidly than Mn catalyst.

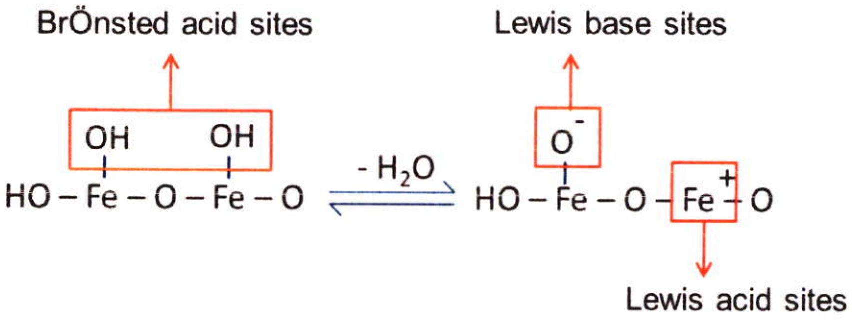

Figure 4.17 Formation process of Lewis acid and basic sites on iron oxide

Source: Wang and Bai (2017)

CHAPTER 5

Conclusion and Suggestions

5.1 Conclusions

1. Fe and Mn catalysts coated on modified WTS were successfully synthesized from water treatment sludge from water treatment plant. XRD analysis showed that addition of Fe and Mn led to decrease in acid modified WTS crystallinity because Fe and Mn attached to the acid modified WTS surface, resulting in the change of its structure. e.g. BET analyses indicated that surface area increased when WTS was activated by phosphoric acid with hydrothermal method. The surface area of acid modified WTS decreased when content of impregnated Fe and Mn increased because the enlargements of pore size and pore volume were attributed to the replacement of Fe and Mn in the structure of acid modified WTS. The XRF results indicated the increasing fraction of Fe content when Fe was impregnated. While the SEM-EDX results confirmed that both Fe and Mn were placed into acid modified WTS structure.

2. As-prepared Fe/WTS and Mn/WTS catalysts were successfully used in catalysts were successfully used in catalytic ozonation for degradation of phenol.

- Increasing pH increase the perform of phenol degradation by catalytic ozonation. At 20 min and pH of 3, 7, and 11, removal efficiencies of phenol by using Fe/WTS as a catalyst in ozonation were 41.98, 65.77, and 78.29 % , respectively, while Mn/WTS catalyst were 40.90, 59.69, and 67.03%, respectively.

-Increasing catalyst dosage from 1 to 3 g/L increased the performance in phenol degradation. However, when catalyst dosage was increased to 5g/L the removal efficiency decrease. At the Fe/WTS dosages of 1, 3, and 5 g/L removal efficiencies for phenol degradation were 64.65, 53.12, and 49.23%, respectively, while Mn/WTS dosage of 1, 3, and 5 g/L removal efficiencies for phenol degradation were 56.86, 61.91, and 52.38%, respectively. The sole ozonation was 26.27% at 60 min.

-Fe and Mn content in Fe/WTS and Mn/WTS catalysts affected removal efficiency. The removal efficiencies by Fe/WTS catalyst with Fe contents of 1, 2, and 3% were 64.65, 81.85, and 55.5%, respectively. While, the removal of phenol by Mn/WTS with Mn content of 1, 2, and 3% were 61.91, 76.36, and 50.31 % respectively.

-As the concentration of TBA increased, the percent phenol removal simultaneously decreased. This phenomenon indicated that Fe/WTS and Mn/WTS catalysts can generate hydroxyl radical mechanism.

- The optimum conditions for catalytic ozonation using Fe/WTS as a catalysts were: Fe content in Fe/WTS of 2%, catalyst dosage of 1 g/L, pH of 11, and reaction time of 120 min. while Mn those for Mn/WTS catalyst were content in Mn/WTS of 2%, catalyst dosage of 3 g/L, pH of 11, and reaction time of 120 min. At the optimum conditions, removal efficiencies of phenol. at 120 min were 99.16 % and 89.96 % for Fe/WTS and Mn/WTS, respectively. which were higher than that of sole ozonation (44.61%).

3. According to kinetic analysis, experimental data fit well with pseudo-first order kinetic model with rate constants (K_{obs}) of 0.0362 min^{-1} for Fe/WTS, 0.019 min^{-1} for Mn/WTS 0.0063 min^{-1} for WTS catalyst, and 0.0046 min^{-1} for sole ozonation. This finding indicated that Fe and Mn catalysts coated on modified WTS accelerated ozone decomposition to generate $OH^{\bullet}$ for degradation of phenol.

5.2 Suggestions

1) Other types of phenolic compound such as chlorophenol, aniline, etc. should be investigated for the removal efficiency by Fe/WTS and Mn/WTS catalytic ozonation.

2) Organic intermediates generated during the degradation process should be studied.

3) The factors affecting the efficiency of ozonation such as temperature should be investigated.

4) The experiment on catalytic ozonation should be scaled up in order to accurately predict the efficiency of catalytic ozonation utilization.

References

Angaji, M.T. Zinali, A.Z. and Qazvini, N.T. 2013. "Study of physical, chemical and morphological alterations of smectite clay upon activation and functionalization via the acid treatment." *World Journal of Nano Science and Engineering.* 3: 161-168.

Ayodele, O.B. 2013. "Effect of phosphoric acid treatment on kaolinite supported ferrioxalate catalyst for the degradation of amoxicillin in batch photo-fenton process." *Applied Clay Science.* 72 : 74-78.

Ayodele, O.B. Lim, J.K. and Hameed, B.H. 2012. "Degradation of phenol in photo-fenton process by phosphoric acid modified kaolin supported ferric-oxalate catalyst: Optomization and kinetic modeling." *Chemical Engineering Journal.* 197 : 181-192.

Benlalla, A. Elmoussaouiti, M. and Dahhou, M. 2015. "Utilization of water treatment plant sludge in structural ceramics bricks." *Applied clay science.* 118: 171-177.

Chen, W. Li, X. Pan, Z. Ma, S. and Li, L. 2016. "Effective mineralization of diclofenac by Catalytic Ozonation." *Chemical Engineering Journal.* 304: 594-601.

Chen, W. Li, X. Pan, Z. Ma, S. and Li, L. 2017. " Synthesis of MnO_x/SBA-15 for Norfloxacin degradation by catalytic ozonation" *Seperation and Purification Technology.* 173: 99-104.

Cheng, WP. Chen, PH. and Yu,RF . 2016. "Treating ammonium-rich wastewater with sludge from water treatment plant to produce ammonium alum. *Sustainable Environmetal Research.*" 26 : 63–69.

Farzadkia, M. Shahamat, Y. D. Nasseri, S. Mahvi, A. H. Gholami, M. and Shahryari, A. 2014. "Catalytic ozonation of phenolic wastewater: Identification and toxicity of intermediates." *Hindawi Publishing Corporation Journal of Engineering.* 1-10.

Fei, C. Li, D. Mao, X. Guo, Y. and Jing, W. "Synthesis of ordered mesoporous manganese titanium composite oxide catalyst for catalytic ozonation" *Chinese Journal of Chemical Engineering.* 26 : 1862-1872.

Gao, L. Zhai, Y. Ma, H. and Wang, B. 2009. “Degradation of cationic dye methylene blue by ozonation assisted with kaolin.” *Applied Clay Science.* 46 : 226-229.

Gao, W. Zhao, S. and Wu, H. 2016. “Direct acid activation of kaolinite and its effects on the adsorption of methylene blue.” *Applied Clay Science*. 126: 98-106.

Ghuge, S.P. and Saroha, A.K. 2018. “Catalytic ozonation for the treatment of synthetic and industrial effluents - Application of mesoporous materials: A review.” *Journal of Environmental Management.* 211: 83-102

Guo, Y. Yang, L. Chang, X. and Wang, X. 2012. “The application and reaction mechanism of catalytic ozonation in water treatment.” *Environmental and Analytical Toxicology.* 2(7): 1-6.

Guo, Y. Wang, H. Wang, B. Deng, S. Hung, J. Yu, G. and Wang, Y. 2018. “Prediction of micropollutant abatement during homogeneous catalytic ozonation by a chemical kinetic model.” *Water Research.* 142: 383-395.

He, K. Dong, Y. M. Li, Zhen, Y. L. Zhang, A. M. and Zheng, Y. C. 2008. “Catalytic ozonation of phenol in water with natural brucite and magnesia.” *Journal of Hazardous Materials.* 159 : 587-592.

Huang, Y. Sun, Y. Xu, Z. Luo, M. Zhu, C. and Li, L. 2017. “Removal of aqueous oxalic acid by heterogeneous catalytic ozonation with MnO_x/sewage sludge derived activated carbon as catalyst.” *Science of the Total Environment.* 575 : 50-57.

Forero, J.A. Duque, J.J. Rios, A And Diaz, J. 2001. “Ozone for phenol treatment in industrial wastewater” *C.T.F Cienc. Tecnol. Futuro*. 2: 1-10

Jozefaciu, G. 2002. "Effect of acid and alkali treatments on surface-charge properties of selected". *minerals* 50 (5): 647-656.

Kasprzyk-Hordern, B. Ziolek, M. and Nawrocki J. 2003. “Catalytic ozonation and methods for enhancing molecular ozone reactions in water treatment” *Applied catalyst B: Environmental.* 46: 639-669.

Kizinievic, O. Zurauskiene, R. Kizinievic, V. and Zurauskas, R. 2013. “Utilisation of sludge waste from water treatment for ceramic products.” *Construction and Building Materials.* 41 : 464-473.

Kormadel P. 2016 "Acid activated clay: Materials in continuous demand." *Applied clay Science.* 131: 84-99.

Kumar, S.P. Achyut K. and Sigha R.K. 2013. "Preparation and characteristic of acid and alkali treated kaolin clay." *Bulletin of Chemical Reaction Engineering and Catalyst.* 8(1) : 61-69.

Lenarda, M. Storaro, L. Talon, A. Moretti, E. and Riello, P. 2007. "Solid acid catalyst from clay: Preparation of mesoporous catalysts by chemical activation of metakaolin under acid condirions." *Journal of Colloids and Interface Science.* 311 : 537-543.

Li, B. Xu, X. Zhu, L. Ding, W. and Mahmood, Q. 2010. " Catalytic ozonation of industrial wastewater containing chloro and nitro aromatics using modified diatomaceous porous filling" *Desalination.* 254 : 90-98.

Li, X. Chen, W. Tang, Y. and Li, L. 2018. "Relationship between the structure of Fe-MCM-48 and its activity in catalytic ozonation for diclofenac minerization." *Chemosphere.* 206 : 615-621.

Ling, Y P. Ooi, C-H. Matsumoto, A. and Yeoh, F-Y. 2018. "Properties evaluation and fabrication of green clay reformulated from water sludge. *Ceramic International.* 44 (2):1411-1419.

Ling, Y P. Tham, R-H. and Lim, S-M. 2017. "Evaluation and reutilization of water sludge from fresh water processing plant as a green clay substituent". *Applied clay science.* 143: 300-306.

Liotta, L.F. Gruttadauria, M. Carlo, G.D. Perrini, G. and Librando, V. 2009. "Heterogeneous catalytic degradation of phenolic substrates : Catalyst activity." *Journal of Hazardous Materials.* 132 : 588-606.

Luo, J. Jiang, T. Li, G. Peng, Z. Rao, M.and zhang, Y. 2017. "Porous Materials from Thermally Activated Kaolinite: Preparation, Characterization and Application" *Materials.* 10(6);1-12.

Lv, K. Guo, X. Wu, X. Li, Q. Ho, W. Li, M. Ye, H. and Du, D. " Photocatalytic selective oxidation of phenol to produce dihydroxylbenzene in a TiO_2/UV system: hydroxyl radical versus hole" *Applied Catalyst B: Environment.* 199: 405-411.

Ma, J. and Graham, N.D. 2000. "Degradation of atrazine by manganese-catalysted ozonation-influence of radical scavengers." *Water Research.* 34(15) : 3822-3828.

Motlagh, M.K. Youzbashi, A.A. and Rigi, Z.A. 2011. "Effect of acid activation on structural and bleaching properties of a bentonite." *Iranian Journal of Materials Science and Engineering.* 8 : 50-56.

Muruganandham, M. Chen, S.H. and Wu, J.J. 2007. "Evaluation of water treatment sludge as a catalyst for aqueous ozone decomposition." *Catalysis Communication.* 8 : 1609-1614.

Nimwinya, E. Arjharn, W. Horpibulsuk, S. Phoo-ngernkham, T. and Poowancum, A. 2016 . "Asustainable calcined water treatment sludge and rice husk ash geopolymer" *Journal of cleaner production.* 19:128-134.

Nawrocki, J. and Kasprzyk-Hordern, B. 2010. "The efficiency and mechanisms of catalytic ozonation." *Applied Catalysis B:Environment.* 99 : 27-42.

Panda, A. K. Mishra, B.G. Mishra, D.K. and Singh, R.K.. 2010. "Effect of sulfuric acid treatment on the physico-chemical characteristics of kaolin clay." *Colloids and Surface A: Physicochemical and Engineering Aspect.* 363 : 98-104.

Parsons, SA. Daniels, SJ. 1999. "The use of recovered coagulants in wastewater treatment. *Environmental Technology.* 20 (9): 979-986.

Pumkumarn C. 2017 . "Synthesis of Geopolymer Composites from Water Treatment Residue (WTR) Reinforced with Polyethylene and Glove fibers". Master of engineering. King Mongkut's University of Technology Thonburi

Qi, F. Xu, B. Chen, Z. Ma, J. Sun, D. Zhang, L. and Wu, F. 2009. "Ozonation catalyzed by the raw bauxite for the degradation of 2,4,6 trichloroanisole in drinking water." *Journal of Hazardous Materials.* 168 : 246-252.

Qi, F. Xu, B. Zhao, L. Chen, Z. Zhang, L. Sun, D. and Ma, J. 2012. "Comparison of the efficiency and mechanism of catalytic ozonation of 2,4,6 trichloroanisole by iron and manganese modified bauxite." *Applied Catalysis B: Environmental.* 121-122 : 171-181.

Rao, Y-F. Luo, H-J. Wei, C-H. and Lou, L-F. 2010. "Catalytic ozonation of phenol and oxalic acid with copper-loaded activated carbon." *Journal of Center South University Technology.* 17 : 300-306.

Rosal, R. Gonzalo, M. S. Rodriguez, A. and Garcia-Calvo, E. 2010. "Catalytic ozonation of fenofibric acid over alumina-supported manganese oxide." *Journal of Hazardous Materials.* 183 : 271-278.

Rozic, L. Novakovic, T. and Petrovic, S. 2008. "Process improvement approach to the acid activation of smectite using factorial and orthogonal central composite design methods." *Journal of Serbian Chemical Society.* 73(4) : 487-497.

Rozic, L. Novakovic, T. and Petrovic, S. 2010. "Modelling and optimization process parameters of acid activation of bentonite by response surface methodology." *Applied Clay Science.* 73(4) : 487-497.

Shahamat, Y.D. Farzadkia, M. Nasseri, S. Mahvi, A H. Gholami, M. and Shahryari, A. 2014. "Magnetic heterogeneous catalytic ozonation : a new removal method for phenol in industrial wastewater." *Journal of Environmental Health Science and Engineering.* 12(50) : 1-12

Shahidi, D. Roy, R. and Azzouz, A. 2014. "Total removal of oxalic acid via synergistic parameter interaction in montmorillonite catalyzed ozonation." *Journal of Environmental Chemical Engineering.* 2 : 20-30.

Seiple, T E. Coleman, A M. and Skaggs, R. L. 2017 "Municipal wastewater sludge as a sustainable bioresource in the United States." *Journal of Environmental Management."* 197 : 673-680.

Suasamserm, P. 2002. "Properties of pre-collected alluvial sediment (sludge) from bangkok metropolitan water supply source." Master of Science (agriculture). Kasetsart university.

Sun, Q. Wang, Y. Li, L. Bing, J. Wang, Y. and Yan, H. 2015. "Mechanism for enhanced degradation of clofibric acid in aqueous by catalytic ozonation over MnO_x/SBA-15" *Journal of Hazardous Materials.* 286: 276-284.

Turhan, K. and Uzman, S. 2008. "Removal of phenol from water using ozone." *Desalination.* 229 : 257-263.

Vinitnantharat, S. Kositchaiyong, S. and Chairakorn, S. 2010. "Removal of fluoride in aqueous solution by adsorption on acid activated water treatment sludge." *Applied Clay Science.* 256 : 5458-5426.

Wang, H C. Liang, H S. and Chang, M B. 2011. " Chlorobenzene oxidation using ozone over iron oxide and manganese oxide catalysts" *Journal of Hazardous Materials*. 186: 1781-1787.

Wang, J. and Bai, Z. 2017." Fe-based catalysts for heterogeneous catalytic ozonation of emerging contaminants in water and wastewater" *Chemical Engineering Journal*. 312: 79-98.

Wang, Y. Yang, W. Yin, X. and Liu, Y. 2016. "The role of Mn-doping for catalytic ozonation of phenol using Mn/y-Al_2O_3 nanocatalyst: Performance and mechanism" *Journal of Environmental Chemical Engineering*. 4 : 3415-3425

Wei, X. Wu, H. Sun, Feng. 2017."Magnetite/ Fe-Al-Montmorillonite as a Fenton catalyst with efficient degradation of phenol" *Journal of Colloid and Interface Science*.504:611-619.

Wetchasat, K. Buchagul, S. Punthong, P. and Heramphakun, S. 2010. "Design and construction of sludge waste disposal system by using sludge dewatering method, Bangkhen water treatment plant." 1-8. In 15th National convention on civil engineering. Ubonratchathani : Ubonratchathani university.

WiŚniowsk, E. and Włodarczyk-Makuła, M. 2018. "The effect of selected acidic or alkaline chemical agents amendment on leachability of selected heavy metals from sewage sludge." *Science of The total Environment*. 663: 463-469.

Wolff, E. Schwabb, W.K. and Conceicao, S. 2015 "Utilization of water treatment plant sludge in structural ceramics" *Journal of cleaner production*. 96 : 282-289.

Wou, G. Jeong, T. Won, C. and Chi, L. 2010. "Comparison of catalytic ozonation of phenol by activated carbon and manganese-supported activated carbon prepared from brewing yeast." *Korian Journal Chemical Engineering*. 27(1) : 168-173.

Yahaya, S. Jikan, S.S. Badarulzaman, N.A. and Adamu, A.D. 2017. " Effects of Acid Treatment on the SEM-EDX Characteristics of Kaolin Clay" *Path of Science*. 3(9); 4001-4005.

Yang, Y. Chun, Y. Sheng, G. and Huang, M. 2004. "pH-Dependence of pesticide adsorption by wheat-residue-derived black carbon." *Langmuir* 20 : 6736-6741.

Zeng, Z. Zou, H. Li, X. Sun, B. Chen, J. and Shao, L. 2012. “Ozonation of acidic phenol wastewater with O_3/Fe(II) in a rotating packed bed reactor : Optimization by response surface methodology.” *Chemical Engineering and Processing : Process Intensification.* 60 : 1-8.

Zhu, X.F. And Xu, X.H. 2004. “The mechanism of Fe (III)-catalyzed ozonation of phenol.” *Journal of Zheijiang University Science.* 5(12) : 1543-1547.

APPENDIX A

EXPERIMENTAL DATA

Table A-1 Removal efficiency of phenol by sole ozonation

Time (min)	pH 3						$\bar{X}$	SD	pH 7						$\bar{X}$	SD	pH 11						$\bar{X}$	SD
	conc.(mg/L)			% removal					conc.(mg/L)			% removal					conc.(mg/L)			% removal				
	R 1	R 2	R 3	R 1	R 2	R 3			R 1	R 2	R 3	R 1	R 2	R 3			R 1	R 2	R 3	R 1	R 2	R 3		
0	53.23	51.58	50.14	0	0.00	0.00	0	0	53.23	53.23	52.73	0.00	0.00	0.00	0	0	54.82	51.58	52.08	0.00	0.00	0.00	0	0
5	48.27	48.41	47.69	0.63	9.32	4.88	5.50	0.63	48.27	47.91	47.77	9.32	10.00	9.41	9.58	0.37	50.21	46.76	48.05	8.40	9.34	7.73	8.49	0.81
10	46.18	47.55	46.11	0.36	13.24	8.03	7.72	0.36	46.18	46.33	45.61	13.24	12.97	13.51	13.24	0.27	49.33	46.43	46.25	9.97	10.04	11.19	10.40	0.68
15	42.87	46.54	45.32	0.24	19.46	9.61	9.56	0.24	42.87	42.23	42.30	19.46	20.68	19.78	19.97	0.63	47.69	44.46	44.46	12.99	13.81	14.64	13.81	0.82
30	41.58	44.60	44.02	0.86	21.89	12.20	13.18	0.86	41.58	41.94	41.29	21.89	21.22	21.69	21.60	0.35	45.18	42.01	42.15	17.59	18.55	19.06	18.40	0.75
60	40.64	40.50	39.56	0.21	23.65	21.09	21.33	0.21	40.64	39.64	39.64	23.65	25.54	24.83	24.67	0.96	39.58	37.41	37.48	27.82	27.48	28.04	27.78	0.28
90	37.19	37.26	36.47	0.28	30.13	27.26	27.59	0.28	37.19	37.26	37.05	30.13	30.00	29.74	29.96	0.20	33.23	31.79	32.08	39.37	38.35	38.40	38.71	0.57
120	34.17	35.97	35.32	0.37	35.81	29.56	29.84	0.37	34.17	34.96	34.02	35.81	34.32	35.47	35.20	0.78	30.07	28.41	29.28	45.14	44.91	43.78	44.61	0.73

Experimental condition: O_3 generation 0.57 mg/min, phenol 50 mg/L

Table A-2 Removal efficiency of phenol by catalyst without ozone applied

Time (min)	WTS*						$\bar{X}$	SD	Fe/WTS**						$\bar{X}$	SD	Mn/WTS***						$\bar{X}$	SD
	conc.(mg/L)			% removal					conc.(mg/L)			% removal					conc.(mg/L)			% removal				
	R 1	R 2	R 3	R 1	R 2	R 3			R 1	R 2	R 3	R 1	R 2	R 3			R 1	R 2	R 3	R 1	R 2	R 3		
0	53.23	51.58	50.78	0.00	0.00	0.00	0.00	0	53.23	51.58	50.78	0.00	0.00	0.00	0.00	0	53.23	51.58	50.78	0.00	0.00	0.00	0.00	0
5	50.44	50.52	50.51	0.50	0.52	0.51	0.51	0.63	50.52	50.52	50.54	0.52	0.53	0.51	0.51	0.37	50.64	50.65	50.65	0.26	0.25	0.26	0.26	0.81
10	50.45	50.42	50.52	0.50	0.51	0.52	0.51	0.36	50.52	50.53	50.52	0.51	0.52	0.51	0.51	0.27	50.52	50.51	50.53	0.51	0.50	0.51	0.51	0.68
15	50.36	50.38	50.39	0.76	0.78	0.77	0.77	0.24	50.39	50.40	50.39	0.71	0.76	0.77	0.77	0.63	50.38	50.40	50.39	0.77	0.75	0.77	0.77	0.82
30	49.73	49.64	49.74	2.04	2.01	2.04	2.05	0.86	49.74	49.74	49.75	2.06	2.05	2.07	2.05	0.35	49.60	49.61	49.62	2.33	2.30	2.30	2.30	0.75
60	49.20	49.21	49.22	3.05	3.04	3.06	3.07	0.21	49.21	49.22	49.22	3.05	3.06	3.07	3.07	0.96	49.09	49.09	49.06	3.34	3.33	3.33	3.33	0.28
90	48.92	48.89	48.96	3.54	3.55	3.58	3.58	0.28	48.96	48.98	48.96	3.51	3.52	3.58	3.54	0.20	48.82	48.83	48.83	3.84	3.86	3.84	3.84	0.57
120	48.81	48.82	48.83	3.81	3.82	3.84	3.84	0.37	48.83	48.83	48.84	3.83	3.82	3.84	3.83	0.78	48.69	48.71	48.70	4.09	4.06	4.09	4.09	0.73

* Experimental condition for WTS: WTS: dosage 1g/L, phenol 50 mg/L, pH11

** Experimental Conditions Fe/WTS: Fe/WTS : Fe1% , dosage 1 g/L , phenol 50 mg/L, pH11

*** Experimental Condition Mn/WTS: Mn/WTS: Mn1%, dosage 1g/L, phenol 50 mg/L, pH11

Table A-3 Removal efficiency of phenol by catalytic ozonation using Fe/WTS as a catalyst

time	pH3						$\overline{X}$	SD	pH7						$\overline{X}$	SD	pH11						$\overline{X}$	SD
	conc.(mg/L)			% removal					conc.(mg/L)			% removal					conc.			% removal				
	R 1	R 2	R 3	R 1	R 2	R 3			R 1	R 2	R 3	R 1	R 2	R 3			R 1	R 2	R 3	R 1	R 2	R 3		
0	50.77	50.77	50.77	0	0	0	0.00	0.00	52.15	52.59	0	0	0	0	0.00	0.00	52.48	52.48	52.48	0	0	0	0.00	0.00
5	44.03	43.95	43.87	13.28	13.43	12.385	13.03	0.57	40.64	40.71	23.33	22.04	22.57	23.33	22.65	0.65	40.00	40.00	40.00	23.78	23.78	23.78	23.78	0.00
10	40.85	40.77	40.93	19.54	19.69	18.267	19.17	0.78	35.75	35.61	33.92	31.42	32.28	33.92	32.55	1.27	30.77	30.62	30.62	41.35	41.65	41.65	41.56	0.17
15	38.14	38.21	38.37	24.88	24.73	23.375	24.33	0.83	31.72	31.65	39.89	39.15	39.80	39.89	39.62	0.40	25.34	25.42	25.42	51.69	51.55	51.55	51.60	0.09
30	35.96	36.04	36.20	29.16	29.00	27.710	28.63	0.80	26.40	26.47	50.61	49.36	49.65	50.61	49.88	0.65	23.64	23.72	23.72	54.94	54.80	54.80	54.85	0.09
60	32.63	32.71	32.94	35.72	35.57	34.211	35.17	0.83	25.10	25.18	52.37	51.84	52.12	52.37	52.11	0.27	18.68	18.76	18.76	64.40	64.25	64.25	64.30	0.09
90	32.55	32.01	32.40	35.87	36.94	35.295	36.04	0.84	21.94	21.87	58.61	57.91	58.41	58.61	58.31	0.36	16.51	16.58	16.58	68.53	68.39	68.39	68.44	0.09
120	29.45	29.30	28.83	41.98	42.29	42.415	42.23	0.22	17.84	17.84	66.62	65.77	66.07	66.62	66.16	0.43	11.39	11.31	11.31	78.28	78.44	78.43	78.39	0.09

Experimental conditions: Fe/WTS : Fe1% , dosage 1 g/L , phenol 50 mg/L

Table A-4 Removal efficiency of phenol by catalytic ozonation using WTS as a catalyst : effect of pH

time	pH 3						$\bar{X}$	SD	pH 7						$\bar{X}$	SD	pH 11						$\bar{X}$	SD
	conc.(mg/L)			% removal					conc.			% removal					conc.			% removal				
	R 1	R 2	R 3	R 1	R 2	R 3			R 1	R 2	R 3	R 1	R 2	R 3			R 1	R 2	R 3	R 1	R 2	R 3		
0	50.81	51.55	51.70	0.00	0.00	0.00	0	0	50.07	50.96	51.33	0.00	0.00	0.00	0	0	50.81	51.63	50.81	0.00	0.00	0.00	0	0
5	46.74	46.51	46.74	8.02	9.77	9.60	9.12	0.97	44.22	44.22	44.14	11.69	13.23	14.00	12.97	1.18	42.96	43.18	43.70	15.45	16.36	13.99	15.26	1.19
10	42.88	42.96	42.88	15.60	16.67	17.05	16.43	0.75	39.85	40.07	39.77	20.41	21.37	22.51	21.43	1.05	40.07	39.77	39.33	21.14	22.96	22.60	22.22	0.96
15	40.96	40.66	40.96	19.39	21.12	20.77	20.42	0.92	37.70	36.81	37.77	24.70	27.76	26.41	26.29	1.53	36.88	37.18	37.40	27.41	27.98	26.39	27.25	0.81
30	38.37	38.88	38.37	24.49	24.57	25.79	24.94	0.73	35.92	35.18	35.77	28.25	30.96	30.30	29.83	1.41	35.11	34.96	34.29	30.90	32.28	32.51	31.89	0.87
60	35.85	35.55	35.85	29.45	31.04	30.66	30.38	0.83	31.03	30.88	30.88	38.02	39.39	39.83	39.07	0.94	29.40	29.55	28.74	42.13	42.76	43.44	42.77	0.66
90	34.29	34.22	34.29	32.51	33.62	33.67	33.26	0.66	29.77	29.55	29.77	40.53	42.01	41.99	41.51	0.85	25.40	25.55	24.8	50.00	50.50	51.17	50.55	0.58
120	30.66	30.96	31.40	39.65	39.94	39.26	39.61	0.35	28.81	29.03	28.88	42.46	43.02	43.72	43.06	0.63	20.59	20.66	21.03	59.48	59.97	58.60	59.34	0.69

Experimental Conditions: WTS 1g/L , phenol 50 mg/l, O_3 generation 0.57 mg/m

Table A-5 Removal efficiency of phenol by catalytic ozonation using Mn/WTS as a catalyst :Effect of pH

time	pH 3						$\bar{X}$	SD	pH 7						$\bar{X}$	SD	pH 11						$\bar{X}$	SD
	conc.(mg/L)			% removal					conc.			% removal					conc.			% removal				
	R 1	R 2	R 3	R 1	R 2	R 3			R 1	R 2	R 3	R 1	R 2	R 3			R 1	R 2	R 3	R 1	R 2	R 3		
0	50.77	50.77	50.77	0	0	0	0.00	0.00	50.07	50.96	51.33	0.00	0.00	0.00	0	0	50.81	51.63	50.81	0.00	0.00	0.00	0	0
5	44.03	43.95	43.87	13.28	13.43	12.38	13.03	0.57	42.88	43.48	44.14	14.35	14.68	14.00	14.34	0.34	41.48	41.70	41.48	18.37	19.23	18.37	18.65	0.50
10	41.62	40.77	40.93	18.01	19.69	18.26	18.66	0.91	36.88	37.11	36.81	26.33	27.18	28.28	27.26	0.98	35.18	35.33	35.11	30.76	31.56	30.90	31.07	0.43
15	38.91	38.21	38.37	23.35	24.73	23.37	23.82	0.79	34.74	35.03	35.11	30.62	31.25	31.60	31.15	0.50	29.48	30.51	30.00	41.98	40.89	40.96	41.27	0.61
30	35.96	36.04	36.20	29.16	29.00	27.71	28.63	0.80	28.51	29.25	29.11	43.05	42.59	43.29	42.97	0.36	24.81	25.25	24.66	51.17	51.08	51.46	51.23	0.20
60	33.41	33.48	33.72	34.19	34.04	32.66	33.64	0.85	26.59	26.96	26.88	46.89	47.09	47.62	47.20	0.37	22.44	22.37	22.29	55.83	56.67	56.12	56.20	0.43
90	31.55	31.24	31.55	37.86	38.47	36.99	37.78	0.74	23.33	24.07	24.07	53.40	52.76	53.10	53.08	0.32	20.22	20.37	20.3	60.20	60.55	59.91	60.22	0.32
120	29.92	30.07	29.61	41.06	40.76	40.86	40.90	0.16	20.37	20.29	20.74	59.32	60.17	59.60	59.69	0.44	16.88	16.96	16.66	66.76	67.15	67.20	67.03	0.24

Experimental Conditions: Mn 1%, dosage 1 g/L, phenol 50 mg/L, O_3 generation 0.57 mg/min

Table A-6 Removal efficiency of phenol by catalytic ozonation using Fe/WTS as a catalyst: Effect of dosage of catalyst

Dosage of Catalyst(g/L)	time	pH 3						$\bar{X}$	SD	pH 7						$\bar{X}$	SD	pH 11						$\bar{X}$	SD
		conc.(mg/L)			% removal					conc.(mg/L)			% removal					conc.(mg/L)			% removal				
		R 1	R 2	R 3	R 1	R 2	R 3			R 1	R 2	R 3	R 1	R 2	R 3			R 1	R 2	R 3	R 1	R 2	R 3		
1	0	50.81	50.07	50.81	0.00	0.00	0.00	35.01	0.73	51.55	50.96	51.63	0.0	0.00	0.00	52.96	0.82	51.70	51.33	50.81	0.00	0.00	0.00	65.24	0.71
	60	32.67	32.51	33.40	35.71	35.06	34.26			24.71	23.77	24.00	52.0	53.34	53.52			17.85	17.55	18.07	65.47	65.80	64.43		
2	0	50.81	50.07	50.81	0.00	0.00	0.00	31.10	0.42	51.55	50.96	51.63	0.00	0.00	0.00	46.95	0.78	51.70	51.33	50.81	0.00	0.00	0.00	52.58	0.18
	60	34.88	34.74	34.88	31.34	30.62	31.34			26.89	27.25	27.63	47.85	46.51	46.49			24.44	24.44	24.07	52.72	52.38	52.62		
3	0	50.81	50.07	50.81	0.00	0.00	0.00	25.49	0.79	51.55	50.96	51.63	0.00	0.00	0.00	40.94	0.58	51.70	51.33	50.81	0.00	0.00	0.00	49.01	0.74
	60	37.78	36.96	38.29	25.66	26.18	24.64			30.53	30.29	30.14	40.66	40.55	41.61			25.96	26.44	26.07	49.86	48.48	48.69		

Experimental Condition: phenol 50 ppm, time 60 min, O_3 generation 0.57 mg/min

Table A-7 Removal efficiency of phenol by catalytic ozonation using Mn/WTS : Effect of dosage of catalyst

Dosage of Catalyst(g/L)	time	pH 3						$\bar{X}$	SD	pH 7						$\bar{X}$	SD	pH 11						$\bar{X}$	SD
		conc.(mg/L)			% removal					conc.(mg/L)			% removal					conc.(mg/L)			% removal				
		R 1	R 2	R 3	R 1	R 2	R 3			R 1	R 2	R 3	R 1	R 2	R 3			R 1	R 2	R 3	R 1	R 2	R 3		
1	0	50.81	50.07	50.81	0.00	0.00	0.00			51.55	50.96	51.63	0.00	0.00	0.00			51.70	51.33	50.81	0.00	0.00	0.00		
	60	33.85	33.25	33.70	33.38	33.58	33.67	33.55	0.15	26.93	26.88	26.96	47.70	47.24	47.78	47.57	0.29	22.26	22.00	22.07	56.88	57.14	56.56	56.86	0.29
2	0	50.81	50.07	50.81	0.00	0.00	0.00	36.86	0.65	51.55	50.96	51.63	0.00	0.00	0.00	51.85	0.24	51.70	51.33	50.81	0.00	0.00	0.00	61.91	0.35
	60	31.70	31.85	32.22	37.61	36.39	36.59			24.81	24.66	24.74	51.87	51.60	52.08			19.55	19.48	19.55	62.18	62.05	61.52		
3	0	50.81	50.07	50.81	0.00	0.00	0.00	27.44	0.29	51.55	50.96	51.63	0.00	0.00	0.00	42.38	0.57	51.70	51.33	50.81	0.00	0.00	0.00	52.38	0.67
	60	37.03	36.22	36.81	27.11	27.66	27.55			29.85	29.55	29.40	42.10	42.01	43.04			24.44	24.22	24.59	52.72	52.81	51.60		

Experimental Condition: Mn/WTS, phenol 50 ppm, time 60 min, Mn/WTS, 1g/L, O_3 generation 0.57 mg/min

Table A-8 Removal efficiency of phenol by catalytic ozonation using WTS as catalyst: effect of catalyst dosage

Catalyst dosage (g/L)	time	pH 3						$\overline{X}$	SD	pH 7						$\overline{X}$	SD	pH 11						$\overline{X}$	SD
		conc.(mg/L)			% removal					conc.(mg/L)			% removal					conc.(mg/L)			% removal				
		R 1	R 2	R 3	R 1	R 2	R 3			R 1	R 2	R 3	R 1	R 2	R 3			R 1	R 2	R 3	R 1	R 2	R 3		
1	0	50.81	51.56	51.70	0.00	0.00	0.00	30.38	0.83	50.07	50.96	51.33	0.00	0.00	0.00	39.08	0.94	50.81	51.63	50.81	0.00	0.00	0.00	42.78	0.66
	60	35.85	35.56	35.85	29.45	31.04	30.66			31.04	30.89	30.89	38.02	39.39	39.83			29.41	29.56	28.74	42.13	42.76	43.44		
2	0	50.81	51.56	51.70	0.00	0.00	0.00	42.54	0.57	50.07	50.96	51.33	0.00	0.00	0.00	47.10	0.69	50.81	51.63	50.81	0.00	0.00	0.00	53.12	0.48
	60	29.48	29.63	29.41	41.98	42.53	43.12			26.89	26.74	26.96	39.83	46.30	47.53			22.07	22.59	22.52	56.56	56.24	55.69		
3	0	50.81	51.56	51.70	0.00	0.00	0.00	47.92	0.46	50.07	50.96	51.33	0.00	0.00	0.00	50.64	0.40	50.81	51.63	50.81	0.00	0.00	0.00	56.16	0.44
	60	27.04	26.96	26.22	46.79	47.70	49.28			26.07	25.11	24.00	47.93	50.73	53.25			22.07	22.59	22.52	56.56	56.24	55.69		

Experimental Conditions: phenol 50 ppm, 60 min, O_3 generation 0.57 mg/min

Table A-9 Removal efficiency of phenol by catalytic ozonation using Fe/WTS as a catalyst : Effect of percent of metal doped

% of metal doped	time	pH 3						X̄	SD	pH 7						X̄	SD	pH 11						X̄	SD
		conc.(mg/L)			% removal					conc.(mg/L)			% removal					conc.(mg/L)			% removal				
		R 1	R 2	R 3	R 1	R 2	R 3			R 1	R 2	R 3	R 1	R 2	R 3			R 1	R 2	R 3	R 1	R 2	R 3		
1	0	50.81	50.07	50.81	0.00	0.00	0.00	35.01	0.73	51.55	50.96	51.63	0.0	0.00	0.00	52.96	0.82	51.70	51.33	50.81	0.00	0.00	0.00	65.24	0.71
	60	32.67	32.51	33.40	35.71	35.06	34.26			24.71	23.77	24.00	52.0	53.34	53.52			17.85	17.55	18.07	65.47	65.80	64.43		
2	0	50.81	50.07	50.81	0.00	0.00	0.00	31.10	0.42	51.55	50.96	51.63	0.00	0.00	0.00	46.95	0.78	51.70	51.33	50.81	0.00	0.00	0.00	52.58	0.18
	60	34.88	34.74	34.88	31.34	30.62	31.34			26.89	27.25	27.63	47.85	46.51	46.49			24.44	24.44	24.07	52.72	52.38	52.62		
3	0	50.81	50.07	50.81	0.00	0.00	0.00	25.49	0.79	51.55	50.96	51.63	0.00	0.00	0.00	40.94	0.58	51.70	51.33	50.81	0.00	0.00	0.00	49.01	0.74
	60	37.78	36.96	38.29	25.66	26.18	24.64			30.53	30.29	30.14	40.66	40.55	41.61			25.96	26.44	26.07	49.86	48.48	48.69		

Experimental Condition: phenol 50 ppm, time 60 min, Fe/WTS 1 g/L, O_3 generation 0.57 mg/min

Table A-10 Removal efficiency of phenol by catalytic ozonation using Mn/WTS :Effect of percent of metal doped

% of metal dope	time	pH 3						X̄	SD	pH 7						X̄	SD	pH 11						X̄	SD
		conc.(mg/L)			% removal					conc.(mg/L)			% removal					conc.(mg/L)			% removal				
		R 1	R 2	R 3	R 1	R 2	R 3			R 1	R 2	R 3	R 1	R 2	R 3			R 1	R 2	R 3	R 1	R 2	R 3		
1	0	50.81	50.07	50.81	0.00	0.00	0.00	36.86	0.65	51.55	50.96	51.63	0.00	0.00	0.00	51.85	0.24	51.70	51.33	50.81	0.00	0.00	0.00	61.91	0.35
	60	31.70	31.85	32.22	37.61	36.39	36.59			24.81	24.66	24.74	51.87	51.60	52.08			19.55	19.48	19.55	62.18	62.05	61.52		
2	0	50.81	50.07	50.81	0.00	0.00	0.00	43.22	0.71	51.55	50.96	51.63	0.00	0.00	0.00	61.94	0.18	51.70	51.33	50.81	0.00	0.00	0.00	76.36	0.23
	60	28.74	28.14	29.25	43.44	43.79	42.42			19.63	19.48	19.55	61.93	61.77	62.12			12.14	12.07	12.14	76.50	76.48	76.09		
3	0	50.81	50.07	50.81	0.00	0.00	0.00	26.75	0.64	51.55	50.96	51.63	0.00	0.00	0.00	41.76	0.31	51.70	51.33	50.81	0.00	0.00	0.00	50.31	0.40
	60	36.96	37.03	37.11	27.26	26.04	26.97			30.00	29.85	29.92	41.81	41.42	42.04			25.55	25.40	25.41	50.57	50.50	49.85		

Experimental Condition: : Mn/WTS, 3g/L, 50 ppm , 60 min, O_3 generation 0.57 mg/min

Table A-11 Removal efficiency of phenol by catalytic ozonation using Fe/WTS as catalyst :Effect of TBA

Conc. of TBA	time	pH 3						X̄	SD	pH 7						X̄	SD	pH 11						X̄	SD
		conc.(mg/L)			% removal					conc.(mg/L)			% removal					conc.(mg/L)			% removal				
		R 1	R 2	R 3	R 1	R 2	R 3			R 1	R 2	R 3	R 1	R 2	R 3			R 1	R 2	R 3	R 1	R 2	R 3		
1 mM	0	50.07	50.07	50.81	1.46	0.00	0.00			50.81	50.96	51.63	1.44	0.00	0.00			51.70	51.33	50.81	0.00	0.00	0.00		
	60	29.70	29.25	29.70	41.55	41.57	41.55	41.55	0.01	24.37	24.14	24.29	52.73	52.62	52.94	52.76	0.17	18.29	18.14	18.07	64.61	64.65	64.43	64.56	0.12
2 mM	0	50.07	50.07	50.81	1.46	0.00	0.00			50.81	50.96	51.63	1.44	0.00	0.00			51.70	51.33	50.81	0.00	0.00	0.00		
	60	31.70	31.25	31.70	37.61	37.57	37.61	37.60	0.02	29.18	28.81	29.18	43.39	43.46	43.47	43.44	0.04	24.22	24.00	23.85	53.15	53.25	53.06	53.15	0.09
3 mM	0	50.07	50.07	50.81	1.46	0.00	0.00			50.81	50.96	51.63	1.44	0.00	0.00			51.70	51.33	50.81	0.00	0.00	0.00		
	60	32.59	32.07	32.59	35.86	35.95	35.86	35.89	0.05	30.74	30.29	30.74	40.37	40.55	40.46	40.46	0.09	28.14	28.00	27.70	45.56	45.45	45.48	45.50	0.05

Experimental Conditions: Fe/WTS, 1g/L, 50 ppm, 60 min, Fe 2 %

Table A-12 Removal efficiency of phenol by catalytic ozonation using Mn/WTS as catalyst :Effect of TBA

Conc. of TBA	time	pH 3						$\bar{X}$	SD	pH 7						$\bar{X}$	SD	pH 11						$\bar{X}$	SD
		conc.(mg/L)			% removal					conc.(mg/L)			% removal					conc.(mg/L)			% removal				
		R 1	R 2	R 3	R 1	R 2	R 3			R 1	R 2	R 3	R 1	R 2	R 3			R 1	R 2	R 3	R 1	R 2	R 3		
1 mM	0	50.81	50.07	50.81	0.00	0.00	0.00	41.26	0.63	51.55	50.96	51.63	0.00	0.00	0.00	57.62	0.35	51.70	51.33	50.81	0.00	0.00	0.00	70.53	0.24
	60	29.48	29.63	30.00	41.98	40.83	40.96			21.85	21.77	21.70	57.62	57.27	57.96			15.18	15.03	15.11	70.63	70.71	70.26		
2 mM	0	50.81	50.07	50.81	0.00	0.00	0.00	39.60	0.45	51.55	50.96	51.63	0.00	0.00	0.00	44.64	0.43	51.70	51.33	50.81	0.00	0.00	0.00	64.76	0.28
	60	30.88	30.00	30.74	39.21	40.09	39.50			28.51	28.44	28.37	44.68	44.19	45.05			18.14	18.00	18.07	64.90	64.93	64.43		
3 mM	0	50.07	50.07	50.81	1.46	0.00	0.00	36.96	0.78	50.81	50.96	51.63	1.44	0.00	0.00	43.39	0.13	51.70	51.33	50.81	0.00	0.00	0.00	49.30	0.86
	60	31.92	32.00	31.70	37.17	36.09	37.61			29.25	28.81	29.18	43.25	43.46	43.47			25.70	26.22	26.07	50.29	48.92	48.69		

Experimental Conditions: Mn/WTS, 1g/L, 50 ppm, 60 min,

Table A-13 Removal efficiency of phenol by ozonation:Effect of TBA

time	pH 3						$\bar{X}$	SD	pH 7						$\bar{X}$	SD	pH 11						$\bar{X}$	SD
	conc.(mg/L)			% removal					conc.(mg/L)			% removal					conc.(mg/L)			% removal				
	R 1	R 2	R 3	R 1	R 2	R 3			R 1	R 2	R 3	R 1	R 2	R 3			R 1	R 2	R 3	R 1	R 2	R 3		
0	50.81	50.07	50.81	0.00	0.00	0.00			51.55	50.96	51.63	0.00	0.00	0.00			51.70	51.33	50.81	0.00	0.00	0.00		
60	4.11	4.12	4.11	20.98	20.83	20.86	20.89	0.05	4.00	3.98	4.12	22.60	22.54	22.48	22.54	0.06	3.93	3.94	3.96	22.43	22.44	22.50	22.45	0.04

Experimental Conditions: sole ozonation, phenol 50 ppm, 60 min, + TBA 3 mM

Table A-14 Kinetic study of catalytic ozonation using Fe/WTS as a catalyst

time	pH 3						$\bar{X}$	SD	ln C/co	pH 7						$\bar{X}$	SD	ln C/co	pH 11						$\bar{X}$	SD	ln C/CO
	conc.(mg/L)			% removal						conc.(mg/L)			% removal						conc.(mg/L)			% removal					
	R 1	R 2	R 3	R 1	R 2	R 3				R 1	R 2	R 3	R 1	R 2	R 3				R 1	R 2	R 3	R 1	R 2	R 3			
0	50.77	50.23	49.76	0	0	0	0.00	0.00	0.00	52.15	52.59	53.02	0	0	0	0.00	0.00	0.00	52.48	52.48	52.48	0	0	0	0.00	0.00	0.00
5	44.03	43.79	43.56	13.28	12.80	12.46	12.85	0.41	-0.14	39.42	39.85	39.85	24.41	24.21	24.83	24.49	0.32	-0.28	39.69	39.45	39.45	24.37	24.81	24.81	24.67	0.26	-0.28
10	40.85	40.15	39.84	19.54	20.06	19.93	19.85	0.27	-0.22	31.87	32.87	32.87	38.89	37.48	37.99	38.12	0.72	-0.48	31.61	31.00	31.00	39.76	40.91	40.91	40.53	0.67	-0.52
15	38.14	38.52	38.14	24.88	23.30	23.36	23.85	0.90	-0.27	27.62	27.48	27.48	47.03	47.74	48.16	47.65	0.57	-0.65	25.27	25.65	25.65	51.84	51.10	51.10	51.35	0.43	-0.72
30	31.31	31.47	31.31	38.32	37.34	37.07	37.58	0.66	-0.47	25.18	24.89	24.89	51.72	52.66	53.05	52.48	0.68	-0.74	22.17	22.17	22.17	57.75	57.75	57.75	57.76	0.00	-0.86
60	27.75	27.51	27.75	45.34	45.21	44.23	44.93	0.61	-0.60	18.41	19.20	19.20	64.68	63.47	63.77	63.98	0.63	-1.02	9.76	9.77	5.89	81.38	81.38	88.77	83.85	4.26	-1.82
90	24.88	24.80	24.88	50.99	50.61	50.00	50.54	0.50	-0.70	15.82	16.40	16.40	69.65	68.81	69.06	69.18	0.43	-1.18	3.56	3.48	1.55	93.20	93.35	97.04	94.53	2.18	-2.91
120	22.01	21.93	22.01	56.64	56.32	55.76	56.24	0.45	-0.83	11.36	11.94	11.94	78.20	77.29	77.47	77.66	0.48	-1.50	0.54	0.31	0.46	98.96	99.40	99.11	99.16	0.23	-4.78

Experimental Conditions: Fe 2% 1g/L, phenol 50 mg/l, O_3 generation 0.57 mg/min,

Table A-15 Kinetic study of catalytic ozonation using Mn/WTS as a catalyst

time	pH 3						$\bar{X}$	SD	ln C/co	pH 7						$\bar{X}$	SD	ln C/co	pH 11						$\bar{X}$	SD	ln C/CO
	conc.(mg/L)			% removal						conc.(mg/L)			% removal						conc.(mg/L)			% removal					
	R 1	R 2	R 3	R 1	R 2	R 3				R 1	R 2	R 3	R 1	R 2	R 3				R 1	R 2	R 3	R 1	R 2	R 3			
0	50.77	50.23	49.76	0	0	0	0.00	0.00	0.00	52.15	52.59	53.02	0	0	0	0.00	0.00	0.00	52.48	52.48	52.48	0	0	0	0.00	0.00	0.00
5	44.03	43.25	43.10	13.28	13.89	13.39	13.52	0.32	-0.15	39.42	40.00	40.07	24.41	23.94	24.42	24.26	0.28	-0.28	42.79	42.24	42.17	18.46	19.49	19.64	19.20	0.64	-0.21
10	41.62	40.93	40.62	18.01	18.51	18.37	18.30	0.26	-0.20	32.23	32.15	32.87	38.20	38.85	37.99	38.35	0.45	-0.48	34.65	35.19	35.27	33.97	32.94	32.79	33.24	0.64	-0.40
15	38.91	38.52	38.14	23.35	23.30	23.36	23.34	0.03	-0.27	27.62	27.48	27.48	47.03	47.74	48.16	47.65	0.57	-0.65	31.08	31.08	30.93	40.76	40.76	41.06	40.87	0.17	-0.53
30	31.55	31.31	31.31	37.86	37.65	37.07	37.53	0.41	-0.47	24.82	24.89	24.89	52.41	52.66	53.05	52.71	0.32	-0.75	25.27	26.04	26.12	51.84	50.37	50.22	50.81	0.90	-0.71
60	28.52	28.29	28.52	43.81	43.67	42.67	43.39	0.62	-0.57	20.57	21.36	20.64	60.55	59.37	61.05	60.33	0.87	-0.92	12.09	12.86	12.09	76.95	75.48	76.95	76.46	0.85	-1.45
90	25.65	25.27	25.42	49.46	49.69	48.90	49.36	0.40	-0.68	18.12	17.84	17.84	65.24	66.07	66.35	65.89	0.58	-1.08	7.28	7.36	7.13	86.11	85.96	86.41	86.16	0.23	-1.98
120	23.56	23.56	23.56	53.58	53.08	52.64	53.11	0.47	-0.76	15.18	14.82	15.54	70.89	71.81	70.69	71.14	0.60	-1.24	5.58	4.96	5.27	89.36	90.54	89.95	89.96	0.59	-2.30

Experimental Conditions: Mn 2% 1g/L, phenol 50 mg/l, O_3 generation 0.57 mg/min,

Table A-16 Kinetic study of catalytic ozonation using WTS as a catalyst

time	pH 3						$\overline{X}$	SD	ln C/co	pH 7						$\overline{X}$	SD	ln C/co	pH 11						$\overline{X}$	SD	ln C/co
	conc.(mg/L)			% removal						conc.(mg/L)			% removal						conc.(mg/L)			% removal					
	R 1	R 2	R 3	R 1	R 2	R 3				R 1	R 2	R 3	R 1	R 2	R 3				R 1	R 2	R 3	R 1	R 2	R 3			
0	50.81	51.55	51.70	0.00	0.00	0.00	0	0	-0.17	50.07	50.96	51.33	0.00	0.00	0.00	0	0	-0.17	50.81	51.63	50.81	0.00	0.00	0.00	0	0	-0.17
5	46.71	46.51	46.74	8.02	9.77	9.60	9.129	0.97	-0.26	44.22	44.22	44.14	11.69	13.23	14.00	12.97	1.18	-0.31	42.96	43.18	43.70	15.45	16.36	13.99	15.26	1.19	-0.33
10	42.88	42.96	42.88	15.60	16.67	17.05	16.43	0.75	-0.35	39.85	40.07	39.77	20.41	21.37	22.51	21.43	1.05	-0.41	40.07	39.77	39.33	21.14	22.96	22.60	22.22	0.96	-0.42
15	40.96	40.66	40.96	19.39	21.12	20.77	20.42	0.92	-0.40	37.70	36.81	37.77	24.70	27.76	26.41	26.29	1.53	-0.48	36.88	37.18	37.40	27.41	27.98	26.39	27.25	0.81	-0.48
30	38.37	38.88	38.37	24.49	24.57	25.79	24.94	0.73	-0.45	35.92	35.18	35.77	28.25	30.96	30.30	29.83	1.41	-0.53	35.11	34.96	34.26	30.90	32.28	32.51	31.89	0.87	-0.55
60	35.85	35.55	35.85	29.45	31.04	30.66	30.38	0.83	-0.53	31.03	30.88	30.88	38.02	39.39	39.83	39.07	0.94	-0.67	29.40	29.55	28.74	42.13	42.76	43.44	42.77	0.66	-0.73
90	34.29	34.22	34.29	32.51	33.62	33.67	33.26	0.66	-0.57	29.77	29.55	29.77	40.53	42.01	41.99	41.51	0.85	-0.71	25.40	25.55	24.81	50.00	50.50	51.17	50.55	0.58	-0.87
120	30.67	30.96	31.40	39.65	39.94	39.26	39.61	0.35	-0.67	28.81	29.03	28.88	42.46	43.02	43.72	43.06	0.63	-0.73	20.59	20.66	21.03	59.48	59.97	58.60	59.34	0.69	-1.07

Experimental conditions: WTS 1 g/L, phenol 50 mg/l, O_3 generation 0.57 mg/min,

Table A-17 Kinetic study of catalytic ozonation using sole ozonation

time	pH 3						$\bar{X}$	SD	ln C/co	pH 7						$\bar{X}$	SD	ln C/co	pH 11						$\bar{X}$	SD	ln C/CO
	conc.(mg/L)			% removal						conc.(mg/L)			% removal						conc.(mg/L)			% removal					
	R 1	R 2	R 3	R 1	R 2	R 3				R 1	R 2	R 3	R 1	R 2	R 3				R 1	R 2	R 3	R 1	R 2	R 3			
0	52.59	51.58	50.14	0.00	0.00	0.00	0	0	0.00	53.23	53.23	52.73	0.00	0.00	0.00	0	0	0.00	54.82	51.58	52.08	0.00	0.00	0.00	0	0	0.00
5	49.70	48.41	47.69	5.49	6.14	4.88	5.50	0.63	-0.06	48.27	47.91	47.77	9.32	10.00	9.41	9.58	0.37	-0.10	50.21	46.76	48.05	8.40	9.34	7.73	8.49	0.81	-0.09
10	48.74	47.55	46.11	7.32	7.81	8.03	7.72	0.36	-0.08	46.18	46.33	45.61	13.24	12.97	13.51	13.24	0.27	-0.14	49.35	46.40	46.25	9.97	10.04	11.19	10.40	0.68	-0.11
15	47.70	46.54	45.32	9.30	9.76	9.61	9.56	0.24	-0.10	42.87	42.23	42.30	19.46	20.68	19.78	19.97	0.63	-0.22	47.69	44.46	44.46	12.99	13.81	14.64	13.81	0.82	-0.15
30	45.33	44.60	44.02	13.80	13.53	12.20	13.18	0.86	-0.14	41.58	41.94	41.29	21.89	21.22	21.69	21.60	0.35	-0.24	45.18	42.01	42.15	17.59	18.55	19.06	18.40	0.75	-0.20
60	41.33	40.50	39.56	21.41	21.48	21.09	21.33	0.21	-0.24	40.64	39.64	39.64	23.65	25.54	24.83	24.67	0.96	-0.28	39.56	37.41	37.48	27.82	27.48	28.04	27.78	0.28	-0.33
90	38.00	37.26	36.47	27.75	27.75	27.26	27.59	0.28	-0.32	37.19	37.26	37.05	30.13	30.00	29.74	29.96	0.20	-0.36	33.23	31.79	32.08	39.37	38.35	38.40	38.71	0.57	-0.49
120	36.44	35.97	35.32	29.70	30.27	29.56	29.84	0.37	-0.36	34.17	34.96	34.02	35.81	34.32	35.47	35.20	0.78	-0.43	30.07	28.41	29.28	45.14	44.91	43.78	44.61	0.73	-0.59

Experimental Conditions: phenol 50 mg/L, O_3 generation 0.57 mg/min,

Table A-18 pH_{pzc} of each catalyst

Sample	pH 5					pH6					pH7					pH8					pH9					
	R1	R2	R3	avg	SD	R1	R2	R3	avg	SD	R1	R2	R3	avg	SD	R1	R2	R3	avg	SD	R1	R2	R3	avg	SD	$\overline{X}$
Fe/WTS	5.7	5.5	5.6	5.60	0.10	5.4	5.3	5.4	5.37	0.06	6.0	5.8	6.0	5.93	0.12	5.6	5.6	5.5	5.57	0.06	5.9	5.8	5.7	5.80	0.10	5.734
Mn/WTS	5.5	5.6	5.5	5.53	0.06	5.4	5.6	5.6	5.53	0.12	6.0	5.8	5.9	5.90	0.10	5.4	5.6	5.5	5.50	0.10	5.9	6.0	6.0	5.97	0.06	5.686
5 M modified WTS	4.5	4.2	4.3	4.33	0.15	4.5	4.2	4.4	4.37	0.15	4.4	4.2	4.3	4.30	0.10	4.4	4.3	4.3	4.33	0.06	4.8	4.8	4.7	4.77	0.06	4.42
WST	5.5	5.7	5.6	5.60	0.10	6.0	6.1	6.1	6.07	0.06	6.0	6.1	6.0	6.03	0.06	6.3	6.4	6.3	6.33	0.06	6.9	6.8	6.8	6.83	0.06	6.172

Table A-19 One way ANOVA test for Fe/WTS+ozonation, Fe/WTS +air and ozonation

Anova: Single Factor						
SUMMARY						
Groups	Count	Sum	Average	Variance		
Fe/WTS+air	8	16.59562	2.074453	2.350825		
Fe/WTS+O_3	8	382.9171	47.86464	656.9447		
O_3	8	162.8413	20.35516	232.2147		
ANOVA						
Source of Variation	SS	df	MS	F	P-value	F crit
Between Groups	8500.525	2	4250.263	14.30246	0.00012	3.4668
Within Groups	6240.572	21	297.1701			
Total	14741.1	23				

Table A-20 One way anova test for Fe/WTS+ozonation, Mn/WTS +air and ozonation

Anova: Single Factor						
SUMMARY						
Groups	Count	Sum	Average	Variance		
Mn/WTS+o_3	8	325.7072	40.7134	523.0927		
Mn/WTS+air	8	15.10156	1.887695	2.895487		
O_3	8	162.8413	20.35516	232.2147		
ANOVA						
Source of Variation	SS	df	MS	F	P-value	F crit
Between Groups	6034.509	2	3017.254	11.93844	0.000344	3.4668
Within Groups	5307.42	21	252.7343			
Total	11341.93	23				

Table A-21 One way anova test for Fe/WTS+ozonation, Mn/WTS +air and ozonation

Anova: Single Factor						
SUMMARY						
Groups	Count	Sum	Average	Variance		
WTS+o_3	8	249.3312	31.1664	374.9716		
WTS+air	8	12.3525	1.544063	2.035907		
O_3	8	162.8413	20.35516	232.2147		
ANOVA						
Source of Variation	SS	df	MS	F	P-value	F crit
Between Groups	3595.263	2	1797.631	8.852096	0.001629	3.4668
Within Groups	4264.556	21	203.0741			
Total	7859.818	23				

APPENDIX B

ANALYTICAL METHODS

B-1: Phenol Determination (Spectrophotometric, Manual 4-AAP With Distillation)

1.0 Scope and Application

1.1 This method is applicable to the analysis of drinking, surface and saline waters, domestic and industrial wastes.

1.2 The method is capable of measuring phenolic materials at the 5 μg/L level when the colored end product is extracted and concentrated in a solvent phase using phenol as a standard.

1.3 The method is capable of measuring phenolic materials that contain more than50 μg/L in the aqueous phase (without solvent extraction) using phenol as a standard.

1.4 It is not possible to use this method to differentiate between different kinds of phenols.

2.0 Summary of Method

2.1 Phenolic materials react with 4-aminoantipyrine in the presence of potassium ferricyanide at a pH of 10 to form a stable reddish-brown colored anti pyrine dye. The amount of color produced is a function of the concentration of phenolic material.

3.0 Comments

3.1 For most samples a preliminary distillation is required to remove interfering materials.

3.2 Color response of phenolic materials with 4-amino antipyrine is not the same for all compounds. Because phenolic type wastes usually contain a variety of phenols, it is not possible to duplicate a mixture of phenols to be used as a standard. For this reason phenol has been selected as a standard and any color produced by the reaction of other phenolic compounds is reported as phenol. This value will represent the minimum concentration of phenolic compounds present in the sample

4.0 Reagents

4.1 Phosphoric acid solution, 1 + 9: Dilute 10 mL of 85% H_3PO_4 to 100 mL with distilled water.

4.2 Copper sulfate solution: Dissolve 100 g $CuSO_4•5H_2O$ in distilled water and dilute to 1 liter.

4.3 Buffer solution: Dissolve 16.9 g NH Cl in 143 mL conc. NH_4OH and dilute to 250 mL with distilled water. Two mL should adjust 100 mL of distillate to pH 10.

4.4 Amino antipyrine solution: Dissolve 2 g of 4 AAP in distilled water and dilute to 100 mL.

4.5 Potassium ferricyanide solution: Dissolve 8 g of $K_2Fe(CN)$ in distilled water and dilute to 100 mL.

4.6 Stock phenol solution: Dissolve 1.0 g phenol in freshly boiled and cooled distilled water and dilute to 1 liter. 1 mL = 1 mg phenol.

4.7 Ferrous ammonium sulfate: Dissolve 1.1 g ferrous ammonium sulfate in 500 mL distilled water containing 1 mL conc. H_2SO_4 and dilute to 1 liter with H_2SO_4 freshly boiled and cooled distilled water.

5.0 Procedure

5.1 To 100 mL of distillate or an aliquot diluted to 100 mL and/or standards, add 2 mL of buffer solution and mix. The pH of the sample and standards should be 8± 0.1.

5.2 Add 1.0 mL amino antipyrine solution and mix.

5.3 Add 1.0 mL potassium ferricyanide solution and mix.

5.4 After 15 minutes read absorbance at 510 nm.

B-2: Analysis of pH_{pzc} (ASTM standard)

pH_{pzc} described the condition when the electrical charge density on a surface is zero. It is usually determined in relation to an electrolyte's pH, The pH_{pzc} value was a pH solution that zero net electrical charge on the surface.

Procedure

1. A solution of 0.005 M $CaCl_2$ was boiled to remove dissolved CO_2 and then cooled in room temperature.

2. The pH of solution was adjusted to a value between 5 to 9 using 0.5 M HCl or 0.5 NaOH.

3.Sample 10 g was added into 100 mL of the pH adjusted solution in a flask 250 mL and equilibrated for 24 h.

4. The final pH was measured and plotted against the initial pH.

5.The pH at which the curve crosses the $pH_{initial}=pH_{final}$ line is taken as $pH_{pzc.}$

Author Biography

NameMs.	Apiradee Sukmilin
Date of Birth	16 June 1980
Address	Pranakhorn Rajabhat University, Bangkok.
Education	(2002) Bachelor of Science in Environmental Resource Chemistry GPA 2.45 King Mongkut's Institute of Technology Ladkrabang (2004) Master of Science in Environmental Chemistry GPA 3.94 King Mongkut's Institute of technology Ladkraba
Scholarship	1.The Office of the Higher Education Commission (OHEC) 2. Pranakhorn Rajabhat University (PNRU)
Publication	-Sukmilin, A. Boonchom, B. and Jarusutthirak, C. 2019. " A Novel Catalyst fromWater Treatment Sludge for catalytic ozonation to degradephenol." *EnvironmentAsia.* 12(2) : -Sukmilin, A. Boonchom, B. and Jarusutthirak, C. 2019. "Catalytic Ozonation using Iron-Doped Water Treatment Sludge as a Catalyst for Treatment of Phenol in Synthetic Wastewater." *Environment and Natural Resources.* 17: